Control and Coordination *of* Robotic Fish

Chen Wang

Invitation

You are cordially invited
to attend the defense of
my thesis:

Control and Coordination *of* Robotic Fish

The defense will take place
on Friday, 10 October 2014,
at 12:45 in the Aula
of the Academy Building
of the University of Groningen,
Broerstraat 5, 9712CP,
Groningen, the Netherlands.

After the defense,
a reception will be held
in the same building.

Chen Wang

chen.wang@rug.nl

Control and Coordination of Robotic Fish

Chen Wang

The research described in this dissertation has been carried out at the Faculty of Mathematics and Natural Sciences, University of Groningen, the Netherlands. The author acknowledges the financial support from the university and the faculty for her Bernoulli Scholarship.

This dissertation has been completed in partial fulfillment of the requirements of the Dutch Institute of Systems and Control (DISC) for graduate study.

Printed by *Ipskamp Drukkers B.V.*
Enschede, the Netherlands

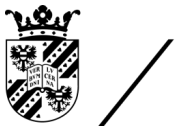

rijksuniversiteit
groningen

Control and coordination of robotic fish

Proefschrift

ter verkrijging van de graad van doctor aan de
Rijksuniversiteit Groningen
op gezag van de
rector magnificus prof. dr. E. Sterken
en volgens besluit van het College voor Promoties.

De openbare verdediging zal plaatsvinden op

vrijdag 10 oktober 2014 om 12.45 uur

door

Chen Wang

geboren op 15 april 1985
te Shaanxi, China

Promotores
Prof. dr. M. Cao
Prof. dr. ir. J.M.A. Scherpen

Beoordelingscommissie
Prof. dr.-Ing S. Hirche
Prof. dr. R. Babuska
Prof. dr. B. Jayawardhana

ISBN (Book): 978-90-367-7371-3
ISBN (Ebook): 978-90-367-7372-0

Contents

Acknowledgments

I would like to thank many people for their guidance, encouragement and support during my years as a Ph.D. student at the group of Discrete Technology & Production Automation (DTPA) at the University of Groningen.

First of all, this dissertation represents a great deal of time and effort not only on my part, but on the part of my supervisor, Prof. Ming Cao, without whom this dissertation would not have happened. I feel grateful that he provided me with the opportunity to pursue a Ph.D. degree. I especially thank him for the guidance, freedom, patience and criticism that he gave me during my research and for his personal and professional advice. I am extremely grateful to him for his consistent and detailed edits of numerous paper drafts and thesis chapters. I am also appreciate his understanding and encouragement when I was in trouble. I want to thank my promotor Prof. Jacquelien Scherpen for carefully reading my thesis and raising a number of suggestions for improvement.

I am grateful to Prof. Charlotte K. Hemelrijk at the Behavioural Ecology and Self-organization (BESO) group, for her discussions on my research project of biomimetic robotic fish and for providing me a lot of valuable suggestions. I especially thank her for inviting me to join the BESO Self-Organisation meeting. I really enjoy the time and gain a lot from the academic experience and the valuable literatures they shared during the meeting each week. I am appreciate Prof. Franjo Weissing at the Theoretical Biology group, for his guidance on the issue of evolutionary game theory and his discussions on my research project of multi-robotic fish systems.

I would like to thank my reading committee members, Prof. Robert Babuska, Prof. Sandra Hirche, and Prof. Bayu Jayawardhana, for reading the manuscript and providing valuable comments regarding my research.

I am very grateful to Prof. Guangming Xie who supervised me when I studied at Peking University, China. His discerning taste for exciting research topics, his ex-

traordinary ability to think clearly and deeply, and his respectful attitude towards scientific research, have had an immense impact on me. I deeply thank him for encouraging me to study abroad, for sharing the valuable academic and life experience with me, and for his constant help, support, patience and encouragement. I am extremely grateful to him for allowing me the freedom to pursue my interests and for helping me build the confidence to tackle challenging problems. I deeply thank Prof. Long Wang at Peking University, China, who is a brilliant scientist, for his guidance and encouragement on my research project.

Thanks to Dr. Bin Wu at Max Planck Institute for Evolutionary Biology, Plön, and Prof. Xiaojie Chen at University of Electronic Science and Technology of China, China, for our nice collaboration and their guidance and discussions on evolutionary game theory. I want to thank Liang Li and Minglei Xiong at Peking University, China, and Linbo Shao at Harvard University, USA, for their kind help with experiments with robotic fish. I also want to thank Fang Wang at Peking University, China, for designing the nice cover for my thesis.

I would like to thank my dear colleagues of the Discrete Technology & Production Automation (DTPA) at the University of Groningen. Especially, I thank Ewoud Vos for his help with the Dutch translation of the summary. I am extremely grateful to Frederika Fokkens, Jianlei Zhang, Mauricio Muñoz Arias, and Fan Zhang for their warm help with various procedures during preparing for my dissertation defense. I also thank Ewoud and Mauricio for being my defense paranymphs. I thank Sietse Achterop and Pim van den Dool for our cooperation and their help with experiments with robotic fish and E-pucks. I am very grateful to Weiguo Xia, Ruiyue Ouyang, Fan Zhang, Tao Liu, Chunyan Zhang, Jianlei Zhang, Hui Liu, and Shuo Zhang for their help, encouragement and companion during my life at Groningen. I am thankful to the former and present members for the valuable conversations and friendship: Robert Huisman, Gunn Larsen, Desti Alkano, Héctor Garcia de Marina Peinado, Prof. Claudio de Persis, Qingkai Yang, Matin Jafarian, Herman Kuis, Manuel Mazo Jr., Marko Seslija, Daniel Alonzo Dirksz, Dustano del Puerto Flores.

Last but not least, I would like to thank my family for their love, support, and encouragement over the years.

Chen Wang
Beijing
September, 2014

Chapter 1

Introduction

Astonishing dynamical behaviors in schools of fish and other social animal groups in nature have become the focus of multi-disciplinary studies in the past years. Rooted in control engineering and reaching out to biology, in this thesis, we aim to use biomimetic robotic fish teams as a powerful means to investigate the control and coordination issues for robotic multi-agent systems. On the one hand, we develop new theoretical results that are useful for control engineers and provide insight for biologists, and on the other, we improve experimental techniques that pave ways for further robotic study.

First, to replicate the outstanding locomotion skills of real fish, we investigate the locomotion control of an individual robotic fish. Second, inspired by the observation that formations of synchronized fish may swim with higher energy efficiency, we design distributed control laws for formations of swimming robotic fish generating antiphase sinusoidal body waves. Third, based on inspiration from the coordination behaviors of fish schooling and other collective motions for social animals, we propose an evolutionary game model to control groups of robotic fish and further study the emergence and evolution of cooperation among them in multi-robot water polo matches. Finally, based on these biomimetically inspired control tools, we develop a multi-robotic fish setup using the evolutionary game theoretic ideas to construct a new framework to study the diversification of personalities and emergence of leadership that are critical for the completion of group tasks.

This chapter introduces some background information and motivation for the research in this thesis. Then the contributions are presented and the outline of the thesis follows.

1.1 Background and motivation

Organisms have probably existed in the world for approximately 3.5 billion years [22, 46]. Their perfect physical structures and excellent locomotion properties emerging from the continuous long-time evolution fascinate all researchers who hope to

design better mobile robots. Recent developments in bionics, material, computer, electronics and fabrication technologies have offered researchers an unprecedented opportunity to design novel mobile robots based on inspiration from animals.

Among all kinds of aquatic organisms, fish are always paid more attention to and are often imitated to design underwater robots. The swimming modes of fish can roughly be divided into four categories: anguilliform mode, carangiform mode, ostraciiform mode, and labriform mode [65]. According to this classification, a variety of biomimetic underwater robots have been constructed. Most of them are designed based on the anguilliform swimming mode and the carangiform mode, such as a lamprey-like robot [33], a salamander-like robot [32] and the well-known RoboTuna [75]. But few underwater robots implement the ostraciiform or the labriform modes, with the box-fish-like robot BoxyBot being an example [15]. There are three control issues that we are interested in the most.

• Control Issue 1: Locomotion control of an individual robotic fish

To replicate the outstanding locomotion skills of fish, how to control the locomotion of an individual robotic fish becomes a basic but important issue in designing robotic fish. The thrust of most fish is achieved by bending their bodies to generate a traveling wave traversing the fish body in a direction opposite to the overall movement [45, 65]. Then the main difficulty of the locomotion control comes from how to coordinate multiple degrees of freedom of a robot and how to generate a real-time locomotion pattern to achieve such a traveling wave.

In the past, the control mechanisms of fish-like robots were commonly based on model-based approaches [48, 53] and sine approaches [47, 76]. Model-based approaches use kinematic [53] or dynamic models [48] of animals or robots to design mechanisms for locomotion control. In these approaches, once the kinematic or dynamic models turn out to be inaccurate, or in some cases even wrong, the performance of the controllers will be unreliable. The high computational cost is another drawback of model-based approaches. Sine-based approaches use simple sine functions to generate traveling waves. Usually, the propulsive wave traverses the fish-like robot body in the direction opposite to the overall movement and at a speed greater than the overall swimming speed to propel the robot. Compared with model-based approaches, sine-based approaches require lower computational costs and are thus convenient for online gait generation. Another advantage of sine-based approaches is that important quantities, such as the frequency and amplitude, are explicitly defined and easy to be controlled. However, a noteworthy disadvan-

tage is that online modifications of the parameters of the sine function will result in discontinuity of the output signals, leading to jerky locomotion.

Due to the drawbacks of the model-based approaches and sine approaches, recently, the central pattern generator (CPG) based methods are increasingly used in controlling a variety of different types of robots and different modes of locomotion. As biologically inspired approaches, CPGs are essential building blocks for the locomotion neural circuits found in both invertebrates and vertebrates [31]. A key feature of CPGs is the capability of producing coordinated patterns of rhythmic activities without any rhythmic inputs from sensory feedback or high-level control signals [16, 24]. There have been a number of projects using CPGs for controlling legged robots [38], amphibian robots [14, 32], swimming robots [15, 87], etc. In [14, 15, 32], Ijspeert proposed a novel CPG model for locomotion control of robots, which is a system of coupled nonlinear amplitude-controlled phase oscillators. This CPG model is not to model a particular biological system or to only replicate biological principles at an abstract level, but the main outcome of this novel model that differs from other CPG-based models is that its limit cycle behavior has an analytical solution with explicit frequency, amplitude and phase lag parameters, which can be used as control parameters[14].

Based on the novel model described above, we set out to design a much simpler but effective CPG model for the locomotion control of an individual robotic fish.

• **Control Issue 2: Formation swimming control for groups of robotic fish**

Besides the study of design principles for individual robotic fish, such as the issue of locomotion control mentioned above, some results have been reported to use proper sensing and planning to control multiple robotic fish [30, 67]. However, less effort has been made to study how robotic fish can benefit from collective hydrodynamics they generate while they are swimming together cooperatively.

While a detailed study on how fish adjust their own motions to exploit vortices to reduce locomotion energy costs can be too complex to be used in the design of coordination control strategies for robotic fish [44], one can nevertheless gain insight from such biological study into the relationship between the patterns of fish collective motion and the corresponding energy costs.

It was first pointed out by Weihs [80, 81] that diamond-shape formations are hydrodynamically advantageous for fish to improve propulsion efficiency while cruising. It was further analyzed in [69] through mathematical modeling that fish in a

diamond-shape formation need to get synchronized with antiphase body waves in order to reduce drag and benefit from the propulsion associated with the generated reverse Kármán vortex street; attempts have also been made to relate the synchronized collective swimming pattern with fish's senses through eyes and lateral lines. Numerical studies in computational fluid dynamics have investigated the interactions of vortices in the wakes of biomimetic fish schools and discussed how fish might adjust the frequencies and amplitudes of their body waves to keep the fixed inphase or antiphase swimming formation [17, 85].

Inspired by the above-mentioned observation that formations of synchronized fish may swim with less energy consumption, we design distributed control laws for groups of robotic fish to lock the phases of their sinusoidal body waves in an antiphase fashion.

• Control Issue 3: Coordination control in multi-robotic fish systems

Biologists have observed that the animal groups can achieve difficult goals though coordination with each other, although the ability of each individual is limited. As a colony, social animals can exhibit great power on foraging, avoiding predators, cruising and so on. The observation that fish schools utilize the vortices produced by others to improve propulsion efficiency, which we have mentioned above, is also a good example.

Inspired by the behaviors of social animals, teams of mobile robots have been utilized more and more often for a growing variety of tasks, such as environmental monitoring [18], surveillance [9], exploration [62], pursuit and evasion [11], search and rescue [3], transportation [67], and maintenance in harsh environments [7, 12]. Various strategies have been proposed and implemented using techniques that are based on robot behavior [2], potential fields [3], or reinforcement learning [8, 70]. Researchers are especially interested in testing new strategies using platforms of robotic team sports and more recently robotic water polo has attracted much attention [86].

One key research topic in the study of coordinating multiple robots is to understand under what conditions the synergy effect emerges, i.e., a collaborative team outperforms the collection of its independent individual members. While most of the previous works confirm the existence of synergy effects, less is known about how to quantify them and more importantly, how they affect autonomous robots' tendencies to cooperate. Here we address these challenging questions taking multi-

robot water polo matches as a case study and provide analysis and simulation results using ideas from evolutionary game theory, which is the application of game theory to evolving populations of lifeform agents and has been applied successfully in the fields of biology and economics [49, 52, 77]. In particular, evolutionary game theory has proven to be powerful in tracking the evolution of cooperation [56]. For this purpose, classic games are often utilized, which include the prisoner's dilemma game and the snowdrift game [19, 23]. A critical difference between the two games is that in the latter a player can still benefit when she opts to cooperate and her opponent chooses to defect.

Using game theoretic ideas, we propose a modified snowdrift game to control groups of robotic fish and study the emergence and evolution of cooperation among them in multi-robot water polo matches.

• A new framework to study effective leadership: An evolving multi-robotic fish system

The above three control issues all focus on investigating how to control biomimetic robotic fish. In particular, the context of the third issue, using an evolutionary game model to control groups of robotic fish and study the emergence and evolution of cooperation among them in multi-robot water polo matches, provides a way of introducing evolutionary game theory to the application of robotic fish teams. To further explore the usefulness of this new methodology, we take a look at its two components. On the one hand, the design of the robotic fish, including the control of its locomotion, imitates the physical structures and locomotion properties of real fish. On the other hand, evolutionary game theory is powerful in understanding interactive behavior in animal groups and societies. Thus, it provides us with a new research opportunity to look into the evolution of cooperation in robotic teams and may lead to new coordination strategies that have not been tested before.

Collective movement is one of the most salient dynamical behaviors of multi-agent systems, from which varieties of animal groups and artificial systems can get benefits [21, 82]. However, consider the collective movement in a social group, several questions should be asked, such as, how does the group decide when and where to go [39, 82]. It is normally agreed that such problems can be efficiently solved by leader-follower patterns. Thus "leadership" has become a key feature of the studies of collective movement, and thus attracted considerable attention from researchers

[39, 41, 57, 82].

In biological studies, plenty of different definitions of "leadership" exist. Krause et al. [40] define leadership as "the initiation of new directions of locomotion by one or more individuals which are then followed by other group members". To avoid the confusion between initiation and any prediction about the next events, such as being followed, Petit and Bon [57] suggest to use "initiator" instead of "leader" when we talk about specific individuals initiating a collective movement. Several studies in biology focus on what makes an individual emerge as an initiator among a group. State-dependent leadership is considered as one of the explanations [58]. For example, in the case of a foraging scenario, a hungrier individual is more likely to initiate a collective movement to forage. Another explanation of the initiator's emergence is that the group members differ in their preferred course of action [13, 26, 34]. In this case, conflicts of interest may occur among the group, since the individual benefits from taking its own preferred action besides keeping together with more companions. In recent years, a number of studies indicate that personality types offer an opportunity to generate an initiator [21, 25, 34, 50, 83]. The observations of experiments with pairs of real fish [25] imply that being bolder increases the willingness of an individual to initiate a collective movement, i.e., to be an initiator while a shyer individual shows stronger willingness to follow an initiator, i.e., to be an follower. Moreover, another study of experiments with pairs of real fish [50] shows that the experience of group members influence their tendency of initiation or following.

Keeping the above in mind, it would be worthwhile further reviewing the three main kinds of research frameworks used to study collective movement in the literature. The theoretical framework based on evolutionary game theory is widely used [34, 83]. Aiming to be analytically trackable, the models are abstract representations of real world, which ignoring lots of realistic factors. Whether the results derived from such models can well present the situations in nature is still needed to be verified. The framework based on simulations, comparing the theoretical methods, introduces more realistic factors and gets a more substantial model. [13, 20]. However, it is still far from the scenarios in real world. Experimental study is without doubt the most intuitive and concrete framework which is quite closed to or even recurs the scenarios in real world [13, 25, 26, 50]. However, there exist a lot of uncontrollable factors, especially for experiments with animals, which may great influence the focus of the research. Moreover, the group size cannot be too large due to the spatial limitation and the complexity of experiments.

As such, we propose a new framework, combining multi-robotic fish system with evolutionary game theory, to investigate how leadership emerges in robotic

fish teams. On the one hand, the experiments with robots, which have the capability of keeping as many realistic factors of real world as possible, allow us to get much closer to the situations in practice. On the other hand, using biomimetic robotic fish instead of real fish reduces a lot of noise caused by many uncontrollable factors of real fish if one wants to understand the fish behavior in nature. It becomes easy to set behaviors and update rules to individuals in the game model. To present how our proposed framework performs when investigating the behaviors of robotic fish groups, we choose leadership as a case study and focus on the evolution of personality and the emergence of effective leadership among groups in an obstacle removing scenario.

1.2 Contributions

The contributions of this thesis can be summarized as follows.

• **Control Issue 1: Locomotion control of an individual robotic fish**

We design a simple but effective CPG model for locomotion control of robotic fish. One key feature in our CPG model is to use partially linearized oscillators. Although only simple oscillators are adopted, we show that the performance of our CPG model is similar to that of Ijspeert's. Moreover, the structural parameters in our model can be selected more reasonably and easily according to the request of the dynamic performance of the CPG. A complete control architecture, mainly composed of the proposed CPG model and a transition layer, is built up. The transition layer is used to transform higher level control commands into the specific control inputs to the CPG for producing suitable coordinated patterns of rhythmic activities. Furthermore, in order to reduce the number of the control parameters, a particle swarm optimization(PSO) based method is used to find an optimal point in the parameter space, where a maximum speed can be achieved. As a result, the speed control is implemented by simply modulating the frequency of the joints. A large number of numerical simulations and physical experiments are performed to test our CPG model and locomotion control method. The performance is reliable and the application is easy and simple.

• Control Issue 2: Formation swimming control for groups of robotic fish

We design distributed control laws for teams of robotic fish to lock the phases of their sinusoidal body waves in an antiphase fashion. We model the phase dynamics of the body waves of the robotic fish by coupled Kuramoto oscillators. We prove that when such phase dynamics are coupled through real-time communications with a diamond-shape topology, they can be synchronized with the desirable relative phase differences of zero or π to mimic the fish swimming patterns predicted in the corresponding biological studies. We perform both computer simulations and physical experiments to show the effectiveness and robustness of the proposed control strategies.

• Control Issue 3: Coordination control in multi-robotic fish systems

We model simplified multi-robot water polo matches as modified snowdrift games and propose to introduce a cooperation coefficient to quantify synergy effects. Thus we are enabled to study the evolutionary stability of reactive strategies in infinite populations when the cooperation coefficient takes different values; in other words, we are able to parameterize the game dynamics by the cooperation coefficient and characterize the evolutionarily stable strategies. Furthermore, we analyze robotic agents' tendencies to collaborate and find that robots prefer to cooperate with teammates when cooperation is efficient and play alone otherwise. To gain insight into how the cooperation coefficient affects the cooperation tendencies, we design an update rule to allow the cooperation coefficient to evolve when robots learn to improve their performances. We find through simulations that the co-evolution of the population dynamics and the cooperation coefficient changes with robots' learning capabilities.

• A new framework to study effective leadership: An evolving multi-robotic fish system

We propose a new framework, combining multi-robotic fish system with evolutionary game theory, to investigate the emergence of effective leadership. Since the design of the robotic fish, including the control of its locomotion, imitates the physical structures and locomotion properties of real fish, the experiments with

biomimetic robotic fish allow us to get much closer to the situations in nature and thus may help biologists to understand better the leadership evolution in real fish schools. To verify the usefulness of our proposed framework, leadership in an obstacle removing scenario is chosen as a case study. We model the scenario as N-player snowdrift games and introduce personality as the player's strategy to present the robotic fish's willingness to initiate a collective movement in an obstacle removing task. Thus we are enabled to carry out experiments by groups of robotic fish to study the evolution of personality and the emergence of effective leadership in the robotic fish team. In addition, the effectiveness of our game model is verified by fitting with the experimental data. Simulations are also carried out as effective complements of the experimental results.

1.3 Outline of this thesis

This thesis is structured as follows.

Chapter 2 introduces the robotic fish and the experimental platform, which is used throughout this thesis.

In Chapter 3, the locomotion control of an individual robotic fish is investigated. A locomotion control architecture, which is based on our proposed CPG model and a transition layer, is presented. We then describe the PSO method, which is used to design the transition layer of the locomotion control method. Finally, simulation and experimental results are shown.

In Chapter 4, we propose distributed control laws for formations of swimming robotic fish generating antiphase sinusoidal body waves. We first present the coupled oscillator model for the robotic fish that we have developed. Then we discuss how distributed control laws can guide oscillators coupled in diamond-shape formations to get synchronized in an antiphase fashion. Finally, results from simulations and experiments are demonstrated.

In Chapter 5, we propose a modified snowdrift game to study the emergence and evolution of cooperation among robots in multi-robot water polo matches. We first formulate a version of simplified multi-robot water polo matches as a modified snowdrift game and introduce a cooperation coefficient to quantify synergy effects. Then we analyze the game evolutions and investigate the stability of the evolutionary dynamics parameterized by the cooperation coefficient. In addition, we study

the co-evolution of the population dynamics and the cooperation coefficient under a proposed update rule for the cooperation coefficient.

In Chapter 6, we develop an evolving multi-robotic fish system to investigate the behaviors of robotic fish teams. Leadership in an obstacle removing scenario is chosen as a case study. We first formulate a game setting in which groups of robotic fish deal with obstacle removing tasks repeatedly that are modeled by N-player snowdrift games. Personality is introduced to the game model as the player's strategy to present the robotic fish's willingness to initiate a collective movement in an obstacle removing task. Then we carry out the experiments by groups of robotic fish and analyze the evolution of personality and the emergence of effective leadership among the robotic fish groups. In addition, simulations are also carried out as effective complements to the experimental results.

Concluding remarks and recommendations for future research are given in Chapter 7.

Chapter 2

Preliminaries

In this chapter, we first introduce the robotic fish, which is the main subject of this thesis that all the subsequent research works focus on. The experimental platform is described as well. Both the robotic fish and the experimental platform used in this thesis are developed by the Intelligent Control Laboratory, Peking University[43, 66, 67].

2.1 Robotic fish

The robotic fish is shown in Fig. 2.1, which consists of a streamlined head, a flexible body and a caudal fin ([67, 79]).

The total length of the robotic fish is $40cm$. The head is made of fiberglass, which accommodates an onboard control unit, a duplex wireless serial-port communication module and a set of rechargeable batteries. The battery pack is placed at the bottom to lower the center of mass and consequently stabilize the vertical posture (Figure 2.1(b)). A pair of fixed pectoral fins is used to ensure the roll stability when the robotic fish swims. Since this pair of fins is rigidly attached to the sides of the head, the robotic fish's locomotion is confined roughly to a horizontal two-dimensional space. The flexible body contains three revolute joints that are linked together by aluminium exoskeletons. Each joint is driven by a R/C servomotor, which controls its relative joint angle with respect to those of its adjacent joints. The caudal fin is attached to the third joint, whose shape is designed to enhance the swimming efficiency. The whole body from the end of the head to the tail is covered by tailor-made waterproof rubber. In order to make the robotic fish swim just below the water surface for the purpose of keeping the antenna above the water, we inject an appropriate amount of air so that the density of the robotic fish is just a little bit smaller than that of the water.

For each robotic fish, all the onboard electronic devices are powered by the four $5V$ rechargeable Ni-MH batteries. The onboard control unit is based on a micro-

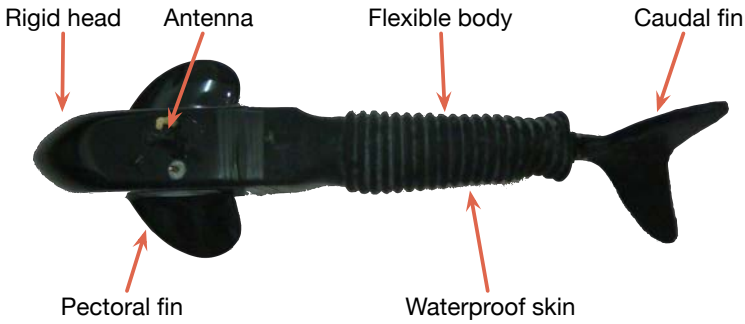

(a) Top view after encapsulation.

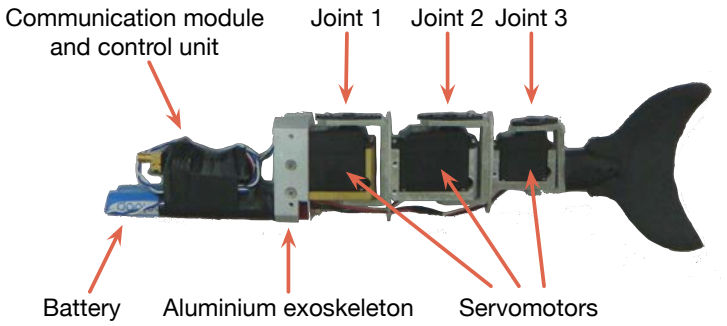

(b) Side view of the interior mechanical structure.

Figure 2.1: Mechanical configuration of a biomimetic robotic fish.

controller, Atmel ATmega 128, which runs the designed control law and generates the control commands in the form of Pulse Width Modulation (PWM) to drive the three R/C servomotors at the three joints in real time. The servomotors at the first two joints are Futaba S3003 with a maximum recommended torque of $3.2kg \cdot cm$ and a working speed of $0.23sec/60deg$ at $4.8V$. The smaller servomotor of the third joint is Futaba S3102 with a maximum recommended torque of $3.7kg \cdot cm$ and a working speed of $0.25sec/60deg$ at $4.8V$. The realtime communication with other robotic fish is achieved through the communication module WAP300C.

2.2 Experimental platform

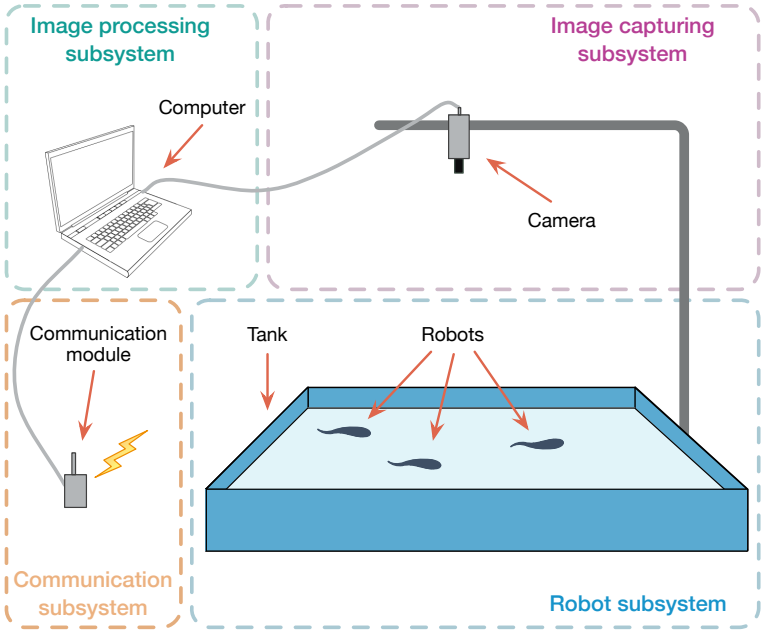

Figure 2.2: Hardware system of the experimental platform.

The experimental platform is used to estimate real-time pose information of the fish-like robot (the position, the direction and the speed).

Figure 2.2 depicts the hardware system which consists of a server computer, an overhead camera, a communication module and a robot subsystem. Images of the pool are captured by the overhead camera per $40ms$ and then sent to the server computer, where images are processed effectively to achieve the pose information of the robots. Through the wireless communication module, the upper computer sends control commands to robot and receives feedback information from the robot.

The schematic diagram of the software system architecture is shown in Figure 2.3. It consists of four modules: GUI (Graphics User Interface) module, robot module, image capturing and processing module and communication module. Through the GUI, one can input control commands and locomotion parameters. Then these signals are sent to the robot by the communication module in real time. In the image

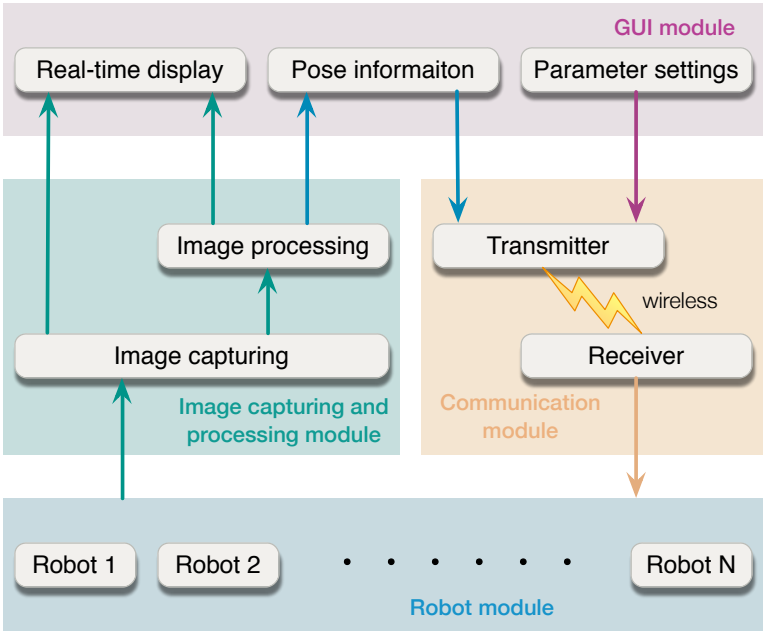

Figure 2.3: Architecture of software platform of the experimental platform.

capturing and processing module, the pose information of the robot is calculated and displayed in the GUI window in real time.

Chapter 3

Locomotion Control of An Individual Robotic Fish

In this chapter, we investigate the locomotion control of an individual robotic fish to learn from the outstanding locomotion skills of real fish in nature. To achieve this goal, we design a control architecture based on a novel central pattern generator (CPG) and implement it as a system of coupled partially linearized oscillators. This design differs from the usual CPG models in which nonlinear oscillators are commonly used. While our CPG contains the basic features of its biological counterparts and is capable of producing coordinated patterns of rhythmic activity, thanks to the linearity of the oscillators used, the computational costs of the CPG is greatly reduced and all the structural parameters can be selected easily. In addition to the proposed CPG model, the complete control architecture in our study also contains a transition layer, which is used to transform higher level control commands into accessible inputs to the CPG. Moreover, particle swarm optimization (PSO) is implemented to reduce the number of the control parameters. As a result, only two control parameters, which are the frequency for speed control and the offset of the motors for direction control, are sufficient for the whole locomotion control implementation. Additionally, a transition layer makes the locomotion control implementation simple and straightforward. Results from both simulation and experiment demonstrate the efficiency of the proposed CPG-based locomotion control approach.

3.1 Locomotion control

The complete locomotion control architecture is shown in Figure 3.1(a). The transition layer, implemented at a server computer, transforms simple control commands to the specific CPG control parameters, and sends them through wireless communication to the robot. The CPG-based model, which is implemented at the robot, can generate the control signals to adjust the deflection angles of the joints [64].

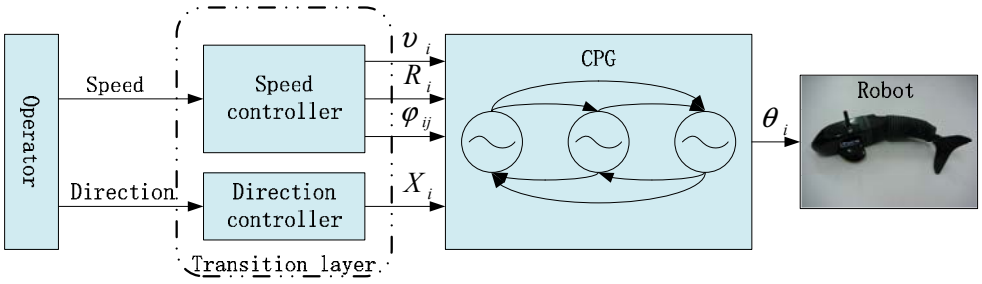

(a)

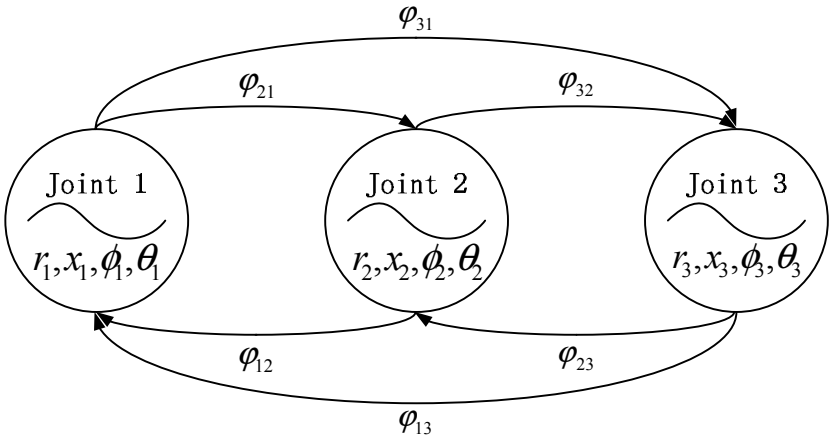

(b)

Figure 3.1: (a) Diagram of the locomotion control architecture. (b) Structure of the CPG-based model used in the robotic fish.

3.1.1 CPG model

In order to make the CPG model easy to be implemented in our robotic fish, a system of N coupled partially linearized oscillators is used to form our CPG model, where N is the number of the body joints and $N \geq 2$. In other words, there is a one-to-one correspondence between the oscillators of the CPG-based model and the joints of the robotic fish. We will demonstrate later that our proposed model performs well although the partially linearized differential equations have been used instead of nonlinear ones in Ijspeert's CPG model. The ith, $i = 1, 2, \ldots, N$, oscillator is

implemented as follows:

$$\ddot{r}_i(t) = \alpha_i[\alpha_i(R_i - r_i(t)) - 2\dot{r}_i(t)] \quad (3.1)$$

$$\ddot{x}_i(t) = \beta_i[\beta_i(X_i - x_i(t)) - 2\dot{x}_i(t)] \quad (3.2)$$

$$\ddot{\phi}_i(t) = \sum_{j=1,j\neq i}^{N} \mu_{ij}[\mu_{ij}(\phi_j(t) - \phi_i(t) - \varphi_{ij}) - 2(\dot{\phi}_i(t) - 2\pi\upsilon_i)] \quad (3.3)$$

$$\theta_i(t) = x_i(t) + r_i(t)\cos(\phi_i(t)) \quad (3.4)$$

where the state variables $r_i(t)$, $x_i(t)$ and $\phi_i(t)$ represent, respectively, the amplitude, the offset and the phase of the ith oscillator at time t. The variable $\theta_i(t)$ is the output of oscillator i, i.e., the desired deflection angle of the corresponding joint i at time t. The parameters υ_i, R_i and X_i are the desired frequency, amplitude and offset of the oscillator i respectively. And the parameter φ_{ij} is the desired phase bias between oscillators i and j, which satisfies the following conditions: i)$\varphi_{ii} = 0$; ii) $\varphi_{ij} = -\varphi_{ji}$; and iii) $\varphi_{ik} + \varphi_{kj} = \varphi_{ij}$. Moreover, α_i, β_i and μ_{ij} are the structural parameters that affect the transient dynamics. To simplify the model, we let $\alpha_i = \alpha$, $\beta_i = \beta$, $\mu_{ii} = 0$ (i.e., all oscillators have no self-couplings); $\mu_{ij} = \mu$ for $i \neq j$. The values of α,β and μ are positive and need to be designed later. In this chapter, we use the same desired frequency $\upsilon_i = \upsilon$ for all the oscillators (i.e., joints). Finally, the CPG model (3.1)-(3.4) can be written as follows:

$$\ddot{r}_i = -\alpha^2(r_i - R_i) - 2\alpha\dot{r}_i \quad (3.5)$$

$$\ddot{x}_i = -\beta^2(x_i - X_i) - 2\beta\dot{x}_i \quad (3.6)$$

$$\ddot{\phi}_i = -\mu^2 \sum_{j=1,j\neq i}^{N} (\phi_i - \phi_j - \varphi_{ji}) - 2(N-1)\mu(\dot{\phi}_i - 2\pi\upsilon) \quad (3.7)$$

$$\theta_i = x_i + r_i\cos(\phi_i), \qquad i = 1, 2, \ldots, N. \quad (3.8)$$

To change the locomotion behavior of the robotic fish, the input signals (i.e., the desired frequency, amplitude and offset) are usually in the form of step signals. Thus we focus on the performance of the step response of the proposed CPG-model in Subsection 3.1.2 and 3.1.3.

3.1.2 Stability analysis

Equation (3.5) and (3.6) are designed to be *critically damped second-order linear systems*. Consider the general form of such a system:

$$\frac{1}{\omega^2}\ddot{y}(t) + \frac{2}{\omega}\dot{y}(t) + y(t) = u(t) \quad (3.9)$$

where $y(t)$ and $u(t)$ represent, respectively, the output and the input. The positive scalar ω is the damping coefficient of the system. The step response of the system converges exponentially, i.e., the output $y(t)$ converges exponentially to $u(t)$. Therefore the amplitude r_i and the offset x_i of the oscillator converge, respectively, to the desired amplitude R_i and offset X_i exponentially.

In Equation (3.7), the phase ϕ_i is not only determined by oscillator i itself but also affected by the other oscillators. We say all the oscillators achieve consensus if, for all $\phi_i(0)$ and $\dot{\phi}_i(0)$ and all $i, j = 1, \ldots, N$, $\phi_i(t) - \phi_j(t) \to \varphi_{ji}$ and $\dot{\phi}_i(t) \to 2\pi\upsilon$, as $t \to \infty$. One can prove that the subsystem (3.7) achieves consensus asymptotically for any $\mu > 0$. In other words, the phase bias between ϕ_j and ϕ_i converges to the desired phase bias φ_{ij} asymptotically. Equation (3.8) is designed to generate the rhythmic output signal θ_i, which is completely determined by the amplitude r_i, the offset x_i and the phase ϕ_i. Since all the amplitude r_i, the offset x_i and the phase ϕ_i can asymptotically and monotonically converge to their desired values from any initial conditions, the output θ_i of oscillator i is modulated smoothly. Based on the above regulations, oscillator i converges to the following limit cycle from arbitrary initial conditions asymptotically:

$$\theta_i^{\infty}(t) = X_i + R_i \cos(2\pi\upsilon t + \phi_0 + \varphi_{1i}), \quad i = 1, \ldots, N \tag{3.10}$$

where ϕ_0 is a constant depending on the initial conditions of the system.

3.1.3 Structure parameters selection

During the following discussion we use $N = 3$ considering our three-joint robotic fish (Figure 3.1(b)). To make the locomotion performance of the robotic fish closer to those of real fish, suitable structure parameters of the CPG model must be chosen.

After a large number of numerical simulations, we observe that with the same α, the influences of the transient period are quite different when different values of υ are used. And the parameters β and μ have similar results. Therefore we assume that the values of the three parameters will change with the frequency υ to achieve better effect of the transient period. We re-analyze the transient behavior of the unit step response of the general system (3.9). By simulation comparison and theoretical analysis, the parameters α, β and μ are selected according as follows

$$\alpha = 11.68\upsilon \tag{3.11}$$

$$\beta = 11.68\upsilon \tag{3.12}$$

$$\mu = 5.84\upsilon. \tag{3.13}$$

Based on the above parameters selection, only four parameters (υ, φ_{ij}, R_i and X_i) need to be set when applied to the CPG model described by Equation (3.5), (3.6),

(3.7), (3.8), (3.11), (3.12) and (3.13) to generate the desired traveling wave for swimming.

3.1.4 Transition layer

For convenience of controlling the locomotion of a robotic fish, we propose a transition layer, composed of a direction controller and a speed controller, to reduce the complexity of the control commands.

Direction controller

The locomotion direction is determined mainly by the three offsets $X_i (i = 1, 2, 3)$. Here, we use the offset to present the difference between the left and right amplitudes of each oscillator. Thus we use a simple direction controller described by $X_i = X(i = 1, 2)$ and $X_3 = 0$ which make $X(rad)$ become the only variable for direction control. We choose $X_3 = 0$ to make the last joint of the robot have no offset with the second joint to ensure enough power for propelling the robot. The command $X > 0$ means turning right and $X < 0$ means turning left.

Speed controller

The locomotion speed (we only discuss swimming forwards in this section) is determined jointly by the frequency υ, the amplitude R_i, the phase bias φ_{ij} and more complicatedly the water environment. Combined activities of all these factors make the design of the speed controller difficult. We carry out extensive experiments with the robotic fish to identify how the speed changes when these parameters change. The observation is that the speed of locomotion monotonically increases with the frequency when all the parameters are within the physical limitation of servomotors. But the amplitude R_i and phase bias φ_{ij} have complex non-monotone influence on the speed of locomotion.

We therefore choose the frequency υ as the only variable for speed control, and design a piecewise linear function $[R_i, \varphi_{ij}] = f_{speed}(\upsilon)$ as the speed controller.

The frequency is limited in $[0.5Hz, 3.0Hz]$ with the step size of $0.25Hz$. For each frequency, the PSO method is used to optimize the other five parameters (R_1, R_2, R_3, φ_{12} and φ_{13}) to obtain the maximum speed (see more details in Section 3.2).

The piecewise linear function, speed controller, is the linear interpolations between these optima acquired by the PSO method. Based on this speed controller, all the specific control inputs of the CPG model ($\upsilon, R_i, \varphi_{ij}$) can be realized by a single control input υ. And the speed controller ensures that the outputs of the proposed

CPG model remain close to the fastest gait for each frequency.

With this transition layer, the direction and the speed of the robotic fish can be simply controlled and modified by manipulating the offset X (resp. the frequency υ) for direction (resp. for speed).

3.2 Parameter optimization via PSO

Particle swarm optimization inspired by social behavior of bird flocking or fish schooling is a stochastic optimization technique [60]. It was originally proposed in 1995 [37]. Similar to the Genetic Algorithm (GA), the PSO method searches for optimal solutions through iterations of a population of individuals, which are called a swarm of particles in PSO. However, the crossover and mutation operation are replaced by moving inside the solution space decided by the so-called velocity of each particle. Many reported results were built on the use of PSO method for developing gaits with better locomotion performance of quadruped robots[27, 61], biped robots[28, 51], modular robots[6], etc.

The PSO method has proved to be faster in computation and easier to be implemented compared with many other optimization algorithms such as GA [10], and it is effective in solving many global optimization problems[6, 35, 42, 74].

To improve the convergence performance of PSO methods, the inertia weight is introduced into PSO [68]. Furthermore, the inertia weight is dynamically adjusted in the PSO evolution process in order to balance the global searching ability and convergence rate. This modified PSO with changing inertia weight is usually called Adaptive PSO (APSO).

In this section, we use the APSO method to optimize the speed of the robotic fish. The APSO iteration equation is given as follows:

$$\begin{aligned} v_{ij}^{k+1} &= w v_{ij}^{k} + c_1 r_{1j}^{k}[p_{ij}^{k} - x_{ij}^{k}] + c_2 r_{2j}^{k}[p_{gj}^{k} - x_{ij}^{k}] \\ x_{ij}^{k+1} &= x_{ij}^{k} + v_{ij}^{k+1} \end{aligned} \tag{3.14}$$

where w is the inertia weight (see [61] for details).

In this chapter, we use a swarm of 10 particles. The state of particle i is a vector $(R_{i1}, R_{i2}, R_{i3}, \varphi_{i12}, \varphi_{i13})$ where R_{i1}, R_{i2} and R_{i3} present, respectively, the amplitude of each joint of robotic fish, φ_{i12} is the phase bias between joint 1 and joint 2, and φ_{i13} between joint 1 and joint 3.

The spectrum of a particle is determined by the physical limitation of servomotors. We use $c_1 = 1.8$ and $c_2 = 2$ to expedite the search process. The inertia weight w, which plays the role of balancing the global searching ability and local searching

ability, is calculated by

$$w = 0.9 - \frac{0.9}{M} \times n, \quad n = 1, 2, ..., M \tag{3.15}$$

where n presents the iteration, and M is the maximum number of iterations (experimentally using $M = 12$ in this case). It is easy to check that the inertia weight starts with a large value 0.825 and linearly decreases to 0 when the iteration number reaches12. Thus both the search is carried out in a broaden area at the beginning and narrows down in a currently effective area at the end.

The speed of the robotic fish is considered to be the performance of each particle. However, the exact objective function of such performance cannot be given because the complexity hydrodynamics result in having no accurate simulator for the robotic fish. Thus, we use the APSO method for real robots within the experimental platform described above. To be more accurate, each result is the average of 5 speed measurements.

Using this APSO method described above, optimization experiments with the real robot are performed for the frequencies from $0.5Hz$ to $3.0Hz$ with a step size of $0.25Hz$. For instance, at the fixed frequency $\upsilon = 2.5Hz$, the other five controller parameters of the proposed CPG model ($R_1, R_2, R_3, \varphi_{12}$ and φ_{13}) have been optimized using the APSO method. Figure 3.2(a) shows the iterative process. The average fitness of all particles is converging quite fast from iteration 1 to 4. Then the average fitness rises slowly but firmly until around iteration 10. The curve rises up to the maximum fitness (i.e., the forwards speed of the robotic fish) of $38.2cm/s$ $(0.955\ body\ lengths/s)$ at iteration 10. The parameter values for the best fitness are $R_1 = 0.42rad, R_2 = 0.31rad, R_3 = 0.40rad, \varphi_{12} = -0.70rad$ and $\varphi_{13} = -1.41rad$. Thus we get a high-speed gait of the robot in a short time by using the above-mentioned APSO method.

Similarly, a series of optimization processes are taken to obtain the maximum speed and the corresponding parameters for each chosen frequency. The results of the optimization are shown in Figure 3.2(b). The maximum speed monotonically increases with the frequency υ up to $2.5Hz$. However, the speed begins to decrease when the frequency υ still increases after $2.5Hz$. The reason is that the amplitude of the servomotors is physical limited when the frequency is too high. Thus the maximum value of the swimming speed is $38.2cm/s$ $(0.955\ body\ lengths/s)$ when $\upsilon = 2.5Hz$. As a result, the speed controller of the transition layer can be obtained using the proposed method in Subsection 3.1.4.

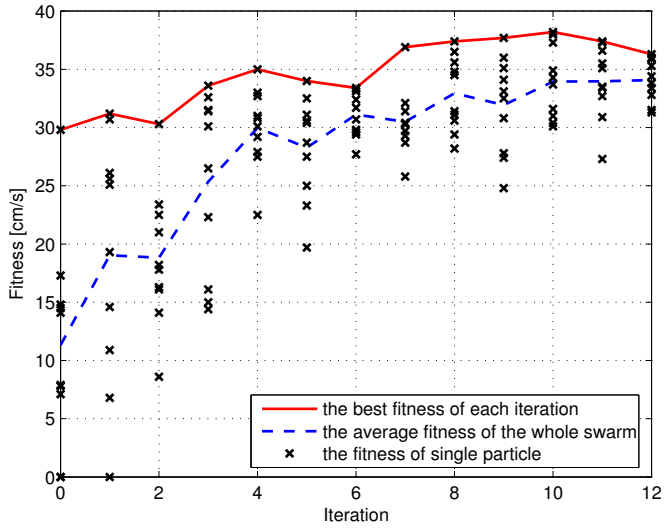

(a)

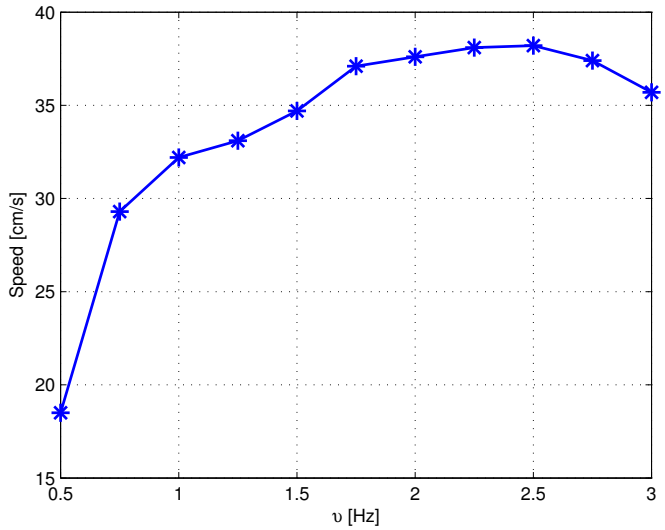

(b)

Figure 3.2: (a) Results of the optimization for swimming at $\upsilon = 2.5Hz$. (b) Optimization results of speed for the frequencies between $0.5Hz$ and $3.0Hz$ (with a step size of 0.25Hz). Each data point is the average of 5 speed measurements.

3.3 Simulations and experiments

For verifying the performance of the proposed CPG-based locomotion control method in Section 3.1, some simulations and experiments are completed in this section.

3.3.1 Comparing with Ijspeert's model

We recall Ijspeert's model [15] for better readability,

$$\dot{\phi}_i = \omega_i + \sum_j [w_{ij} r_j \sin(\phi_j - \phi_i - \varphi_{ij})] \tag{3.16}$$

$$\ddot{r}_i = a_r[\frac{a_r}{4}(R_i - r_i) - \dot{r}_i] \tag{3.17}$$

$$\ddot{x}_i = a_x[\frac{a_x}{4}(X_i - x_i) - \dot{x}_i] \tag{3.18}$$

$$\theta_i = x_i + r_i \cos(\phi_i) \tag{3.19}$$

where θ_i is the output signal (in radians) extracted out of oscillator i, and ϕ_i, r_i and x_i represent the phase, the amplitude, and the offset of the oscillations (in radians), respectively. The parameters w_{ij} and φ_{ij} are respectively coupling weights and phase biases. The parameters a_r and a_x are constant positive gains ($a_r = a_x = 20rad/s$).

We first simulate our CPG model and Ijspeert's model [15] when the phase biases are modified. We take the parameters $\upsilon = 1.0Hz, R_i = 0.5rad, X_i = 0$ for our CPG model, while the parameters $\omega_i = 2\pi rad/s, R_i = 0.5rad, X_i = 0(i = 1, 2, 3)$ and $w_{ij} = 5/s(i \neq j)$ for Ijspeert's model. The phase biases $(\varphi_{12}, \varphi_{13})$ change from $(-0.7, -1.6)rad$ to $(1.2, 0.7)rad$ at $t = 3s$ (resp. $t = 2.92s$) for our model (resp. Ijspeert's model). The reason we choose different changing time of $(\varphi_{12}, \varphi_{13})$ for two models is to make the change occur in the same position of the output waveforms for convenience of comparing the results. One can see that both of the two models converge to the new limit cycle smoothly and quickly (Figure 3.3). The results show that the performance of our CPG model within partially linearized oscillators is similar to that of Ijspeert's model [15] where more complicated differential equations are used.

3.3.2 Frequency variation

We then simulate the proposed CPG model when the frequency changes (Figure 3.4). In this experiment, we take $R_i = 0.5rad, X_i = 0(i = 1, 2, 3)$ and $(\varphi_{12}, \varphi_{13}) = (-0.7, -1.6)rad$. It is shown that when the frequency υ changes, the corresponding output is still continuous and smooth (Figure 3.4). It demonstrates the efficiency of the proposed CPG model when the frequency changes.

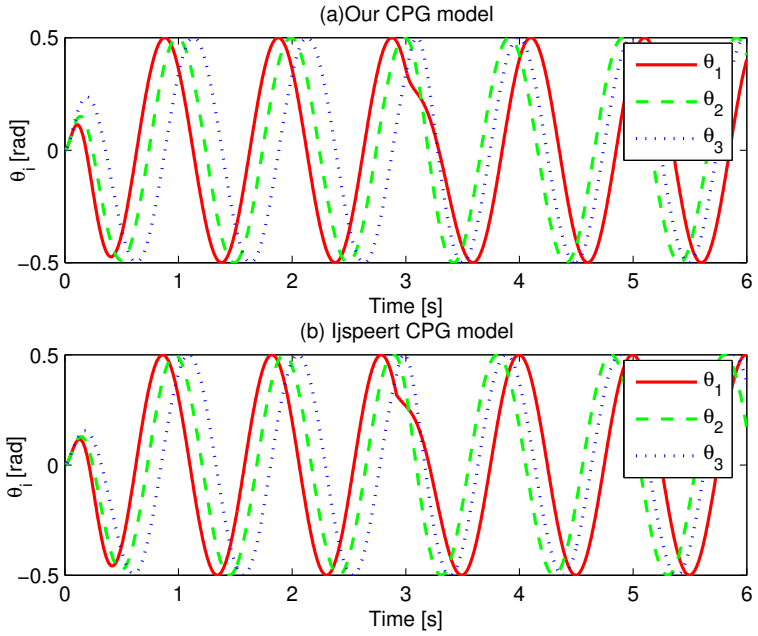

Figure 3.3: Comparing with Ijspeert's CPG model. (a) Output of our CPG model with the parameters $\upsilon = 1.0Hz, R_i = 0.5rad, X_i = 0$; (b) Output of the Ijspeert's model with the parameters values $\omega_i = 2\pi rad/s, R_i = 0.5rad, X_i = 0, a_r = a_x = 20rad/s (i = 1, 2, 3)$ and $w_{ij} = 5/s (i \neq j)$. The phase biases $(\varphi_{12}, \varphi_{13})$ change from $(-0.7, -1.6)rad$ to $(1.2, 0.7)rad$ at $t = 3s$ (resp. $t = 2.92s$) for our model (resp. Ijspeert's model).

3.3.3 Locomotion behaviors variation

Based on the designed transition layer, locomotion behaviors of the robotic fish are divided into two basic categories. (i) *Swimming forwards*: we set $\upsilon \in [0.5, 3]Hz$ and $X = 0$ so that the CPG model can generate the traveling wave from head to tail to make the robot swim forwards. (ii) *Turning*: we set $\upsilon \in [0.5, 3]Hz$ and $X \neq 0$ so that the robot turns. When $X > 0$ the robot turns right, and when $X < 0$ it turns left.

Based on the above basic categories, we try four typical locomotion behaviors to verify the performance of the CPG model: swimming forwards slowly, swimming forwards fast, turning right sharply and turning left gently(Figure 3.5). In the sequence shown in Figure 3.5, the CPG makes transitions in sequence following: swimming forwards fast ($0 \leq t \leq 4s$), swimming forwards slowly ($4 < t \leq 8s$), turning left gently ($8 < t \leq 12s$) and turning right sharply ($12 < t \leq 16s$). We gener-

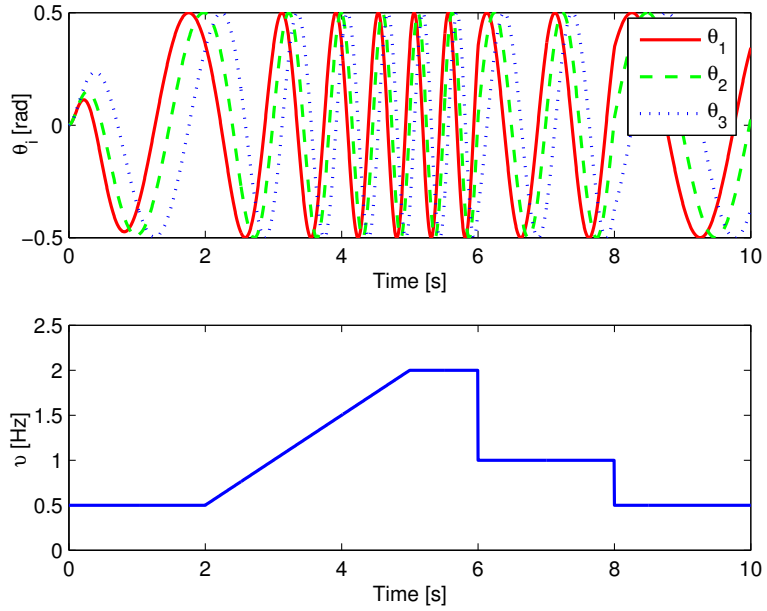

Figure 3.4: Output signals of the CPG model when the frequency changes.

ate different locomotion behaviors by changing the control commands υ and X, and then the specific control inputs of the CPG model (υ, R_i, X_i and φ_{ij}) are obtained by the designed transition layer. Although these parameters are changed abruptly, the output signals of all oscillators are still continuous and smooth.

Then some physical experiments are performed. The swimming forwards gait of the robotic fish is shown in Figure 3.6(a) with the control commands $\upsilon = 1.0Hz$ for speed and $X = 0$ for direction. When the control command X is not zero, the robotic fish will swim on a circle. The experiment results are shown in Figure 3.7(a). It is easy to see that the radius R monotonically increases when the command X changes from 0 to 1 rad. The smaller radius (R) results in the sharper turning. In Figure 3.7(a), it is shown that the sharpest turning is $R = 13.34cm$ (0.334 $body$ $lengths/s$) when $|X| = 1rad$. Figure 3.6(b) shows the turning gait of the robotic fish with the control commands $\upsilon = 1.0Hz$ for speed and $X = -0.5rad$ for direction. And the swimming trajectory of the robot is shown in Figure 3.7(b).

3.4 Conclusion

In this chapter, a novel CPG-based locomotion control method has been proposed and used for a robotic fish. The proposed CPG model, which is a system of coupled partially linearized oscillators, has some unique advantages. First, linear differential equations have been used instead of nonlinear ones to make the CPG model easy to be implemented. Second, the adaptive structural parameters have ensured satisfying dynamic performance. And explicitly presented parameters in the CPG model have brought clarity in applications. The experimental results have shown that our CPG model is well implemented in locomotion control of a three-joint robotic fish. We believe that our model could be applied to other biomimetic multi-joint underwater robots with link structures.

We are currently extending our work in the following directions. First, the stability performance of the locomotion has been ignored in this chapter because we choose the locomotion speed as the only optimization goal. We are testing some optimization methods to optimize the parameters for better stability and transient performance. Second, the optimization has been dependent on the experimental platform because the robotic fish has no sensor. Some pose sensors are being integrated into the robot body. Then the locomotion controller may be implemented on board, and on-line optimization can be applied which may be easier and faster to get the optimization goal. Third, the proposed CPG model is open-loop. Some posture information is being added as coupling terms to obtain a CPG with feedback. Finally, based on the designed transition layer, higher-level intelligent control methods such as neural network based control may be realized for the robotic fish.

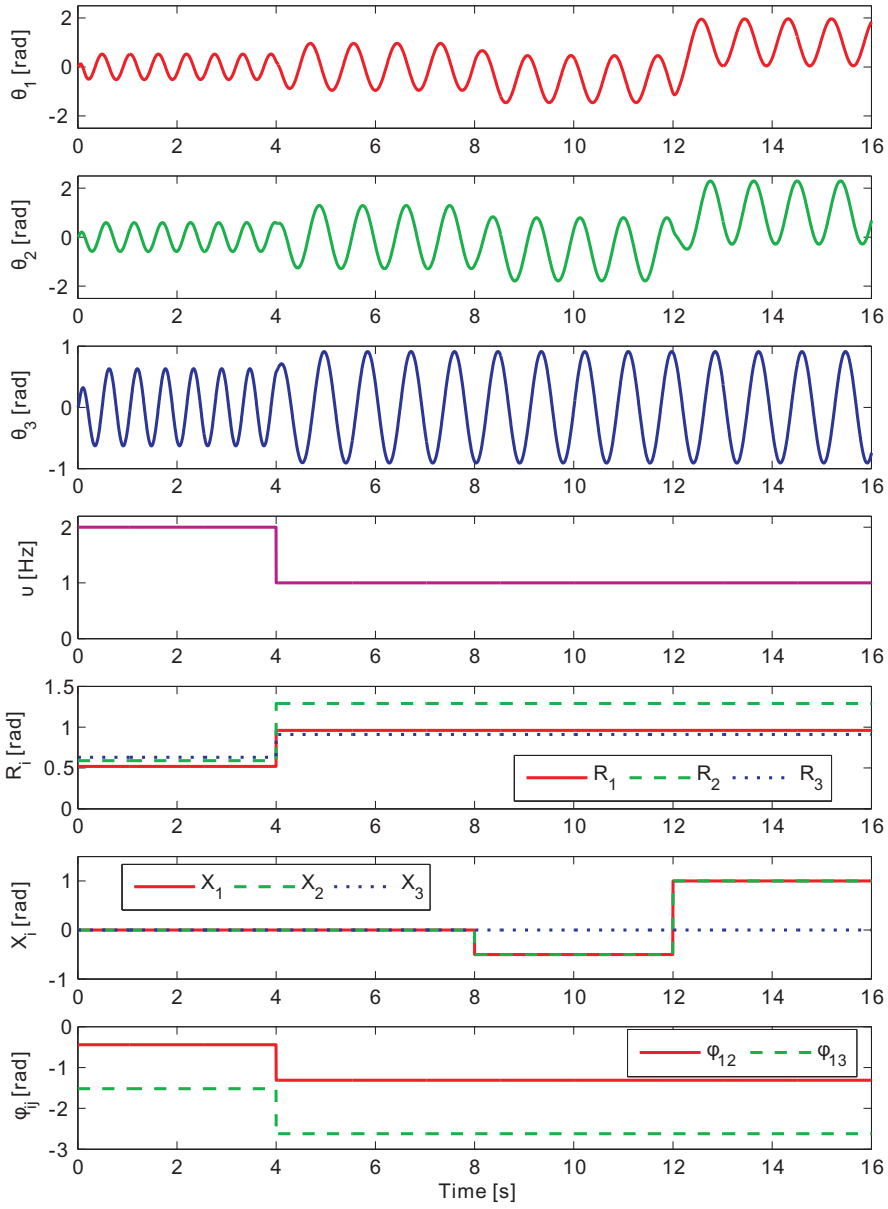

Figure 3.5: Sequence of different locomotion behaviors. The figure shows the output signals of our CPG model while the locomotion model is changing. See text for details.

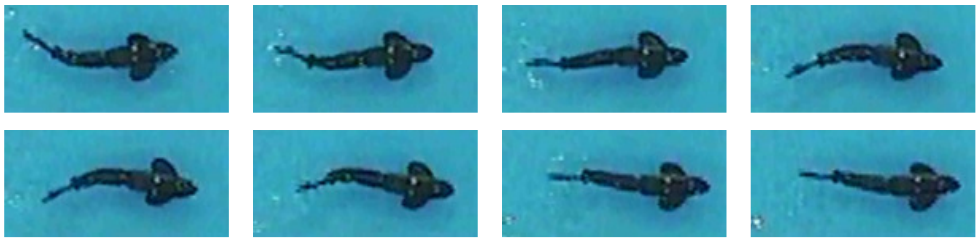

(a)

(b)

Figure 3.6: (From left to right, from top to bottom.) (a) The robotic fish is swimming forwards with the control commands $v = 1Hz$ and $X = 0$. The time step between the snapshots is $0.125s$. (b) The robotic fish is turning left at the control command for direction: $X = -0.5rad$. The control command for speed is set to $v = 1.0Hz$. The time step between the snapshots is $0.5s$.

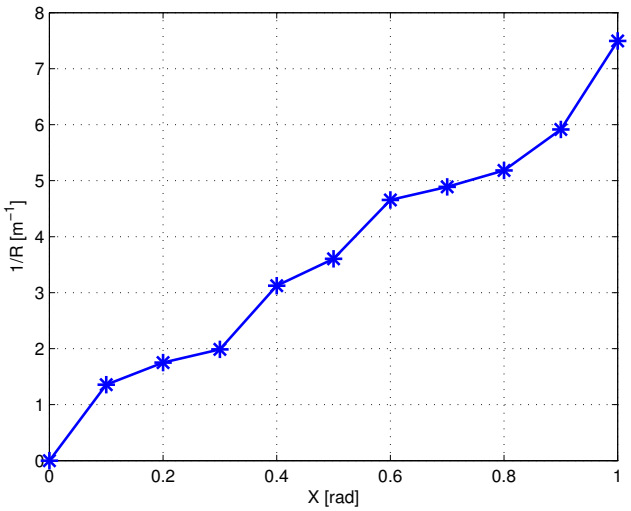

(a)

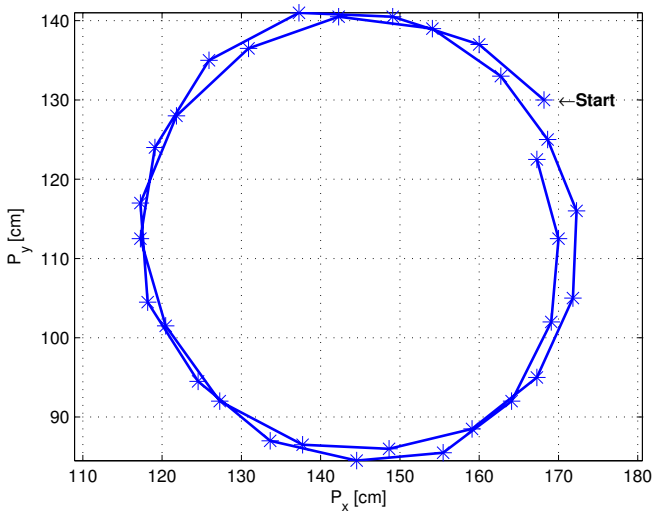

(b)

Figure 3.7: (a) Control of direction. Each data point is the average of 5 direction measurements. (b) Trajectory of the robot with the control commands $X = -0.5rad$ for direction and $v = 1.0Hz$ for speed. The position of the robot is obtained by the experimental platform per $0.4s$.

Chapter 4

Formation Swimming Control for Groups of Robotic Fish

This chapter proposes distributed control laws for formations of swimming robotic fish generating antiphase sinusoidal body waves. The control laws are inspired by the mathematical model for the hydrodynamics of schools of cruising fish, which reveals that fish swimming in diamond-shape formations with synchronized antiphase body waves can benefit greatly from energy saving. The phase dynamics of the body waves of the robotic fish are modeled by coupled Kuramoto oscillators and the stability analysis for the phase dynamics are carried out for coupling topologies corresponding to diamond-shape formations. It is proven that the body waves can be synchronized in specific antiphase patterns. Simulations and experiments further validate the effectiveness of the proposed control laws.

4.1 Coupled oscillator model for robotic fish

Following the research line developed in the previous chapter, the propulsion of each robotic fish is achieved through generating a traveling wave traversing the robotic fish's body towards the tail. The traveling wave ([45]) can be described by

$$y(x,t) = (c_1 x + c_2 x^2)\sin(kx + \omega t + \theta_0) \tag{4.1}$$

where x denotes the displacement along the main axis that starts at the first joint and points towards the opposite direction of motion, y is the body displacement with respect to the axis, c_1 and c_2 are the constants for the amplitude of the envelope of the traveling wave, k is a constant called the body wave number, ω is the body wave frequency, θ_0 is the initial phase and $\omega t + \theta_0$ is the phase. In the sequel, we use θ to denote $\omega t + \theta_0$. An illustrative drawing is shown below.

Obviously, the hydrodynamics that the robotic fish generates are mainly determined by the amplitude and phase of the traveling wave, which, in fact, can be controlled by implementing the CPG-based model [79]. We have discussed in Chapter 3 how to control the three joints once the desired values of the amplitude and phase

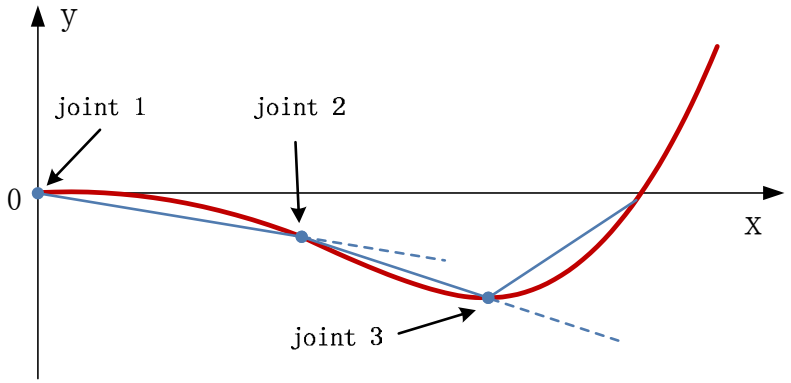

Figure 4.1: Three links connected by revolute joints that generate traveling waves.

of the body wave are set. In this chapter, we are less concerned with the lower level control to adjust the motors at the three joints to obtain a desired body wave, but rather concentrate on how to find the desired values of the phases of the body waves of the robotic fish in a formation such that the collective hydrodynamics of the formation of robotic fish to the advantage of the fish to swim forward.

For the sake of clarity of analysis, we assume that the traveling waves associated with all the robotic fish are identical except that they may have different phases. In other words, the parameters c_1, c_2 and k in (4.1) are all the same for all robotic fish. The setting can be further idealized by assuming that the frequencies ω of all the robotic fish are also the same. We will show in Section 4.3 that such simplifying assumptions are meaningful and can help us gain insight into how robotic fish can be coordinated together by just focusing on the key determining factor of their phase dynamics. Consequently the only state that we need to control is θ. Consider a formation of n robotic fish labeled by $1, \ldots, n$. Then the dynamics of the phase of robotic fish i, $1 \leq i \leq n$, are

$$\dot{\theta}_i = \omega + u_i \tag{4.2}$$

where u_i is the control input. So the aim of this chapter is to design the distributed control law u_i such that the collective dynamics of the formation of robotic fish may evolve into a "desirable" equilibrium and here by the *desirable* dynamics we mean the collective behaviors that have been proven to be advantageous through mathematical modeling for schools of real fish in nature. Note that system (4.2) itself has the form of the dynamics of coupled oscillators with the phases as the system's state.

4.2 Antiphase synchronization in diamond-shape formations

It was reported and analyzed in [80, 81] and [69] that fish swimming in elongated diamond-shape formations can save locomotion energies by up to 20%. The main ideas of the explanation are as follows. Each swimming fish sheds vortices behind its body. Now consider the vortex streets behind a column of fish swimming parallel to each other as shown in Fig. 4.2, the fish that is swimming laterally midway behind the two fish in the column that is immediately in front of it can utilize the favorable flow at the sides of the vortex streets. This hydrodynamical advantage is strengthened when the phases of the body waves of the neighboring fish differ by π, i.e. the body waves of these fish are antiphase synchronized. This leads to the

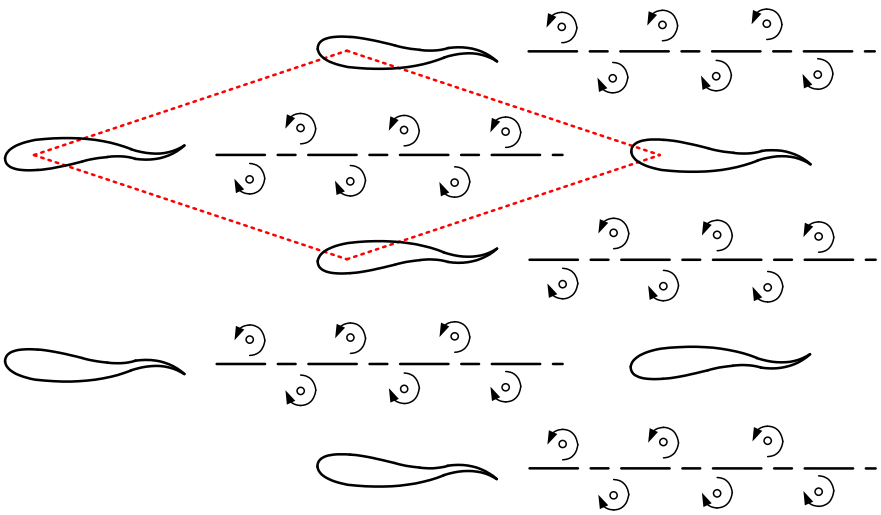

Figure 4.2: Fish swimming in elongated diamond-shape formations with neighboring fish being synchronized in antiphase (Adapted from [81]).

fact that the elongated diamond-shape patterns with antiphase synchronized body waves are preferred basic structure for cruising fish schools. Hence, the goal of this section is to design u_i in (4.2) utilizing only the information of the phases of robotic fish i's neighbors in the diamond-shape formation topologies such that when the relative positions of the robotic fish have been determined by elongated diamond-shape building blocks, one can guarantee that the body waves of the neighboring fish in the same column of the diamond formation are antiphase synchronized and

as a result the formation of robotic fish can maintain the elongated diamond-shape patterns and fully utilize the benefit of energy saving from the collective hydrodynamics of the robotic fish formation.

4.2.1 Control law

For a real fish in a diamond-shape fish school, the phases of its adjacent fish can be acquired through visual information by eyes and fluid pressure information by lateral lines. Usually one side of the vision is preferred than the other (namely the two eyes have asymmetric sensing capabilities), so only that adjacent fish that is on the preferred side is taken as the fish's neighbor ([69]); on the other hand, there is usually no preferences between the lateral lines on the two sides of the body, so both of those two fish that are adjacent in the same column are the fish's neighbors. Hence, in this biological model a fish may have at most three neighbors in the school. To mimic the neighbor relationships in real fish schools, we adopt the same local rule of picking neighbors in the model of real fish school for the robotic fish formation. For robotic fish i, let $\mathcal{N}_i$ denote the set of indices of its neighbors. Then there are at most three elements in $\mathcal{N}_i$. Here, without loss of generality, a robotic fish always takes the front left adjacent robotic fish (if there is one) as its neighbor instead of the one on the front right, although these two have similar distances to this robotic fish. This particular choice of neighbors turns out to be key in proving stability in Section 4.2.2.

Let graph $\mathbb{G}$ with vertex set $\mathcal{V} = \{1, \ldots, n\}$, where vertex i in the graph corresponds to robotic fish i in the formation, be the graph associated with the diamond-shape robotic fish formation describing the neighbor relationships. Then for $i, j \in \mathcal{V}$, there is a directed edge (i, j) in the edge set $\mathcal{E}$ of $\mathbb{G}$ if and only if $i \in \mathcal{N}_j$. For clarity of expression, we denote the robotic fish formation by $\mathbb{F}$. We emphasize below two facts about the edges of $\mathbb{G}$ that are inherited from the properties of neighbor relationships in $\mathbb{F}$.

1. If (i, j) is an edge in $\mathbb{G}$ and i, j are in the same column of $\mathbb{F}$, then (j, i) is also an edge in $\mathbb{G}$. This is due to the fact that the neighbor relationships in the same columns of $\mathbb{F}$ are symmetric.

2. If (i, j) is an edge in $\mathbb{G}$ and i, j are in different columns of $\mathbb{F}$, then (j, i) is *not* an edge of $\mathbb{G}$. This is due to the fact that the neighbor relationships in different columns of $\mathbb{F}$ are asymmetric.

We say that a graph is *connected* if each of its vertices can reach every other vertex and that a graph *contains a spanning tree* if there is a vertex in the graph that can reach all the other vertices.

After clarifying the neighbor relationships in $\mathbb{F}$ and defining the graph $\mathbb{G}$, we are ready to present the control law that is used in this chapter:

$$u_i = \sum_{j \in \mathcal{N}_i} \sin(\theta_i - \theta_j), \qquad i = 1, \ldots, n. \tag{4.3}$$

This control law is in the form of the coupling terms in the Kuramoto model for oscillators coupled through sinusoidal signals ([1]). The Kuramoto model has been studied intensively in the past two decades mainly to study the *in-phase* synchronization behavior where, in the case of all the oscillators having the same frequency, the phases of all the oscillators become the same asymptotically. Recently oscillator models have been used to stabilize different patterns of collective motion for multi-agent systems ([55]). In this chapter, to study the behavior of the phase dynamics of robotic fish formation $\mathbb{F}$, we are in fact exploring the stability properties of coupled Kuramoto oscillators with a specific local neighbor relationship graph $\mathbb{G}$ and with respect to a specific type of equilibrium point corresponding to the "antiphase synchronization". Here, we say that a connected network of coupled oscillators has reached *antiphase synchronization* if any pair of neighboring oscillators has a phase difference of $2k\pi + \pi$ for some integer k.

4.2.2 Stability analysis

Denote the number of columns in $\mathbb{F}$ by a positive number m. Let $\mathbb{F}_i$, $1 \leq i \leq m$, denote the sub-formation in $\mathbb{F}$ that corresponds to the ith column from the front. Correspondingly let graph $\mathbb{G}_i$ be the subgraph of $\mathbb{G}$ associated with $\mathbb{F}_i$. Denote the number of elements in $\mathcal{V}_i$ by l_i, and thus $l_1 + \cdots + l_m = n$. We label the robotic fish in $\mathbb{F}$ following the rule that a fish in the front always has a smaller index than another in the back and if two fish are in the same column, and the one on the left always has a smaller index than the one on the right. Hence, the fish in $\mathbb{F}_1$, from the left to right, are assigned with indices $1, \ldots, l_1$, those in $\mathbb{F}_2$ with indices $l_1 + 1, \ldots, l_1 + l_2$, and so on.

Note that as a standard procedure by a simple argument using coordinate transformation, the systems

$$\dot{\theta}_i = \omega + \sum_{j \in \mathcal{N}_i} \sin(\theta_i - \theta_j), \qquad i = 1, \ldots, n \tag{4.4}$$

and

$$\dot{\theta}_i = \sum_{j \in \mathcal{N}_i} \sin(\theta_i - \theta_j), \qquad i = 1, \ldots, n \tag{4.5}$$

have the same stability properties. In the sequel, we take (4.5) to be the system of interest.

It is easy to check that there is no edge in $\mathbb{G}$ that starts from a vertex in $\bigcup_{i=2}^{m} \mathbb{G}_i$ and ends at a vertex in $\mathbb{G}_1$. So the phase dynamics of the robotic fish in $\mathbb{F}_1$ are not influenced by the robotic fish in $\bigcup_{i=2}^{m} \mathbb{F}_i$. This motivates us to study the collective phase dynamics of $\mathbb{F}_1$ first.

4.2.1. PROPOSITION. *For almost all initial phase configurations and all $l_1 > 1$, the phases of the robotic fish in $\mathbb{F}_1$ reach antiphase synchronization asymptotically if $\mathbb{G}_1$ is connected.*

To prove this proposition, we first look at the possible equilibrium points of the system. Let

$$\mathcal{E}_1 \triangleq \left\{ \begin{bmatrix} \theta_1 & \dots & \theta_{l_1} \end{bmatrix}^T \in \mathbb{R}^{l_1} \mid (\theta_i - \theta_{i+1}) \bmod \pi = 0, \qquad i = 1, \dots, l_1 - 1 \right\}.$$

Then it is easy to check the following result based on which we will get the main conclusion of this chapter later.

4.2.2. LEMMA. *When $\mathbb{G}_1$ is connected, the set of all the equilibrium points of the phase dynamics of $\mathbb{F}_1$ is $\mathcal{E}_1$.*

It can be further checked that the antiphase synchronized state is in $\mathcal{E}_1$.

4.2.3. LEMMA. *When $\mathbb{F}_1$ reaches antiphase synchronization, it is at an equilibrium point in $\mathcal{E}_1$.*

Proof of Proposition 4.2.1: For the phases θ_i and θ_j, we define the distance between them to be

$$d_{ij} \triangleq \sin^2 \frac{\theta_i - \theta_j}{2}.$$

Let D denote the sum of the distances between all pairs of neighboring robotic fish in $\mathbb{F}_1$

$$D \triangleq \sum_{i \in \mathcal{V}_1} \sum_{j \in \mathcal{N}_i} d_{ij}.$$

Then for $\mathbb{F}_1$ with a connected $\mathbb{G}_1$, D can be further written as

$$D = 2 \sum_{i=1}^{l_1 - 1} \sin^2 \frac{\theta_i - \theta_{i+1}}{2} = \sum_{i=1}^{l_1 - 1} [1 - \cos(\theta_i - \theta_{i+1})] \geq 0,$$

which reaches its maximum

$$D_{\max} = 2l_1 - 2$$

when $(\theta_i - \theta_{i+1}) \bmod 2\pi = \pi$ for all $1 \leq i < l_1$. Consider the following Lyapunov function

$$V \triangleq 2l_1 - 2 - D. \tag{4.6}$$

Then V reaches its minimum zero when $D = D_{\max}$ in which case $\mathbb{F}_1$ reaches antiphase synchronization. Furthermore,

$$\dot{V} = -\sum_{i=1}^{l_1-1} \dot{\theta}_i^2 \leq 0$$

where the equality signs holds if and if only if $\begin{bmatrix}\theta_1 & \dots & \theta_{l_1}\end{bmatrix}^T \in \mathcal{E}_1$. Since the antiphase synchronized state corresponds to the unique global minimum of V and in view of Lemma 4.2.3, we know that the antiphase synchronized state is asymptotically stable.

Let $\overline{\mathcal{E}}_1$ denote the subset of $\mathcal{E}_1$ that contains all the equilibrium points not corresponding to antiphase synchronization. To show further that for almost all initial conditions, the phases of $\mathbb{F}_1$ can be antiphase synchronized, it suffices to show that all the equilibrium points in $\overline{\mathcal{E}}_1$ are not stable. For any $\bar{\theta} \triangleq \begin{bmatrix}\bar{\theta}_1 & \dots & \bar{\theta}_{l1}\end{bmatrix}^T \in \overline{\mathcal{E}}_1$, one can always find $1 \leq i < l_1$ such that $(\bar{\theta}_i - \bar{\theta}_{i+1}) \bmod 2\pi = 0$. Although $V(\bar{\theta}) = 0$, the value of V always decreases if we perturb $\bar{\theta}$ in a direction that changes the difference between $\bar{\theta}_1$ and $\bar{\theta}_2$. Hence, $\bar{\theta}$ cannot be stable. □

After investigating the stability of the antiphase synchronized state of the subformation $\mathbb{F}_1$, we continue to look at the stability of the phase dynamics of the overall formation $\mathbb{F}$.

Let

$$\theta \triangleq \begin{bmatrix}\theta_1 & \cdots & \theta_n\end{bmatrix}^T. \tag{4.7}$$

We define the set of antiphase states $\mathcal{E}^*$ to be

$$\mathcal{E}^* \triangleq \{\theta \mid (\theta_i - \theta_j) \bmod 2\pi = \pi,\ i = 1, \dots, n \text{ and } j \in \mathcal{N}_i\}. \tag{4.8}$$

We first examine the local stability of $\mathcal{E}^*$ using the linearization technique.

4.2.4. THEOREM. *When $\mathbb{G}$ contains a spanning tree, any point in $\mathcal{E}^*$ is locally stable.*

Proof: We linearize system (4.5) at any point $\theta^* \in \mathcal{E}^*$:

$$\dot{\theta} = -L(\theta - \theta^*)$$

where L is the Laplacian matrix of graph $\mathbb{G}$. Since $\mathbb{G}$ contains a spanning tree, from the existing result [59] we know that L has a simple zero eigenvalue and all its other eigenvalues are strictly positive. We define an $(n-1)$-dimensional column vector $\widetilde{\theta} \triangleq \begin{bmatrix}\theta_1 - \theta_2 & \cdots & \theta_{n-1} - \theta_n\end{bmatrix}^T$. Then we have

$$\begin{bmatrix} \widetilde{\theta} \\ \theta_n \end{bmatrix} = \begin{bmatrix} \theta_1 - \theta_2 \\ \theta_2 - \theta_3 \\ \vdots \\ \theta_{n-1} - \theta_n \\ \theta_n \end{bmatrix} = U\theta$$

where

$$U = \begin{bmatrix} 1 & -1 & 0 & \dots & 0 \\ 0 & 1 & -1 & \dots & 0 \\ \vdots & \vdots & \ddots & \ddots & \vdots \\ \vdots & \vdots & \dots & 1 & -1 \\ 0 & 0 & \dots & 0 & 1 \end{bmatrix},$$

and one can further have

$$U^{-1} = \begin{bmatrix} 1 & 1 & \dots & \dots & 1 \\ 0 & 1 & 1 & \dots & \vdots \\ \vdots & \vdots & \ddots & \ddots & \vdots \\ \vdots & \vdots & \dots & 1 & 1 \\ 0 & 0 & \dots & 0 & 1 \end{bmatrix}.$$

One can easily check that it holds for the system after linearization that

$$\begin{bmatrix} \dot{\widetilde{\theta}} \\ \dot{\theta_n} \end{bmatrix} = -A \begin{bmatrix} \widetilde{\theta} - \widetilde{\theta}^* \\ \theta_n - \theta_n^* \end{bmatrix}$$

where $\widetilde{\theta}^*$ is defined as $\begin{bmatrix}\theta_1^* - \theta_2^* & \cdots & \theta_{n-1}^* - \theta_n^*\end{bmatrix}^T$ and

$$A = ULU^{-1}.$$

It implies that A and L have the same eigenvalues. Moreover, the last column of A can be calculated by

$$\begin{bmatrix} \sum_{j=1}^{n}(l_{1j}-l_{2j}) & \sum_{j=1}^{n}(l_{2j}-l_{3j}) & \dots & \sum_{j=1}^{n}(l_{n-1,j}-l_{nj}) & \sum_{j=1}^{n} l_{nj} \end{bmatrix}^T = \begin{bmatrix} 0 & 0 & \dots & 0 \end{bmatrix}^T,$$

since that the sum of each row of the Laplacian matrix $L = [l_{ij}]$ is equal to zero. Thus the matrix A can be written as

$$A = \left[\begin{array}{c|c} & 0 \\ \widetilde{A} & \vdots \\ & 0 \\ \hline * & 0 \end{array}\right].$$

It follows that

$$\dot{\widetilde{\theta}} = -\widetilde{A}(\widetilde{\theta} - \widetilde{\theta}^*),$$

and $\widetilde{A}$ is the projection matrix that projects $\mathbb{R}^n$ to the eigenspace of all the nonzero eigenvalue of the Laplacian matrix L. Hence, all the eigenvalues of $\widetilde{A}$ are positive and thus $\widetilde{\theta}$ converges to $\widetilde{\theta}^*$. So we have proved that θ^* is stable. Since this holds for any θ^* in $\mathcal{E}^*$, we arrive at the conclusion. □

In view of the almost global convergence result in Proposition 4.2.1 for the subformation $\mathbb{F}_1$, we want to study the global stability of $\mathcal{E}^*$.

4.2.5. THEOREM. *For almost all initial phase configurations, the phases of the robotic fish in $\mathbb{F}$ reach antiphase synchronization asymptotically if $\mathbb{G}$ contains a spanning tree.*

Proof: We prove by induction. As shown in Proposition 4.2.1, the robotic fish in $\mathbb{F}_1$ can reach antiphase synchronization. Now we look at the phase dynamics of the fish in $\mathbb{F}_2$. For $i \in \mathcal{V}_2$, we define the distance between phases θ_i and θ_j, $j \in \mathcal{N}_i$, to be

$$d_{ij} \triangleq \begin{cases} \sin^2 \frac{\theta_i - \theta_j}{2} & \text{when } j \in \mathcal{V}_2 \\ 2\sin^2 \frac{\theta_i - \theta_j}{2} & \text{when } j \in \mathcal{V}_1 \end{cases}.$$

Let D denote the sum of the distances between all pairs of neighboring robotic fish in $\mathbb{F}_2$ and with their neighbors in $\mathbb{F}_1$

$$D \triangleq \sum_{i \in \mathcal{V}_2} \sum_{j \in \mathcal{N}_i} d_{ij}.$$

Then for $\mathbb{F}_2$, D can be further written as

$$D = \sum_{i \in \mathcal{V}_2} \sum_{j \in \mathcal{N}_i, j \in \mathcal{V}_2} \sin^2 \frac{\theta_i - \theta_j}{2} + 2 \sum_{i \in \mathcal{V}_2} \sum_{j \in \mathcal{N}_i, j \in \mathcal{V}_1} \sin^2 \frac{\theta_i - \theta_j}{2} \geq 0,$$

which reaches its maximum

$$D_{max} = h_1 + 2h_2$$

when the phases of each robotic fish in $\mathbb{F}_2$ are antiphase synchronized with respect to all its neighbors, where h_1 is the number of the edges in column 2 of $\mathbb{F}$ and h_2 is the number of the edges from column 1 to column 2. Considering the following Lyapunov function

$$V \triangleq h_1 + 2h_2 - D.$$

Then V reaches its minimum zero when $D = D_{\max}$ in which case $\mathbb{F}_2$ reaches antiphase synchronization. Furthermore,

$$\dot{V} = -\sum_{i \in \mathcal{V}_2} \dot{\theta}_i^2 \leq 0$$

where the equality signs holds if and if only if $(\theta_i - \theta_j) \mod \pi = 0$ for all $i \in \mathcal{V}_2, j \in \mathcal{N}_i$. Since the antiphase synchronized state corresponds to the unique global minimum of V and in view of Lemma 4.2.3, we know that the antiphase synchronized state is asymptotically stable. Using the argument similar to that in the proof of Proposition 4.2.1, for any equilibrium points $\bar{\theta}$, which are not corresponding to antiphase synchronization, one can always check that the value of V always decreases if we perturb $\bar{\theta}$ in a direction although $V(\bar{\theta}) = 0$. Hence $\bar{\theta}$ cannot be stable. So we have proved that the phase of each robotic fish in $\mathbb{F}_2$ are antiphase synchronized with respect to all its neighbors. Thus the robotic fish in $\mathbb{F}_1 \cup \mathbb{F}_2$ can reach antiphase synchronization. Now we assume that for any $1 < p < m$, the robotic fish in $\bigcup_{i=1}^{p} \mathbb{F}_i$ can reach antiphase synchronization. Then one can again check that the only possible stable equilibrium points for $\mathbb{F}_{p+1}$ are those corresponding to the case when the phases of all robotic fish in $\mathbb{F}_{p+1}$ are antiphase synchronized with respect to all its neighbors. So using the argument similar to that in the proof of Proposition 4.2.1 again, one can shown that all the robotic fish in $\bigcup_{i=1}^{p+1}$ can reach antiphase synchronization. This completes the proof. □

In the next section, we carry out simulations and experiments to verify the theoretical results that we have obtained in this section.

4.3 Simulations and experiments

We first simulate the phase dynamics of a formation of fourteen robotic fish as shown in Fig. 4.3. The initial phases take random values in $[0, 2\pi)$. The phases of the robotic fish, without considering the shared ωt term, are presented in Fig. 4.4 and the phase differences for all pairs of neighboring robotic fish are shown in Fig. 4.4 as well. The results show that the robotic fish school swimming in diamond-shape formations can achieve antiphase synchronization under the proposed phase control law.

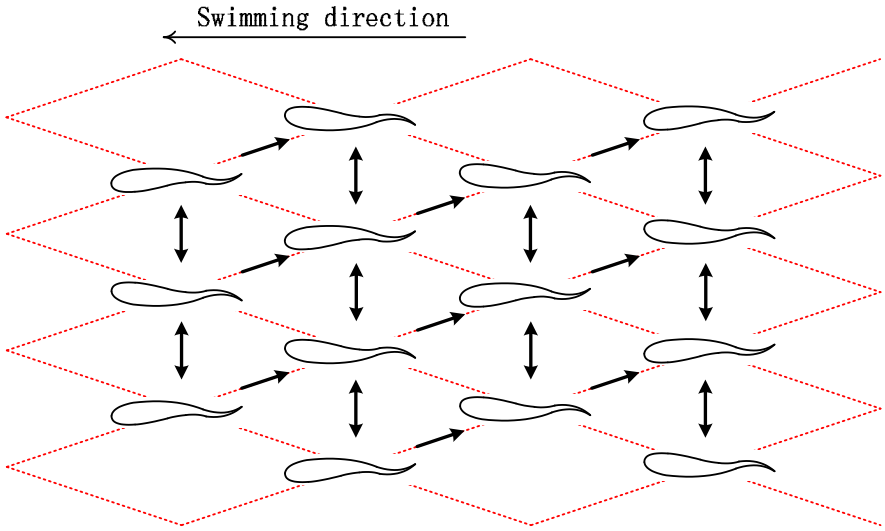

Figure 4.3: A formation of fourteen robotic fish.

We further test the proposed phase control law using two robotic fish that have been introduced in Chapter 2. The lower lever control of an individual robotic fish, which aims to generate the desired traveling wave for swimming, has been discussed in Chapter 3.

To implement our phase control law (4.3), we modify the CPG model proposed in Chapter 3 and describe it by the diagram in Fig. 4.5. The detailed equations for

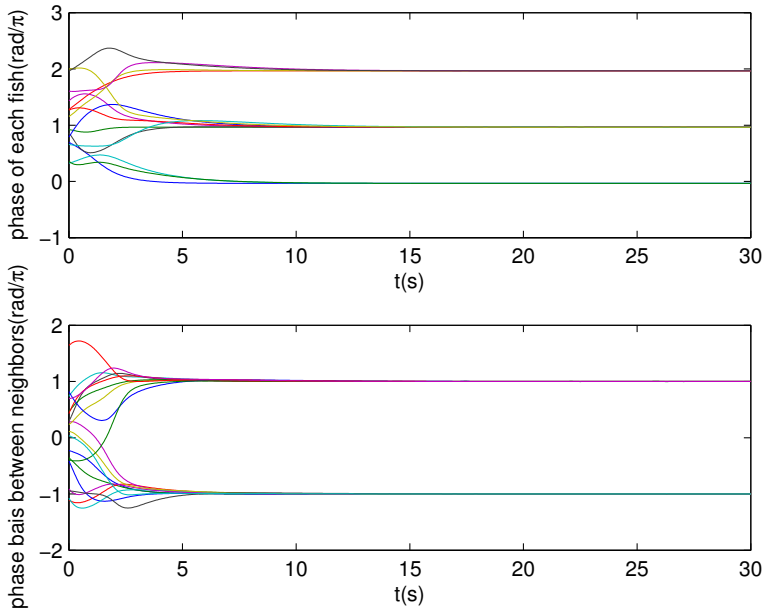

Figure 4.4: The phases and phase differences of the robotic fish formation.

such a modified CPG model can be written as follows:

$$
\begin{aligned}
\ddot{r}_{im} &= \alpha[\alpha(R_{im} - r_{im}) - 2\dot{r}_{im}], \text{ for } m = 1,2,3 \\
\ddot{x}_{im} &= \beta[\beta(X_{im} - x_{im}) - 2\dot{x}_{im}], \text{ for } m = 1,2,3 \\
\ddot{\phi}_{im} &= \sum_{l=1,l\neq m}^{3} \mu[\mu(\phi_{il} - \phi_{im} - \varphi_{iml}) - 2(\dot{\phi}_{im} - \omega_{im})], \\
&\quad \text{for } m = 2,3 \\
\ddot{\phi}_{i1} &= \sum_{l=2,3} \mu[\mu(\phi_{il} - \phi_{i1} - \varphi_{i1l}) - 2(\dot{\phi}_{i1} - \omega_{im} \\
&\quad -\gamma \sum_{j\in\mathcal{N}_i} \sin(\phi_{i1} - \phi_{j1}))] \\
y_{im} &= x_{im} + r_{im}\cos(\phi_{im}), \text{ for } m = 1,2,3
\end{aligned}
\tag{4.9}
$$

Here, $r_{im}(t)$, $x_{im}(t)$ and $\phi_{im}(t)$ are the amplitude, the offset and the phase of the mth joint of the ith robotic fish at time t respectively. $y_{im}(t)$ are the desired deflection angle of the mth joint of the ith robotic fish at time t. The parameters ω_{im},

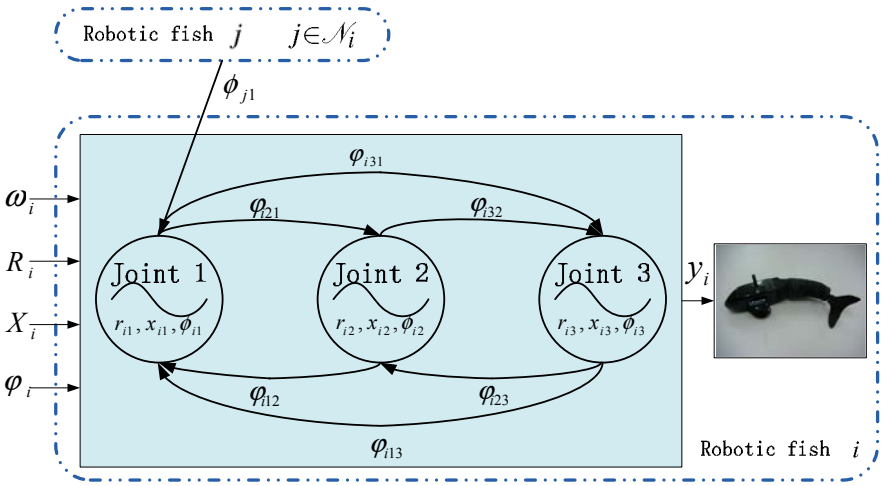

Figure 4.5: Diagram of CPG-based locomotion control architecture.

R_{im} and X_{im} are the desired frequency, amplitude and offset of the mth joint of the ith robotic fish respectively. The parameter φ_{iml} are the desired phase difference between joints m and l of the ith robotic fish. Finally, α, β, μ and γ are structural parameters that affect the transient dynamics. As we have mentioned above, the CPG-based model is used to generate the desired traveling wave for each robotic fish. Note that the coupling $-\gamma \sum_{j\in\mathcal{N}_i} \sin(\phi_{i1} - \phi_{j1})$ is used for antiphase synchronization. We choose the parameters $\omega_{im} = 4.69rad/s$, $R_{i1} = 0.26rad$, $R_{i2} = 0.44rad$, $R_{i3} = 0.52rad$, $\varphi_{i12} = -1.33rad$, $\varphi_{i13} = -1.85rad$ ($m = 1, 2, 3$ and $i = 1, 2$), $\alpha = \beta = 8.72/s$, and $\mu = 4.36/s$ for both of the two robotic fish, then both of them performs the behavior of swimming forwards. Additionally, we set $\gamma = 1.5/s$ to couple the phases of body waves of the robotic fish. We run the above detailed robotic fish model through simulations and experiment with the initial conditions $\phi_{i1}(0) = 2.79rad, \phi_{i2}(0) = 2.88rad$, namely the two robotic fish start swimming almost in-phase. The controllers are activated at the time instance 2s. For the simulations, we show in Fig. 4.6 both the phases of the six joints of the two robotic fish and the phase differences between the first joints. The snapshots during the experiment are provided in Fig. 4.7. The data collected per 0.2s from the experiment are shown in Fig. 4.8 where we present the phases of the first joints and the phase difference of the first joints.

The results of simulations and experiment show that the two robotic fish can

achieve antiphase synchronization using the proposed phase control law together with our CPG-based model. In Fig. 4.8, the final value of phase differences is not exactly equal to π because of the low-precision data format we have used to reduce the communication cost.

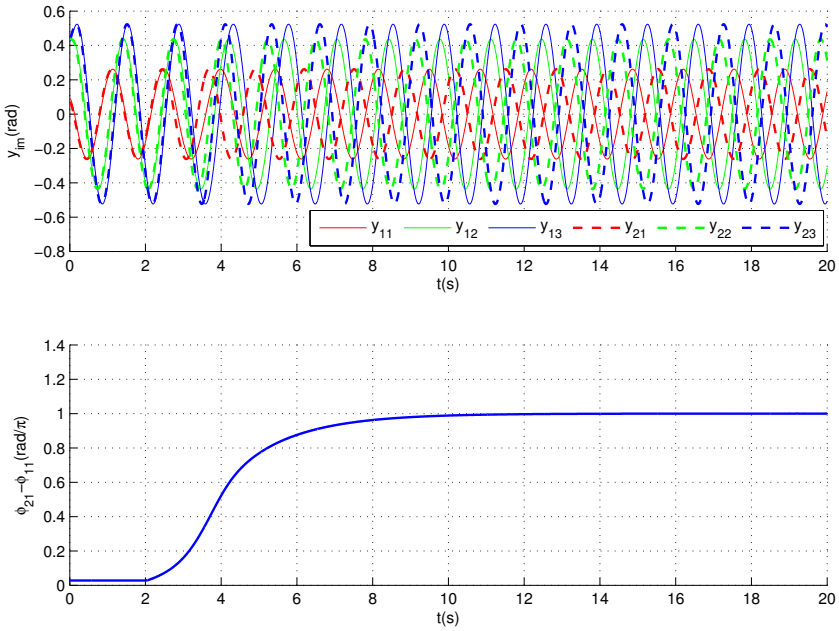

Figure 4.6: Two simulated robotic fish in the antiphase synchronization process.

4.4 Conclusion

We have shown an effective antiphase synchronization strategy in the form of the coupled Kuramoto model that can coordinate the body waves of a formation of swimming robotic fish. While the achieved antiphase body waves of the neighboring robotic fish have a clear biological explanation from the existing theoretical hydrodynamical models for fish school swimming in nature, much more questions remain to be answered. For example, we are interested in what the best combination of the parameters are for lower level motor control such that the best antiphase

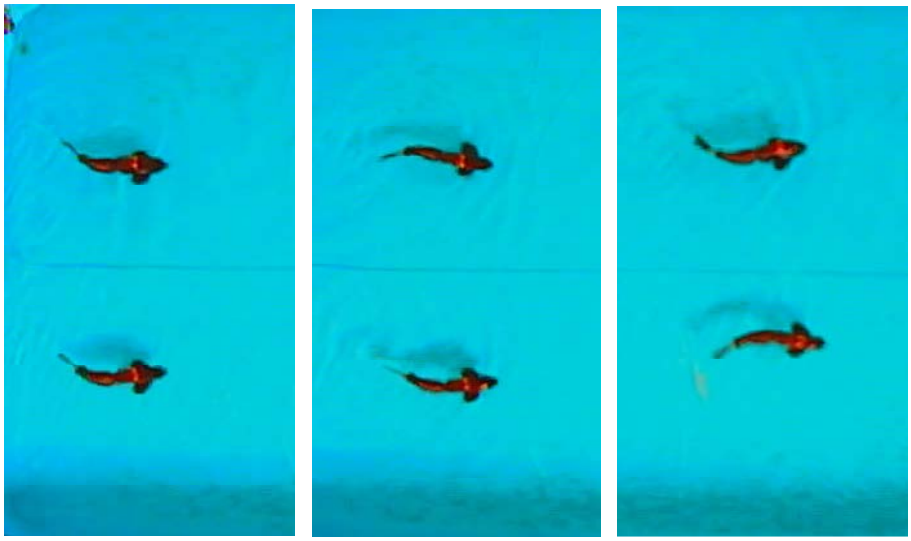

(a) t=2s (b) t=8s (c) t=14s

Figure 4.7: Snapshots of the experiment.

body waves can be achieved in terms of the energy efficiency.

We are also exploring to study a more comprehensive coordination control strategy that considers not only the phase dynamics but the amplitudes and frequencies of the oscillator model as well. Although by relying on a lower level CPG-type of strategy we have obtained an acceptable performance of the robotic fish decoupling the phase dynamics from the rest, a joint consideration of all aspects of the robotic fish motion dynamics that may affect their interactions in water is of a clear advantage. The main challenge in such a comprehensive study lies in the possible complicated analysis for fluid dynamics that are related to the motion of robotic fish.

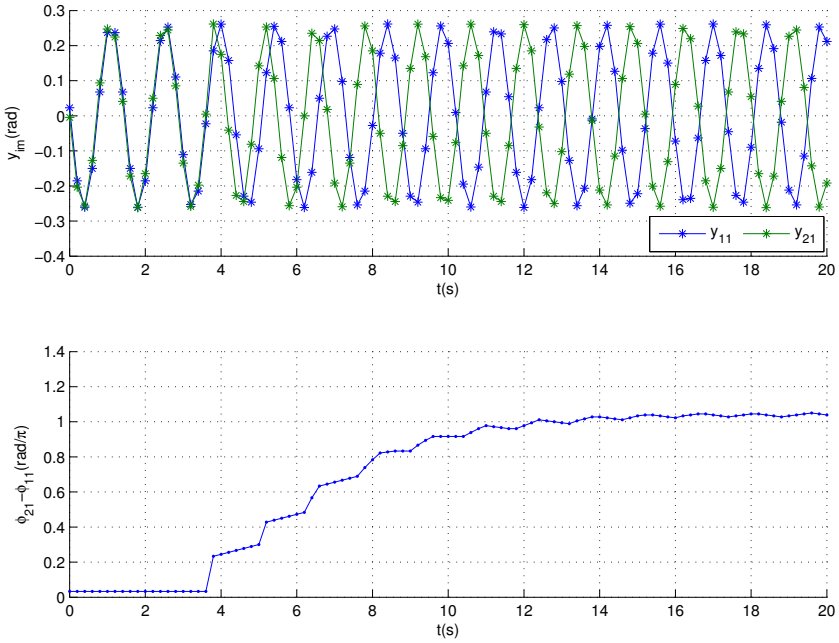

Figure 4.8: Two robotic fish in the antiphase synchronization process.

Chapter 5

Coordination Control in Multi-robotic Fish Systems

In this chapter, using game theoretic ideas, we propose a modified snowdrift game to study the emergence and evolution of cooperation among robots in multi-robot water polo matches [29, 72]. We first formulate a game setting in which groups of robots play matches repeatedly that are modeled by modified snowdrift games. Then by introducing a cooperation coefficient we investigate how evolutionary stability is affected by cooperation efficiency through replicator dynamics in infinite populations. We identify evolutionarily stable strategies (ESS) under different fixed values of the cooperation coefficient. We further study the co-evolution of the cooperation efficiency with game dynamics using simulations of Fermi processes in finite populations. It is found that the cooperation efficiency improves when robots are capable to learn [78].

5.1 Modified snowdrift game

5.1.1 Problem formulation

We consider a simplified scenario in robotic water polo matches, in which the team of players under study cares only scoring more goals without paying attention to the defense. We assume all the players of the team are equipped with the same hardware and software. The match is played in repeated rounds and in each round there are two field players from the team who may choose to or not to shoot. The strategies can be described in a game theoretic setting as follows: strategy C, to cooperate, is to shoot while strategy D, to defect, is to wait for the other teammate to shoot. The base game can then be described by a two-player, two-strategy symmetric game, whose payoff matrix M is

$$M = \begin{array}{c} \\ C \\ D \end{array} \begin{array}{c} \begin{array}{cc} C & D \end{array} \\ \begin{pmatrix} b-kc & b-c \\ b & 0 \end{pmatrix} \end{array}, \tag{5.1}$$

where b is the benefit when at least one player shoots because of the potential to score, c is the cost of shooting alone, and $k > 0$ is a parameter, we call which the *cooperation coefficient*, introduced to quantify the synergy effect between the two players. Here we assume $b > c > 0$. When both of the two players opt for C, each of them shares the cost c discounted by the cooperation coefficient k. So smaller k implies higher cooperation efficiency and thus greater synergy effects. We assume there is a broadcasting mechanism that guarantees the same k between all possible pairs of players. We use G to denote this base game and call it a modified snowdrift game since the standard snowdrift game [19] is a special case of G when $k = \frac{1}{2}$.

5.1.2 Nash Equilibria of the base game

Denote the mixed strategy of player i, $i = 1, 2$, by $\mathbf{w_i} = (w_i, 1 - w_i)$ with which player i chooses C with probability w_i, $0 \leq w_i \leq 1$. One can easily check that the base game G has three Nash equilibria, denoted by NE_i, $i = 1, 2, 3$, such that

$$\text{NE}_1 \quad : \quad w_1 = 1, w_2 = 0; \tag{5.2}$$

$$\text{NE}_2 \quad : \quad w_1 = 0, w_2 = 1; \tag{5.3}$$

$$\text{NE}_3 \quad : \quad w_1 = w_2 = \frac{b - c}{b - (1 - k)c}, \tag{5.4}$$

where NE_1 and NE_2 are strict, pure-strategy Nash equilibria, and NE_3 is a weak, mixed-strategy equilibrium [72]. Let $u_i(\mathbf{w_1}, \mathbf{w_2})$, $i = 1, 2$, denote the expected payoff of player i under the strategy profile $(\mathbf{w_1}, \mathbf{w_2})$ and S the social welfare of the two players. Then

$$\begin{aligned} & S(\mathbf{w_1}, \mathbf{w_2}) \\ = \; & u_1(\mathbf{w_1}, \mathbf{w_2}) + u_2(\mathbf{w_1}, \mathbf{w_2}) \\ = \; & w_1(w_2(b - kc) + (1 - w_2)(b - c)) + (1 - w_1)w_2 b \\ & + w_2(w_1(b - kc) + (1 - w_1)(b - c)) + (1 - w_2)w_1 b \\ = \; & 2w_1 w_2(c - b - kc) + (w_1 + w_2)(2b - c). \end{aligned} \tag{5.5}$$

Now we compare the social welfare of the three Nash equilibria and the strategy profile (C, C):

$$S = \begin{cases} 2b - c & \text{for } \text{NE}_1, \text{NE}_2 \\ \frac{2b(b-c)}{ck+b-c} & \text{for } \text{NE}_3 \\ -2ck + 2b & \text{for } (C, C) \end{cases} \tag{5.6}$$

for which we plot the correspoinding curves that are parameterized by k when fixing $b = 1.5, c = 1$ as shown in Fig. 5.1. It is clear that the social welfare of NE_1

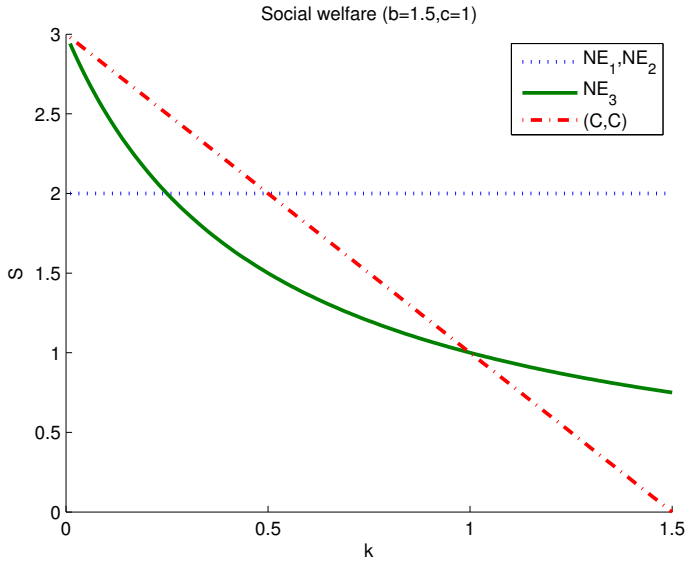

Figure 5.1: The social welfare for NE_i, $i = 1, 2, 3$, and (C, C) when $0 < k \leq 1.5$, $b = 1.5$ and $c = 1$.

and NE_2 are constants independent of k since the corresponding strategies are pure and no cooperation takes place. For the strategy profile (C, C), its social welfare decreases linearly since the cooperation cost grows linearly as k increases. The social welfare of NE_3 decreases convexly since the probability with which both players choose C decreases as k increases. More can be said comparing the social welfare of the four strategy profiles. It is clear that which strategy profile maximizes the social welfare depends on the value of k. When $0 < k < \frac{1}{2}$, in which case the cooperation efficiency is sufficiently high, the social welfare of two cooperators is greater than that of one cooperator and one defector. When $k > \frac{1}{2}$, in which case the cooperation is not efficient, the social welfare of one cooperator and one defector is greater than that of two cooperators. These observations motivate us to study how the evolutionary game dynamics are affected by the cooperation coefficient k.

5.2 Evolutionary game

Motivated by the base game discussed in the previous section, we now study the repeated games with *reactive strategies*, under which a player's choice of strategies in a given round is only determined by the opponent's choice in the previous round

[72]. We then further investigate how the evolutionary dynamics are affected by k using replicator dynamics.

5.2.1 Repeated game

We denote a stochastic reactive strategy s by the triple $s = (u, p, q)$, where u is the probability to cooperate in the first round, and p and q are the conditional probabilities to cooperate in later rounds, given that the opponent's previous choice was to cooperate or defect, respectively [72].

We consider three reactive strategies in this chapter: (a) the *ALLC strategy* $s_C = (1, 1, 1)$ is the strategy that a player always plays C; (b) the *tit-for-tat (TFT) strategy* $s_T = (1, 1, 0)$ is the one that the player plays C in the first round and does what his opponent did in the previous round; (c) the *suspicious Tit-for-tat (STFT) strategy* $s_{ST} = (0, 1, 0)$ is the one that the player plays D in the first round and does what his opponent did in the previous round.

For a given constant $m > 0$, every time when the base game G has been played m times, one has a stage game and can calculate the corresponding stage-game payoff matrix. In what follows, we fix $b = 1.5$, $c = 1$ and $m = 5$ and denote the stage game in this case by $\overline{G}$ and its associated payoff matrix by A

$$A = \begin{array}{c} \\ s_C \\ s_T \\ s_{ST} \end{array} \begin{array}{c} \begin{array}{ccc} s_C & s_T & s_{ST} \end{array} \\ \begin{pmatrix} -5k + 7.5 & -5k + 7.5 & -4k + 6.5 \\ -5k + 7.5 & -5k + 7.5 & 4.5 \\ -4k + 7.5 & 5.5 & 0 \end{pmatrix} \end{array} \tag{5.7}$$

Then $\overline{G}$ is a two-player, three-strategy, symmetric game. Note that although the conclusions to be drawn later on are based on these set of chosen values, they apply to a rather wide range of values of b, c and m.

5.2.2 Evolutionary dynamics

We use $\rho = (\rho_1, \rho_2, \rho_3)^T$ to denote the distribution of the three strategies in the population, and then ρ takes value in the simplex $S = \{(x_1, x_2, x_3)^T | \sum_{i=1}^{3} x_i = 1, x_i \geq 0\}$. In view of (5.7), one has the replicator equations

$$\dot{\rho}_i = \rho_i(e_i^T A\rho - \rho^T A\rho), \qquad i = 1, 2, 3, \tag{5.8}$$

where e_i is the ith standard-basis unit vector. Now we list all the equilibria of (5.8), which are labeled by superscripts. It is easy to check that there are three trivial

equilibrium points:

$$\begin{aligned}\rho^1 &= (1,\ 0,\ 0)^T,\\ \rho^2 &= (0,\ 1,\ 0)^T,\\ \rho^3 &= (0,\ 0,\ 1)^T.\end{aligned}$$

There are other possible equilibrium points, whose existence depends on the value of k, on the boundary of S:

$$\begin{aligned}\rho^4 &= (0,\ \frac{9}{10k+5},\ \frac{10k-4}{10k+5})^T, \text{only when } k > \frac{2}{5};\\ \rho^5 &= (\frac{8k-13}{6k-13},\ 0,\ \frac{-2k}{6k-13})^T, \text{only when } 0 < k < \frac{13}{8};\\ \rho^6 &= (\frac{5k-2}{4k-2},\ \frac{-k}{4k-2},\ 0)^T, \text{only when } 0 < k < \frac{2}{5}.\end{aligned}$$

Also on the boundary of S, there is a continuous set of equilibrium points

$$\Phi^7 = \{\rho^7 \mid \rho^7 = (1-\theta,\ \theta,\ 0)^T \text{ for } 0 < \theta < 1\}.$$

In the interior of S, there is a possible equilibrium set

$$\begin{aligned}\Phi^8 &= \{\rho^8 \mid \rho^8 = (-\theta + \frac{9}{10},\ \theta,\ \frac{1}{10})^T,\\ &\qquad \text{for } 0 < \theta < \frac{9}{10} \text{ and only when } k = \frac{1}{2}\}\end{aligned}$$

We emphasize again that the existence of ρ^4, ρ^5, ρ^6 and Φ^8 is determined completely by k. For later ease of expression, when $0 < k < \frac{2}{5}$, we divide the set Φ^7 into two subsets $\widehat{\Phi}^7$ and $\widetilde{\Phi}^7$ where

$$\widehat{\Phi}^7 = \{\rho^7(\theta) \mid \rho^7 \in \Phi^7, \frac{k}{2-4k} \le \theta < 1\},$$

and

$$\widetilde{\Phi}^7 = \{\rho^7(\theta) \mid \rho^7 \in \Phi^7, 0 < \theta < \frac{k}{2-4k}\}.$$

Now we are ready to present the main result of this section on the evolutionary stability parameterized by k of all the equilibria.

For mixed strategies $\alpha, \beta \in S$, with the payoff matrix A, the expected payoff of α against β can be computed by

$$E(\alpha, \beta) = \alpha^T A \beta \tag{5.9}$$

Now we analyze the stability of the equilibria of the replicator dynamics (5.8). For completeness we provide the definitions for the ESS and ES set below, the equations in which will be used later on in the proofs to be developed.

5.2.1. DEFINITION. *(Evolutionarily stable strategy (ESS) [29])* $\rho^* \in S$ *is an ESS if and only if the following two conditions are satisfied:*
(1) equilibrium condition:

$$E(\rho^*, \rho^*) \geq E(\rho, \rho^*) \quad \textit{for all } \rho \in S; \tag{5.10}$$

(2) stability condition:

$$\begin{aligned} &\textit{if} \quad \rho \neq \rho^* \ \textit{ and } E(\rho^*, \rho^*) = E(\rho, \rho^*) \\ &\textit{then} \quad E(\rho^*, \rho) > E(\rho, \rho). \end{aligned}$$

5.2.2. DEFINITION. *(Evolutionarily stable set (ES set) [29]) A closed nonempty subset* Φ^* *of* S *is an ES set if for each* $\rho^* \in \Phi^*$ *there exists a neighborhood* W *such that*

$$E(\rho^*, \rho) \geq E(\rho, \rho) \tag{5.11}$$

for all $\rho \in W$ *and the equality sign holds only when* $\rho \in \Phi^*$.

Among all the equilibria of (5.8), ρ_1, ρ_2 and ρ_3 are always equilibrium points independent of the values of k. We first analyze their stabilities and the results are summarized in the following three propositions.

5.2.3. PROPOSITION. *The equilibrium point* ρ^1 *is not an ESS.*

Proof: For any $\rho = (\rho_1, \rho_2, \rho_3)^T \in S$ with $\rho_3 > 0$

$$E(\rho^1, \rho^1) - E(\rho, \rho^1) = -k\rho_3 < 0, \tag{5.12}$$

which implies that $E(\rho^1, \rho^1) < E(\rho, \rho^1)$. So the equilibrium condition in Definition 5.2.1 is violated, and thus ρ^1 is not an ESS. □

5.2.4. PROPOSITION. *The equilibrium point* ρ^2 *is not an ESS.*

Proof: We pick $\rho = (\rho_1, \rho_2, 0)^T \in S$ that is different from ρ^2. Then $E(\rho^2, \rho^2) = E(\rho, \rho^2) = 0$ and $E(\rho^2, \rho) = E(\rho, \rho)$, which imply that the stability condition in Definition 5.2.1 is violated. So ρ^2 is not an ESS. □

5.2.5. PROPOSITION. *The equilibrium point ρ^3 is not an ESS.*

Proof: We pick $\rho = (0, \rho_2, \rho_3)^T \in S$ with $\rho_2 > 0$. Then $E(\rho^3, \rho^3) < E(\rho, \rho^3)$. So the equilibrium condition in Definition 5.2.1 is violated and thus ρ^3 is not an ESS. □

The existence of the other equilibrium points or sets depends on the values of k. Now we analyze their stabilities one by one considering only those values of k under which the corresponding equilibrium points or sets exist. We summarize our results in the next five propositions.

5.2.6. PROPOSITION. *The equilibrium point ρ^4 is an ESS for $k > \frac{2}{5}$.*

Proof: For any $\rho = (\rho_1, \rho_2, \rho_3)^T \in S$, we have

$$E(\rho^4, \rho^4) - E(\rho, \rho^4) = \frac{4\rho_1(10k^2 - 9k + 2)}{5(2k+1)} \geq 0. \tag{5.13}$$

So the equilibrium condition in Definition 5.2.1 is satisfied.

Now we check the stability condition in Definition 5.2.1. We pick $\hat{\rho} = (\hat{\rho_1}, \hat{\rho_2}, \hat{\rho_3})^T \in S$ such that $\hat{\rho} \neq \rho^4$ and $E(\rho^4, \rho^4) = E(\hat{\rho}, \rho^4)$, and one can check that such a $\hat{\rho}$ always exists. Then it must be true that $(10k+5)\hat{\rho_2} - 9 \neq 0$, which implies that $E(\rho^4, \hat{\rho}) - E(\hat{\rho}, \hat{\rho}) = \frac{[(10k+5)\hat{\rho_2} - 9]^2}{10(2k+1)} > 0$. So the stability condition is also satisfied and we arrive at the conclusion. □

5.2.7. PROPOSITION. *The equilibrium point ρ^5 is an ESS for $0 < k < \frac{1}{2}$ and not for $\frac{1}{2} \leq k < \frac{13}{8}$.*

Proof: When $0 < k < \frac{1}{2}$, for any $\rho = (\rho_1, \rho_2, \rho_3)^T \in S$, we have

$$E(\rho^5, \rho^5) - E(\rho, \rho^5) = \frac{4k\rho_2(2k-1)}{6k-13} \geq 0. \tag{5.14}$$

So ρ^5 satisfies the equilibrium condition in Definition 5.2.1. We then pick $\hat{\rho} = (\hat{\rho_1} \;\; \hat{\rho_2} \;\; \hat{\rho_3})^T \in S$ such that $\hat{\rho} \neq \rho^5$ and $E(\rho^5, \rho^5) = E(\hat{\rho}, \rho^5)$, and one can check that such a $\hat{\rho}$ always exists. Then it must be true that $(6k-13)\hat{\rho_1} - (8k-13) \neq 0$ and hence $E(\rho^5, \hat{\rho}) - E(\hat{\rho}, \hat{\rho}) = \frac{-[(6k-13)\hat{\rho_1} - (8k-13)]^2}{2(6k-13)} > 0$. So the stability condition in Definition 5.2.1 is also satisfied. We conclude that ρ^5 is an ESS for $0 < k < \frac{1}{2}$.

When $k = \frac{1}{2}$, we pick $\tilde{\rho} = (\tilde{\rho_1}, \tilde{\rho_2}, \frac{1}{10})^T \in S$ that is different from ρ^5, then $E(\rho^5, \rho^5) = E(\tilde{\rho}, \rho^5)$. However $E(\rho^5, \tilde{\rho}) - E(\tilde{\rho}, \tilde{\rho}) = \frac{(9 - 10\tilde{\rho_1} - 10\tilde{\rho_2})^2}{20} = 0$ since $\tilde{\rho_1} + \tilde{\rho_2} = \frac{9}{10}$. Thus, ρ^5 does not satisfy the stability condition in Definition 5.2.1, and so it is not an ESS.

When $\frac{1}{2} < k < \frac{13}{8}$, we pick $\overline{\rho} = (\overline{\rho_1}, \overline{\rho_2}, \overline{\rho_3})^T \in S$ such that $\overline{\rho_2} > 0$. Then from (5.14) we know that $E(\rho^5, \rho^5) - E(\overline{\rho}, \rho^5) < 0$. So ρ^5 does not satisfy the equilibrium condition in Definition 5.2.1 and it is not an ESS. □

5.2.8. PROPOSITION. *The equilibrium point ρ^6 is not an ESS for $0 < k < \frac{2}{5}$.*

Proof: Pick $\tilde{\rho} = (\tilde{\rho_1}, \tilde{\rho_2}, 0)^T \in S$ that is different from ρ^6. Then $E(\rho^6, \rho^6) = E(\tilde{\rho}, \rho^6)$. However, $E(\rho^6, \rho) - E(\rho, \rho) = \frac{\rho_3[(6k-13)\tilde{\rho_1} - (10k+5)\tilde{\rho_2} - (10k-13)]^2}{2} = 0$, which violates the stability condition in Definition 5.2.1. The proof is complete. □

5.2.9. PROPOSITION. *The equilibrium set $\widehat{\Phi}^7$ is and $\widetilde{\Phi}^7$ is not an ES set for $0 < k < \frac{2}{5}$; Φ^7 is not an ES set for $k \geq \frac{2}{5}$.*

Proof: When $0 < k < \frac{2}{5}$, for any $\rho^7(\theta) \in \widehat{\Phi}^7$, we consider the neighborhood $W(\theta) \subset S$ that contains all those $\rho = (\rho_1, \rho_2, \rho_3)^T = (1 - \theta - \delta, \theta - \epsilon + \delta, \epsilon)^T$, with $\delta \geq 0$ and $\epsilon \geq 0$, satisfying $E(\rho^7, \rho) - E(\rho, \rho) = \frac{-\epsilon}{2}[2(k - 2\theta + 4k\theta) - 5\epsilon(2k+1) - 8\delta(1-2k)] \geq 0$, where the equality sign holds if and only if $\epsilon = 0$. One can check that such a W is always nonempty. Then for any $\rho \in W(\theta)$ and $\rho \notin \widehat{\Phi}^7$, we have $E(\rho^7, \rho) - E(\rho, \rho) = \frac{-\rho_3[(13-6k)\rho_1 + (10k+5)\rho_2 - (8k\theta - 8k - 4\theta + 13)]}{2} > 0$. So according to Definition 5.2.2, $\widehat{\Phi}^7$ is an ES set.

Also when $0 < k < \frac{2}{5}$, for any $\rho^7(\theta) \in \widetilde{\Phi}^7$, one can always find a $\tilde{\rho} = (\tilde{\rho_1}, \tilde{\rho_2}, \tilde{\rho_3})^T \in S$ with $\tilde{\rho_3} > 0$ such that $E(\rho^7, \rho^7) - E(\tilde{\rho}, \rho^7) = -\tilde{\rho_3}(k - 2\theta + 4k\theta) < 0$. So ρ^7 violates the equilibrium condition in Definition 5.2.1 and cannot be a Nash equilibrium. Hence, $\widetilde{\Phi}^7$ is not an ES set. Using the same argument, when $k \geq \frac{2}{5}$, for any $\rho^7(\theta) \in \Phi^7$, one can pick the same $\tilde{\rho}$ to show that ρ^7 is not an Nash equilibrium, and thus Φ^7 is not an ES set. □

5.2.10. PROPOSITION. *The equilibrium set Φ^8 is an ES set for $k = \frac{1}{2}$.*

Proof: For any $\rho^8 \in \Phi^8$, we have $E(\rho^8, \rho) - E(\rho, \rho) = \frac{(10\rho_3 - 1)^2}{20} \geq 0$ for all $\rho = (\rho_1, \rho_2, \rho_3)^T \in S$ and the equality sign holds if an only if $\rho \in \Phi^8$. So we conclude Φ^8 is an ES set. □

We summarize the result in Table 5.1 distinguishing evolutionarily stable strategies (ESS) or set (ES set).

We choose six typical values of k and draw the resulted flow pattern for the stage game $\overline{G}$ in Fig. 5.2 using the game dynamics simulation software Dynamo [63].

To better understand the flow patterns, we take a closer look at the three basic deterministic reactive strategies. We call the player, who plays the $ALLC$ strategy, the $ALLC$ player; similarly, we also have TFT players and $STFT$ players. When two $ALLC$ or TFT players meet each other, they both always play C for m rounds. But when two $STFT$ players meet, they both always play D. When an $ALLC$ player meets a TFT player, both of them play C all the time. When an $ALLC$ player meets a $STFT$ player, the former always plays C while the later plays D in the first round and switch to C after that. The more interesting case is the one when a TFT player

Table 5.1: Evolutionary stability of equilibria

	ESS or ES set	neither ESS nor ES set
$0 < k < \frac{2}{5}$	$\rho^5, \widehat{\Phi}^7$	$\rho^1, \rho^2, \rho^3, \rho^6, \widetilde{\Phi}^7$
$k = \frac{2}{5}$	ρ^5	$\rho^1, \rho^2, \rho^3, \Phi^7$
$\frac{2}{5} < k < \frac{1}{2}$	ρ^4, ρ^5	$\rho^1, \rho^2, \rho^3, \Phi^7$
$k = \frac{1}{2}$	ρ^4, Φ^8	$\rho^1, \rho^2, \rho^3, \rho^5, \Phi^7$
$\frac{1}{2} < k < \frac{13}{8}$	ρ^4	$\rho^1, \rho^2, \rho^3, \rho^5, \Phi^7$
$k \geq \frac{13}{8}$	ρ^4	$\rho^1, \rho^2, \rho^3, \Phi^7$

meets a $STFT$ player. In this case, in the first round, the former plays C and the later plays D and then both of them repeat the other's previous strategy. Thus, the oscillation of strategies appears, which takes the form of $(C, D) \rightarrow (D, C) \rightarrow (C, D) \rightarrow$...

Now we are ready to explore how the cooperation coefficient k influences the evolutionary dynamics. Since the three trivial equilibrium points ρ^1, ρ^2, and ρ^3 are never evolutionarily stable, we only need to examine the rest of the equilibria.

When $0 < k < \frac{2}{5}$, ρ^5 is an ESS while ρ^6 is not; $\widehat{\Phi}^7$ is an ES set while $\widetilde{\Phi}^7$ is not as shown in Fig. 5.2(a) and Fig. 5.2(b). When k is close to 0, the ESS ρ^5 is close to the vertex $ALLC$ and the ES set $\widehat{\Phi}^7$ almost coincides with the boundary of the line interval connecting the vertices $ALLC$ and TFT. In this case, cooperation is the best choice, since two players can get benefit with almost zero cost. As k increases, ρ^5 moves away from the vertex $ALLC$ to $STFT$ and $\widehat{\Phi}^7$ shrinks and moves from $ALLC$ to TFT. The reason is that cooperation is no longer the best choice with decreasing cooperation efficiency as k increases.

When $\frac{2}{5} \leq k < \frac{1}{2}$, ρ^6 disappears and ρ^4 appears. The set $\widehat{\Phi}^7$ is not an ES set any more and in fact, the whole set Φ^7, corresponding to the open line connecting the vertices $ALLC$ and TFT, is not an ES set. Since the cooperation efficiency gets worse and worse, a TFT player and an $STFT$ player outperform two $ALLC$ players. In other words, a player prefers to alternate between C and D in turn with her opponent, and thus oscillating strategies win.

When $k = \frac{1}{2}$, ρ^5 turns out not to be an ESS and Φ^8 is an ES set as shown in Fig. 5.2(c). The existence of Φ^8 is a consequence of the fact that an $ALLC$ player and

a TFT player play the same role in this case. This can be easily verified from the payoff matrix A in (5.7) since the first two rows and columns are the same when $k = \frac{1}{2}$.

When $k > \frac{1}{2}$, ρ^5 keeps moving towards the vertex $STFT$ along the boundary until it disappears when $k = \frac{13}{8}$; ρ^4 becomes the only ESS when $k \geq \frac{13}{8}$ as shown in Fig. 5.2(d) - (f).

Combining the analysis above, we identify a very interesting phenomenon. As k increases, some ESSs and ES sets move from the vertex $ALLC$ to $STFT$ passing through TFT along the boundaries of S. In other words, when k increases, the ESS ρ^6 and the ES set $\widehat{\Phi}^7$ move from $ALLC$ to TFT and disappear, while at the same time ρ^4 appears and moves from TFT to $STFT$. On the other hand, the ESS ρ^5 moves from $ALLC$ to $STFT$ along a different boundary line and turns out not to be ESS.

We provide some explanation for this phenomenon as follows. The payoffs of the strategy profiles (C, D), (D, C) and (D, D) are not influenced by k while the payoff of (C, C) is as shown in Fig.5.1. On the other hand, the increasing k implies the decreasing cooperation efficiency. Thus, when k is very small, (C, C) is the best choice for every stage game, and then $ALLC$ is the dominating strategy. When k increases, $ALLC$ plays worse and worse, while (C, D) and (D, C) do better than (C, C). So the performance of alternating between TFT and $STFT$ exceeds that of (C, C). Finally, when k keeps increasing, (D, D) also performs better and better.

We can reinterpret the above analysis result in the context of the robotic water polo matches. A robot player prefers to shoot together with its teammate when cooperation efficiency is high. In contrast, when the cooperation efficiency is low, robots are more motivated to shoot alone.

In this section, we have analyzed the evolutionary stability of the formulated modified snowdrift games with the cooperation coefficient k as the parameter with fixed different values. After we have gained insight into how stability is affected by different k's, in the next section we explore further the more exciting topic of what happens when k is allowed to co-evolve with the game dynamics.

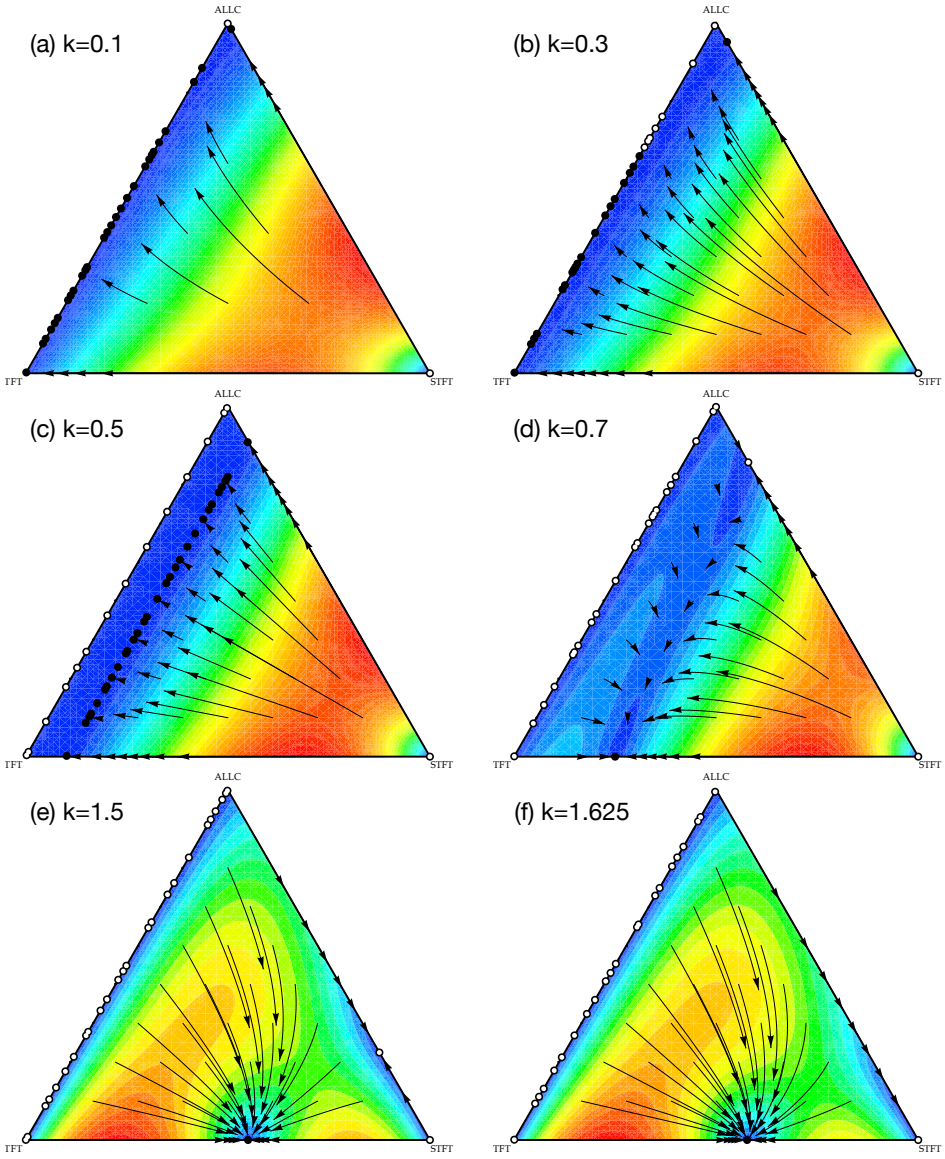

Figure 5.2: Flow patterns for the stage game $\overline{G}$ defined by (5.7). Color temperatures describe motion speeds where blue corresponds to the slowest motion and red the fastest. Black circles denote stable equilibria while white circles unstable ones.

5.3 Adaptive cooperation efficiency

From the analysis using replicator dynamics in infinite populations in the previous section, it is clear that the cooperation coefficient k has great influence on the evolutionary dynamics. It has been reported that robots implemented with learning algorithms are capable to improve their performances [8, 70]. Hence, we are interested in studying how k and cooperation may co-evolve in evolutionary games. Towards this end, we use the tool of Fermi processes in this section for a finite population.

5.3.1 Evolutionary games with evolving k

Using the same stage game $\overline{G}$ defined in (5.7), we now look at an evolutionary game for a team of N robots with an evolving k. In the gth stage game , two players P_a and P_b are chosen randomly. Then for P_a, we choose randomly from the rest of the $N-1$ players a player P_c to play $\overline{G}$ together. Consequently, P_a gains a payoff E_a. Similarly, P_b plays a game with P_d and gains E_b. The frequency of the strategy profile (C, C) chosen in these two games is recorded by $n_{cc}(g)$; in other words, $n_{cc}(g)$ describes the number of base games G, in which both players opt for C during the gth stage game. At the end of the gth stage game, P_a updates its strategy to P_b's current strategy with probability p [5, 73, 84]

$$p = \frac{1}{1 + e^{-\beta(E_b - E_a)}}, \tag{5.15}$$

where $\beta > 0$ is called the *imitation intensity*, which describes the sensitivity to the difference between payoffs. We assume that k is bounded by $k_{min} \leq k \leq k_{max}$. The update rule of k is

$$k(g+1) = \begin{cases} k_{max} & \text{if } \tilde{k}(g) > k_{max} \\ k_{min} & \text{if } \tilde{k}(g) < k_{min} \\ \tilde{k}(g) & \text{otherwise} \end{cases} \tag{5.16}$$

where

$$\tilde{k}(g) = k(g) + 1 - \eta \frac{n_{cc}(g)}{2m}, \tag{5.17}$$

and $\eta > 0$ is called the *learning coefficient*, which quantifies the robots' learning capability to improve their cooperation efficiency. When $n_{cc} < \frac{2m}{\eta}$, $\tilde{k}(g)$ is greater than $k(g)$, which implies that the cooperation is not frequent enough to improve the cooperation efficiency; when $n_{cc} > \frac{2m}{\eta}$, $\tilde{k}(g)$ is less than $k(g)$, which implies that the cooperation efficiency is improved due to the high cooperation frequency. Hence,

with greater η robots can improve their cooperation efficiency with lower cooperation frequency. This agrees with the intuition that if the robots cooperate more, they perform better, which in turn intensifies their willingness to cooperate. Since the robots are assumed to be homogeneous and a broadcasting mechanism is available among robots, we can use the same η for all possible pairs of robots. We will investigate the co-evolution of k and game dynamics under different η mainly through simulations.

5.3.2 Simulation results

We choose $N = 12$, $\beta = 2$, $k(0) = 0.5$, $k_{max} = 1.5$, $k_{min} = 0.1$ and initialize the robots in such a way that there are equal numbers of robots that opt for each of the three strategies. We increase η from 1.0 to 3.0 with step size 0.05 and run the evolutionary game for 10^4 times. Then the population distribution as a function of η is shown in Fig. 5.3(a). In Fig. 5.3(b), a measure $0 \leq \epsilon_k \leq 1$ is used to show the frequency, with which the cooperation coefficient k converges to k_{min} in the simulations for each η. Because of the finiteness of population and the linearity of the dynamics of k, we know that k converges either to k_{min} or k_{max}, and so the frequency of k converging to k_{max} is $1 - \epsilon_k$. It can be seen that ϵ_k increases fast when η grows from 1 to about 1.85.

It is shown that k improves with better learning capabilities. However, ϵ_k does not increase any more after reaching around 0.6 when η grows to about 1.85. This is because of the discretization of $n_{cc}(g)$. To be more precise, $n_{cc}(g)$ has six possible values $0, m-1, m, 2m-2, 2m-1$, and $2m$. When $\eta > \frac{2m}{m-1} = 2.5$, almost all the values of $n_{cc}(g)$ can make k decrease except for $n_{cc}(g) = 0$. So ϵ_k does not increase with η when η is large enough. Also when η increases, the frequency of the $ALLC$ strategy increases smoothly, the frequency of the TFT strategy increases in general, and the frequency of the $STFT$ strategy decreases. Hence, the robots are more willing to cooperate with each other when their learning capabilities become better.

We further find that the trend of the $STFT$ strategy is exactly the opposite to that of ϵ_k, while the sum of the frequencies of $ALLC$ and TFT is almost equal to ϵ_k. This can be explained by our analysis in the previous section that when $k = k_{min} = 0.1$, the ESS ρ^5 is close to $ALLC$ and the ES set $\widehat{\Phi}^7$ almost coincide with the line interval between $ALLC$ and TFT.

In short, the capability of the robots to improve their cooperation efficiency has great influence on the dynamics of the adaptive cooperation coefficient k and the dynamics of the strategies. Better learning capability leads to better cooperation efficiency and cooperation is preferred.

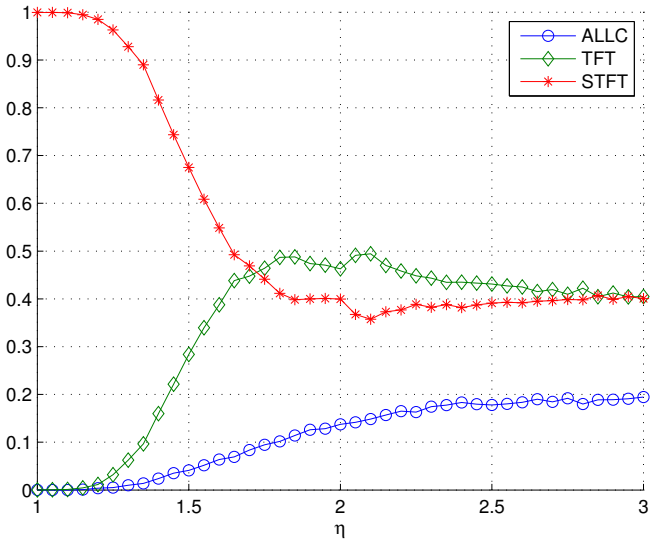

(a)

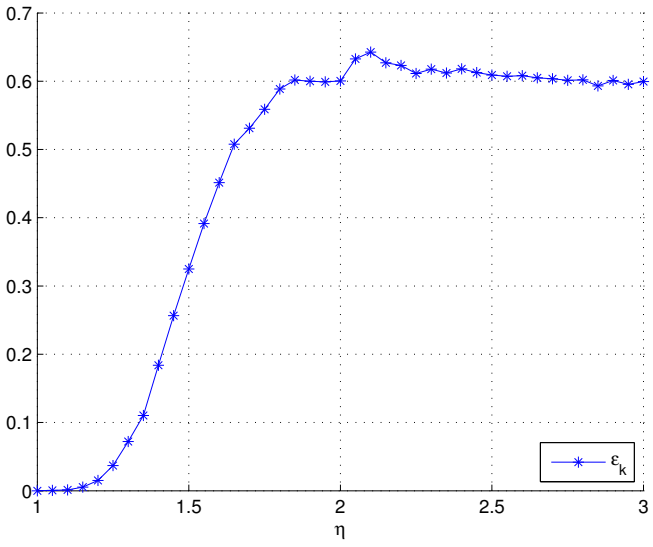

(b)

Figure 5.3: Evolutionary dynamics under different η. Each data point is the average of 10^4 simulation runs.

5.4 Conclusion

In this chapter, a novel modified snowdrift game has been proposed and used to model multi-robot water polo matches. The cooperation coefficient has been introduced to quantify the well-known synergy effect and the learning coefficient has been defined to describe the robots' learning capability. An update rules for the cooperation coefficient has been studied and we have shown that cooperation efficiency can be improved when robots cooperate more. Theoretical analysis has shown that the evolutionary stability is affected by the cooperation efficiency while computer simulations have shown that when the cooperation coefficient co-evolves with the evolutionary dynamics, cooperation efficiency gets improved under better learning capabilities.

Our proposed modified snowdrift game is tailor designed to model multi-robot water polo matches. Compared with standard evolutionary snowdrift games, the proposed game with the adaptive cooperation coefficient is no longer an open-loop model, but a fully co-evolved game, which fits well practical water polo matches.

Currently we are exploring to improve our model by incorporating the defense of the opponent team. We are also implementing robotic experiments using robotic fish to further test our game theoretic model.

Chapter 6

Group Tasks for Evolving Multi-Robotic Fish Systems

how personality evolves and effective leadership emerges

In Chapter 5, an evolutionary game model is used to control groups of robotic fish and study the emergence and evolution of cooperation among them in multi-robot water polo matches. It provides a way of introducing evolutionary game theory to the application of robotic fish teams. In this chapter, we develop a new framework, using multi-robotic fish system as the experimental tool and evolutionary game theory as the theoretical tool, to investigate the evolution of personalities and the emergence of effective leadership in bio-inspired robotic fish groups.

As we mentioned in Chapter 1, a variety of animal groups and artificial systems can benefit from their collective movement. Collective movement can be induced by "leadership" of one or a few individuals. Personality types offer an opportunity to generate the leadership in such multi-individual systems. Inspired by such studies [21, 25, 34, 39, 41, 50, 57, 82, 83], leadership in an obstacle removing scenario is chosen as a case study in this chapter to verify the usefulness of our proposed framework in investigating phenomena in coordinated multi-agent systems.

We propose an N-player evolutionary game model to investigate the evolution of personality and the emergence of effective leadership among groups of robotic fish in obstacle removing scenarios. We first formulate a game setting in which groups of robotic fish deal with obstacle removing tasks repeatedly that are modeled by N-player snowdrift games. Then the personality, which is considered in this research to be each fish's willingness to initiate a collective movement in an obstacle removing task, is introduced to the game model as the player's strategy. It is identified by experiments that the diversity of personalities in a group, which emerges in the short-term evolution, is a crucial factor in determining the group's performance in the obstacle removing tasks. We further analyze how the groups solve the tasks with and without diversity of personalities, respectively. Moreover, it is found that the robotic fish group has the ability of self-adaptation to cope with the level of difficulties of obstacle removing tasks. In addition, it is worth to know that the effectiveness of our proposed game model is verified by fitting with the ex-

perimental data, then simulations are also carried out as effective complements to the experimental results.

6.1 Problem formulation

In this section, we first formulate an obstacle removing task for a group of robotic fish and describe the corresponding experimental set-up. Then we introduce personality to such robotic fish, with which, in the context of the group obstacle removing task, each fish will adopt one of three possible roles - initiator, follower or free-rider - and effective leadership may emerge in completing the tasks.

6.1.1 Obstacle removing task for a robotic fish group

We consider an obstacle removing scenario, in which a group of robotic fish need to remove an obstacle to complete the obstacle removing task. The schematic view of the experimental set-up is shown in Fig. 6.1. The experimental tank ($300 \times 200 \times 40$ cm, length $\times$ width $\times$ height) consists of two areas, the "starting area" on its left-hand side and the "feeding area" on the right-hand side, which are separated from each other by a removable obstacle ($98 \times 8 \times 26$ cm, length $\times$ width $\times$ height). A group of robotic fish is placed in the starting area of the tank at the beginning. To gather food in the feeding area, the fish group must remove the obstacle between the two areas. To simplify the scenario, we assume that the obstacle removing task is completed if and only if the obstacle is removed.

We assume all the robotic fish of the group are equipped with the same hardware and software, i.e., each fish has the same capacity of pushing the obstacle, and they cannot communicate with each other and can only observe whether the rest are engaged in pushing the obstacle. In view of the fact that such capacity is limited, a minimum number of fish must cooperate to push the obstacle so that the obstacle can be removed. Obviously, the required threshold depends on the obstacle's weight, i.e., heavier obstacles in general require more fish to push. The fact that some fish, when pushing together, can remove the obstacle, implies that not all fish need to participate in pushing obstacle to accomplish the obstacle removing task. Yet, more fish contribute, the effort to be invested by a single fish of the cooperated group will be smaller. In addition, we assume that the benefits of completing the obstacle removing task, do not increase with the number of fish that contributed in removing obstacle.

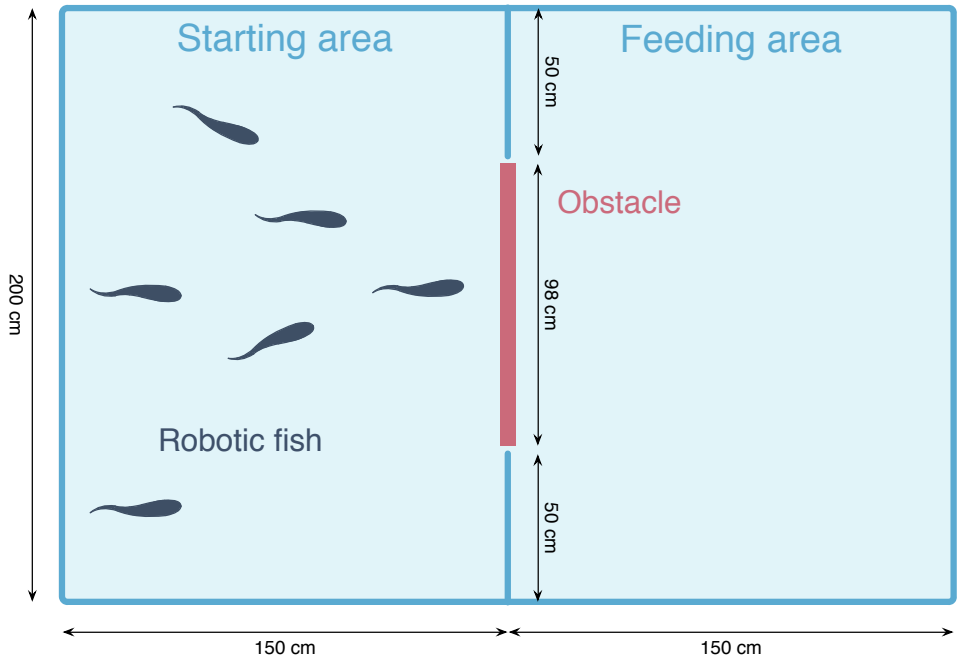

Figure 6.1: Schematic view of the experimental set-up.

6.1.2 Personality and effective leadership

As we mentioned, personality types offer an opportunity to generate the leadership which is a key feature of collective movement in a variety of multi-individual systems. Consider the robotic fish system we studied in this chapter, collective movement is also required to complete the obstacle removing task. To this end, we introduce *personality* to such robotic fish, which presents the willingness of a fish to initiate a collective movement (i.e., to be an *initiator*) in doing the obstacle removing task. We further assume that its willingness to follow an initiator (i.e., to be a *follower*) is inversely correlated with that to be an initiator. This assumption is in accordance with biological studies [21, 50, 54, 83]. More specifically, a robotic fish with a bolder personality should have a higher probability of being an initiator and lower probability of being a follower, while a fish with a shier personality should have a lower probability of being an initiator and higher probability of being a follower. Obviously, both the initiator and its followers (if any) in the group cooperate to push the obstacle. However, the fish may choose to wait until the other fish remove the obstacle. We call such kind of robotic fish *free-riders*. Figure 6.2 shows the

snapshots of one experiment.

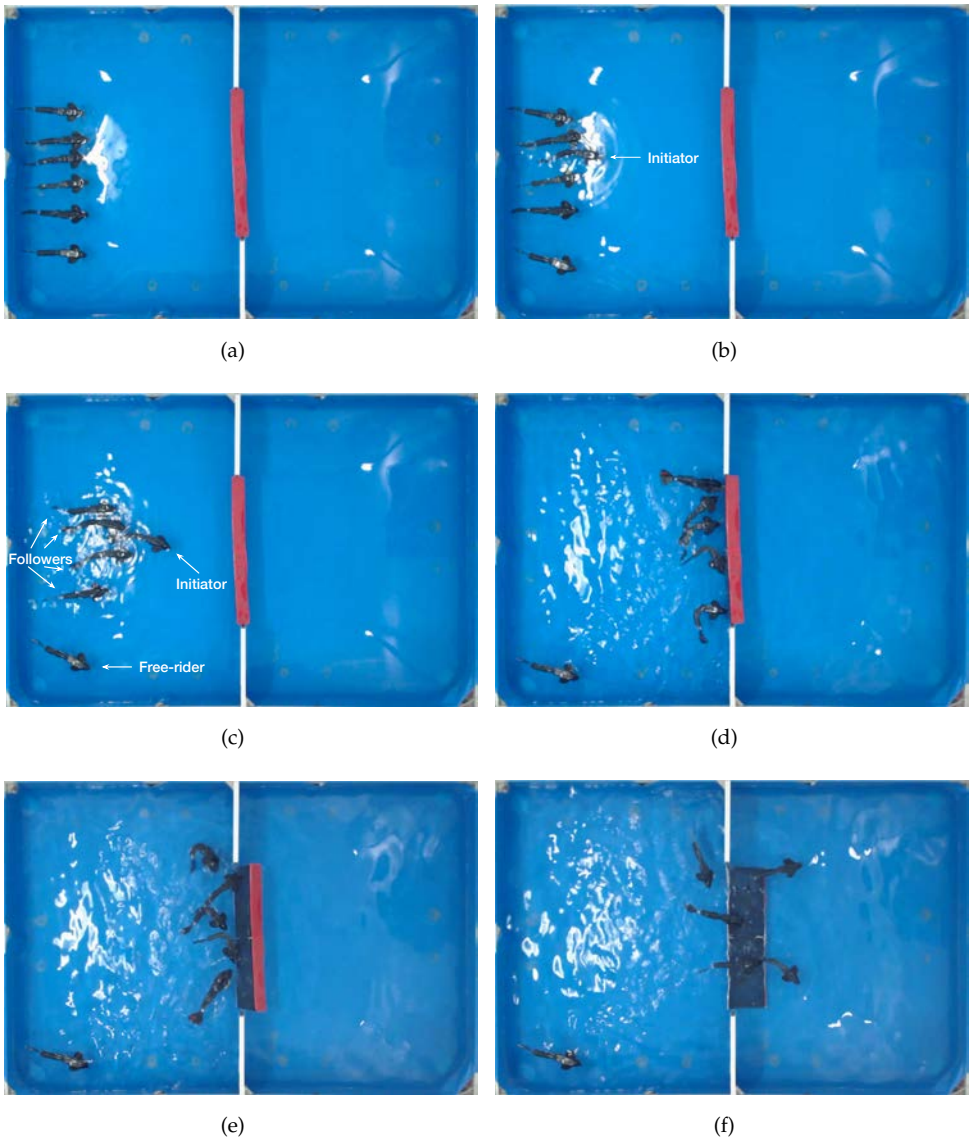

Figure 6.2: Snapshots of the experiments. (a) start; (b) an initiator emerges; (c) four robotic fish follows the initiator; (d) and (e) the five C-players push the obstacle; (f) succeed.

Furthermore, we say *effective leadership* emerges in the group of robotic fish if the initiation by one fish leads to a collective movement by which the obstacle can be removed. In other words, the success of the obstacle removing task implies the emergence of effective leadership in the fish group. Note that the emergence of the effective leadership does not require all the fish to participate in pushing the obstacle. This assumption is natural in the study of cooperation tasks for groups of robotic fish.

6.2 Evolutionary game model

In the previous section, we have formulated an obstacle removing task for a group of robotic fish with personalities which describe their willingness to be an initiator, follower, or free-rider. In order to investigate the evolution of personality and the emergence of effective leadership in the group of robotic fish, we model the obstacle removing scenario as an N-player snowdrift game since the snowdrift game is a typical anti-coordination game that models precisely the type of contributing versus free-riding tendencies in multi-player games. Considering the three possible roles adopted by a fish, a special rule for generating an initiator among the group members is introduced to the game model. Then we discuss the choice of the parameters in the model, and give several variables which should be focused on when analyzing the experimental and simulation results of the model.

6.2.1 N-player snowdrift game with an initiator

We consider an evolving group of N robotic fish engaged in a repeated game, where each stage game is the same N-player snowdrift game that models the obstacle removing task.

Set-up of basic model

In the stage game, each fish must choose between action C (to push the obstacle) and action D (not to push the obstacle). We assume each fish has the same limited capacity when pushing the obstacle, that is, when the fish adopts action C the cost she contributes to the group is at most $c > 0$. A threshold $0 < T \leq N$, $T \in \mathbb{R}$, is defined to represent the difficulty of the obstacle removing task (i.e., the difficulty of removing the obstacle). Then the total costs required for removing the obstacle is defined by $g(T)$ which is a function of the threshold T. Here we assume

$$g(T) = cT, \tag{6.1}$$

which implies that the more difficult the obstacle removing task is, the lager the total cost is required. Denote $n_C \geq 0$ to be the number of C-players in the group. Note that the C-player can contribute c at most. It follows that when $n_C \geq T$, each C-player pays a cost $\frac{g(T)}{n_C} = c\frac{T}{n_C}$. On the other hand, when $n_C < T$, each C-player gives her best to pay a cost c. Considering the environmental noises, the likelihood of the success of the obstacle removing task is assumed to be described by the probability function

$$f(n_C, T) = \frac{1}{1 + \exp[-\beta(n_C - T)]}, \tag{6.2}$$

where β is a constant that denotes the steepness of the function. For $\beta = 0$, the probability of success $f(n_C, T)$ is a constant 0.5 which implies that the success of the obstacle removing task is independent of the number of the fish participating in pushing the obstacle. On the other extreme, for $\beta = +\infty$ the probability of success becomes steplike so that the obstacle removing task is success exactly when the number of C-players exceeds the threshold T (i.e., $n_C \geq T$). For clarity, the probability of success $f(n_c, T)$ is plotted in Fig. 6.3 for different values of β. Here we take the success of probability $f(n_C, T)$ as the benefit of completing the obstacle removing task for each fish.

So each fish gets the benefit $f(n_C, T)$, while C-players try their best to share the total costs $g(T)$ and D-players pay nothing. Then we summarize the payoffs of C-player and D-player, denoted by P_C and P_D respectively, as follows:

$$\begin{aligned} P_C &= \begin{cases} f(n_C, T) - c & \text{when } 0 \leq n_C < T \\ f(n_C, T) - c\frac{T}{n_C} & \text{when } n_C \geq T \end{cases}; \\ P_D &= f(n_C, T). \end{aligned} \tag{6.3}$$

Introduce personalities as strategies

To decide how to choose between actions C and D in the stage game, we introduce strategies $s_i \in (0, 1]$ for fish i, $i = 1, 2, \ldots, N$, as their personalities. It means that a robotic fish with a bolder personality has a higher value of strategy. Thus the strategy corresponds to the fish's willingness to initiate a collective movement in the obstacle removing task. For convenience of description, a robotic fish is called "bold fish" if its strategy satisfies $s_i > 0.7$; while the one is called "shy fish" if its strategy satisfies $s_i < 0.3$. Moreover, denote n_B to be the number of bold fish in the group.

To reflect the biological observation that a bold fish is more likely to become an initiator, we associate each robotic fish with an exponentially distributed random

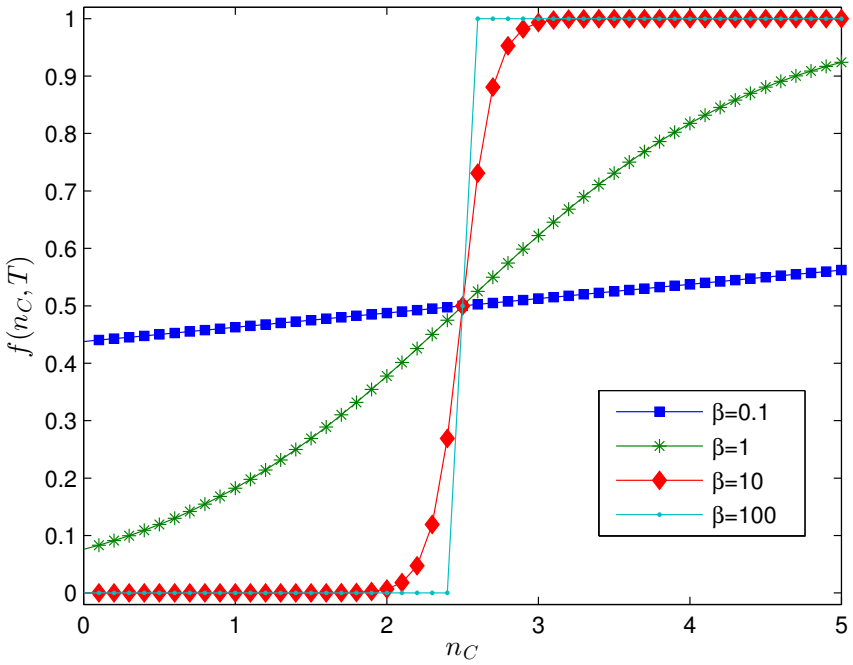

Figure 6.3: The probability of success $f(n_c, T)$ for different values of β where $N = 5$ and $T = 2.5$.

variable t_D, called "decision time", whose mean (expected value) is $\frac{1}{s_i}$; a fish will take the initiative to lead the group task if when its decision time comes, no other fish has become the initiator yet. Thus, the fish whose decision time is the shortest becomes an initiator, but since no fish knows about the t_D of other fish, each fish does not know a priori whether itself might be an initiator or leader in the group. Once an initiator appears, with the probability $1 - s_i$ each of the other $N - 1$ fish becomes a follower participating in pushing, and consequently each of them becomes a free-rider with the probability s_i. Here we have chosen the inverse correlation between boldness and likelihood to become a follower that we described before because of the assumption that the willingness to be an follower is inversely correlated with that to be an initiator. So we have specified how a fish takes its role of initiator, follower or free-rider. Accordingly, the single initiator and its followers (if any) are considered as C-players, while the free-riders as D-players.

Rules for evolving personalities

After each stage game, the initiator's strategy evolves according to the following standard update rule [4, 36, 71]

$$s_0(k+1) = r\lambda + s_0(k)(1-\lambda), \quad k = 0, 1, 2, \ldots \tag{6.4}$$

where $s_0(k)$ and $s_0(k+1)$ denote the initiator's strategy in the current stage game and that in the next stage game, respectively. Here $\lambda \in (0, 1)$ is the strategy update rate and r is the reinforcement value used to update the strategy. In our case, the reinforcement value is $r = 1$ if the group of robotic fish complete the obstacle removing task, while it is $r = 0$ if the group fails at the task. Thus the update rule (6.4) implies a positive feedback for the initiator. If the initiator successful leads an collective movement with which the obstacle can be removed and the obstacle removing task is completed, her willingness to be an initiator will increase; otherwise, her willingness to initiate a collective movement in doing the obstacle removing task will decrease. Notice that the main idea of this update rule is self-learning, while the rule (5.15) we used in the previous chapter is a different kind of update rule, which focuses on comparison and imitation of others.

6.2.2 Parameters and variables

Based on the N-player evolutionary game model which describes the obstacle removing scenario we are interested in, we further discuss the choice of the parameters, and also mention several quantities which should be focused on when analyzing the experimental and simulation results.

Choice of parameters

Considering the space limitation and hardware constraints, such as the battery life, of the real robotic fish system, we choose a small group size N (up to 5) and large strategy update rate λ (0.9) in the experiments, so that a short-term evolution is able to characterize the evolutionary process. In other words, the total number of tasks within a single evolution process does not need to be too large. Thus we assume each evolution consists of 100 tasks for the experiments. Fortunately, the simulations do not have such limitation or constraints. It allows us to investigate more possible situations as effective complements to the experimental results. So we choose different group size N (from 2 to 30) and strategy update rate λ (from 0.1 to 0.9), and study the long-term evolution within 10000 tasks by simulations.

In addition, the time limit of each task is necessary for the experiments. When the time limit is passed, the group of robotic fish in effect fails the task and has to

stop. In other words, the fish group succeeds if and only if they can remove the obstacle within the time limit. Here we set the time limit to be 30s.

The threshold T and steepness β, which imply the difficulty of an obstacle removing task, are not used in experiments. It is because whether the task was successful or not can be directly seen from the experiment (i.e., whether the obstacle has been removed or not), rather than calculated the probability of success $f(n_C, T)$ by Eq. (6.2). Nevertheless, we will show that the expression of $f(n_C, T)$ in our game model is suitable for describing the difficulties of obstacle removing tasks in experiments. Based on this experience from the real robotic fish system, we choose the steepness $\beta = 10$ and different numbers for T (from $0.1N$ to N) according to the group size N in simulations. Please see more details in Section 6.3.2.

The fish's maximal cost c, which only affects the calculation of the payoffs, can be seen as a coefficient of the benefit and cost in Eq. (6.3). However, in order to gain insight into the evolutions, we prefer to investigate the benefit and cost separately in the following analysis. Thus we ignore the value of the maximal cost c here. Note that the maximal cost c would be important when the payoffs react on the update of the strategies. This situation will be studied in our future work.

Moreover, we will validate by simulations that the robots' strategies at the beginning of the evolution would hardly ever affect the results. Thus we set the initial strategy of each fish to 0.5 in all the experiments and simulations.

Quantities to be analyzed

The aim of our research is to study how personality evolves and effective leadership emerges in the group of robotic fish when doing obstacle removing tasks. Thus, we focus on the evolving strategies s_i and further the roles of the robots. We also pay attention to the performance of the fish groups.

As we have mentioned above, the strategy of fish i is denoted by s_i and the bold fish is the one whose strategy satisfies $s_i > 0.7$. Here we use $n_B \geq 0$ to denote the number of bold fish in the group. Considering the evolving roles of the robots, n_C shows the number of C-players in the group. In order to investigate the change of the key role, initiator, we denote I_n as the label of the initiator in each task. Moreover, we also analyze the percentage of the roles for each fish during a single evolution.

To study the performance of a fish group when doing obstacle removing tasks, the success rate, the percentage of successful tasks during an evolution, is considered as an important index. In addition, we also record the time used for each task in the experiments. Because of the time limit (30s) mentioned previously, one can easily check that the time-cost of a certain task is smaller than (resp. equals to) 30s

means that the group succeeds (resp. fails) in this task. Furthermore, the finishing time also implies the efficiency of the group to complete a task which cannot be shown in our model or from simulations. This inspires us to improve the proposed model to get closer to the real situations in our future work.

In this section, we model the obstacle removing scenario as an evolutionary game and discuss the choice of the parameters in the model. Furthermore, we emphasize several quantities which should be focused on when analyzing the model. In the following two sections, we will show the results from experiments and simulations, respectively.

6.3 Experimental results

In this section, we first choose three different obstacles for three obstacle removing tasks with different difficulties, respectively. We further show that the expression of $f(n_C, T)$ in Eq. (6.2) can describe the probability of success for real robotic fish system. Then we run experiments of the obstacle removing tasks with a group of N robotic fish and analyze the results.

6.3.1 Obstacle and its difficulty

We choose three obstacles and label them by obstacle 1, 2, and 3 according to the ascending order of their weights; more concretely, the weights of obstacle 1, 2, and 3 are 1.6 kg, 2.0 kg, and 2.5 kg, respectively. Note that the property we are interested in of an obstacle is the difficulty of its corresponding obstacle removing task. In other words, we mainly focus on the success rate when a group of robotic fish containing n_C C-players is doing the obstacle removing tasks with a certain obstacle. For this purpose, experiments are carried out to estimate the success rate when n_C C-players engage in removing the obstacle together. We choose $n_C = 1, 2, 3, 4, 5, 6$ and obstacles $1, 2, 3$, and then run 100 experiments for each pair of n_C and an obstacle to calculate the corresponding success rate. The time limit of each experiment is still 30s.

We summarize the results in Table 6.1. One can see that the success rate is sensitive to n_C, the number of the fish participating in pushing the obstacle, in a certain range. More precisely, it is impossible to remove any of the three obstacles when $n_C = 1$. When n_C increases to 2, the fish players succeed in 57% of the 100 runs for obstacle 1 while still fail for obstacles 2 and 3. When $n_C = 3$, the players always achieve success for obstacle 1 and succeed in 88% of the 100 runs for obstacle 2; however it still fails for obstacle 3. When n_C goes to 5, the players always achieve

Table 6.1: Properties of three chosen obstacles

Success Rate	$n_C = 1$	$n_C = 2$	$n_C = 3$	$n_C = 4$	$n_C = 5$	$n_C = 6$
obstacle 1	0%	57%	100%	100%	100%	100%
obstacle 2	0%	0%	88%	100%	100%	100%
obstacle 3	0%	0%	0%	0%	86%	100%

success for both obstacles 1 and 2, and succeed in 86% of the 100 runs for obstacle 3. Additionally, the above data agree with the fact that obstacle 1 is the easiest one while obstacle 3 is the most difficult one among the three. Note that there is a chance for potential free-riders no matter which obstacle is present, so the appearance of effective leadership does not require all the fish to become cooperative.

Until now, we have the success rates of different numbers of C-players for each obstacle, which will be used to select the parameters of function $f(n_C, T)$ (6.2) in the model.

6.3.2 Selection of parameter β via experiments

In the proposed N-player game, the probability of success for the obstacle removing task is modeled by the function $f(n_C, T)$ with the parameter β in Eq. (6.2). Notice that T denoting the difficulty of the obstacle removing task differs for tasks with different obstacles, while β is assumed to be a common constant for different T. To estimate the parameter β, the Curve Fitting Tool from MATLAB is used to fit the proposed model $f(n_C, T)$ in Eq. (6.2) to the experimental data of three obstacles shown in Table 6.1. Since n_C can only be an integer, the experimental data are too few to get an exclusive examination of the pair (β, T). However, one can check that when β satisfies $\beta \geq 9$, the goodness-of-fit (the SSE's are in the order of 10^{-6}; RMSE's are less than 0.001) is acceptable. On the other hand, when β goes to $+\infty$ the probability of success becomes steplike which is a quite special case. In order to mimic a more general case, we fix $\beta = 10$ in our studies.

We further use the Curve Fitting Tool to fit the model (6.2) under $\beta = 10$. Then one can get an exclusive examination of T for each obstacle in this case. We show the fitting results for the three obstacles in Fig. 6.4 and Table 6.2. The results demonstrate that the proposed model (6.2) with the estimated T fits the experimental data.

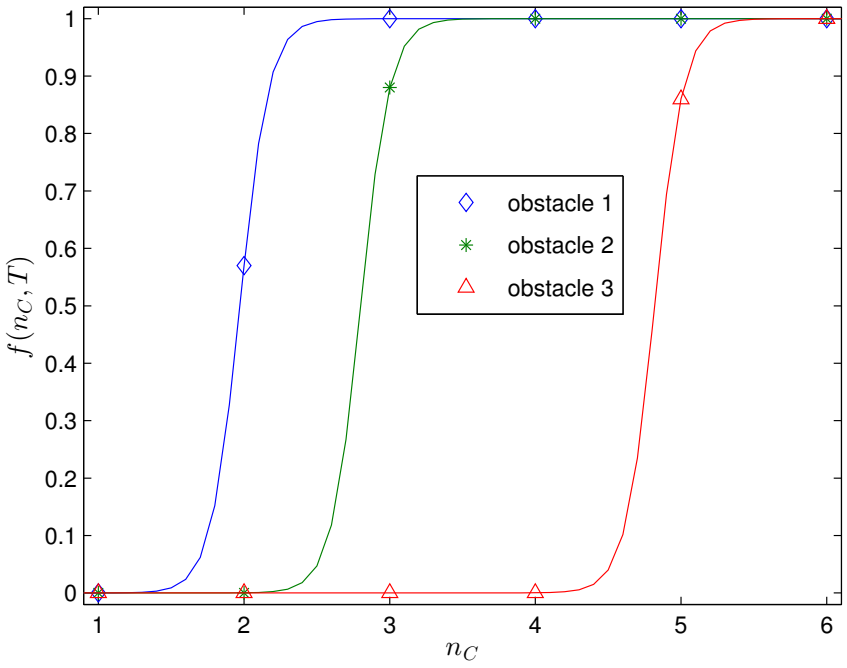

Figure 6.4: Use the Curve Fitting Tool from MATLAB to fit the propose model $f(n_C, T)$ in Eq. (6.2) to the experimental data of three obstacles in Table 6.1 when $\beta = 10$.

Table 6.2: Estimation of T and goodness-of-fit under $\beta = 10$

	T	SSE	R-square	RMSE
obstacle 1	1.972	4.974×10^{-9}	1	3.097×10^{-5}
obstacle 2	2.801	1.108×10^{-7}	1	0.0001489
obstacle 3	4.818	7.779×10^{-8}	1	0.0001247

6.3.3 Evolution with fixed tasks

Using the chosen obstacles, we run experiments of the obstacle removing tasks with a group of N robotic fish. As we have mentioned, we choose a small group size

$N = 2, 3, 4, 5$ and a large strategy update rate $\lambda = 0.9$ to investigate the short-term evolution. Then each evolution consists of 100 tasks. The time limit of each task is set to be 30 seconds. We use $T = T_1, T_2, T_3$ ($T_1 < T_2 < T_3$) to represent obstacle $1, 2, 3$, respectively. Notice that the threshold T is not directly used in the experiments, but just shows the difficulty of the obstacle removing tasks with a certain obstacle. Furthermore, considering the properties of three chosen obstacles shown in Table 6.1, we set $N = 2, 3, 4, 5$ for $T = T_1$, $N = 3, 4, 5$ for $T = T_2$, and $N = 5$ for $T = T_3$.

We summarize the results in Table 6.3, and show the corresponding evolutionary processes in Fig. 6.5−6.12. In each figure, the strategies s_i of the N fish, the label of the initiator I_n, the number of C-players n_C, the number of bold fish n_B, and the time cost are shown for each task contained in the evolution. The average of n_C and n_B during each single evolution, which are denoted by $\bar{n}_C$ and $\bar{n}_B$ respectively, as well as the success rate are shown in Table 6.3.

Table 6.3: Summary of Experimental results ($\bar{n}_C, \bar{n}_B$, Success Rate)

	T_1	T_2	T_3
$N = 2$	$1.9300, 0.4158, 41\%$	/	/
$N = 3$	$2.7500, 0.9109, 86\%$	$2.7500, 0.5545, 56\%$	/
$N = 4$	$2.8800, 1.6949, 87\%$	$3.1000, 0.7723, 66\%$	/
$N = 5$	$3.3700, 2.2673, 91\%$	$3.9600, 0.9109, 76\%$	$4.7900, 0.6931, 69\%$

To get a general idea of the experimental results, we first focus on the data in Table 6.3. For a group of N robotic fish, the number of C-players $\bar{n}_C$ increases as T increases. It means that more fish in the group participate in pushing the obstacle when the task is more difficult. It is consistent with the fact that a more difficult task requires more C-players to deal with while the easier one does not need too many C-players. However, note that in our case, the difficulty of the task is unknown to the fish group and the fish do not communicate with each others. Thus, this phenomenon implies that *the fish group has some ability of self-adaptation to fit with the difficulties of the obstacle removing tasks*. On the other hand, the number of bold fish $\bar{n}_B$ decreases as T increases. It shows that fewer fish are willing to push the obstacle first for a more difficult task, while more fish want to be an initiator for an easier task. Considering the difficult tasks for which a lot of C-players are required to remove the obstacle, the initiator may fail the task because of lack of enough followers with a high probability so that its willingness to initiate is more likely to decrease because

of the feedback by the update rule (6.4). In comparison, for easy tasks, the initiator is more likely to succeed with its followers since the easy tasks do not need too many C-players. Then its willingness to initiate may increase with a high probability. In summary, *more bold fish emerge in the group when the tasks are easier*. Moreover, one can find that the success rate decreases as T increases.

To gain insights into the evolution, we then focus on Fig. 6.5−6.12. It is shown in the figures that the strategies s_i of the individuals in the group do not converge to a common value but show a strong tendency for diversity. As a consequence, the process of role differentiation has occurred after a few steps of the evolution, which is clearly shown by the label of the initiator I_n in the figures. Concretely, the curve of I_n shows that an initiator emerges in the group and remains to initiate the group for a period of time. Note that it also shows the phenomenon of role-switch in the group that such a relative fixed role of initiator may be switched among some of the group members. Moreover, combining the dynamics of the strategies s_i and the corresponding task time, one can find that when the strategies show a clear diversity for a period of time, the group always keep succeeding in the tasks within a short time during this period. See Fig. 6.12 as an example. From around the 54th to the 66th task of the evolution, the group members are separated into two clusters in which their strategies are close to 1 and 0 respectively; while the task time, which is much smaller than the time limit, implies the group quickly achieves success in this case. We can conclude that *more diversity of personalities in the group results in a better performance of succeeding within a short time when doing the obstacle removing tasks*.

Up to now, we have already identified some interesting phenomena from the experimental results. However, as we have mentioned before, only a small region in the parameter space of our game model can be explored by experiments since the real robotic fish system has some limitation and constraints. In the next section, we will run lots of simulations to investigate more possible situations of the game model. These simulations based on the model can be seen as effective complements to the above experimental results, since our proposed model has been verified by fitting the experimental data in Section 6.3.2.

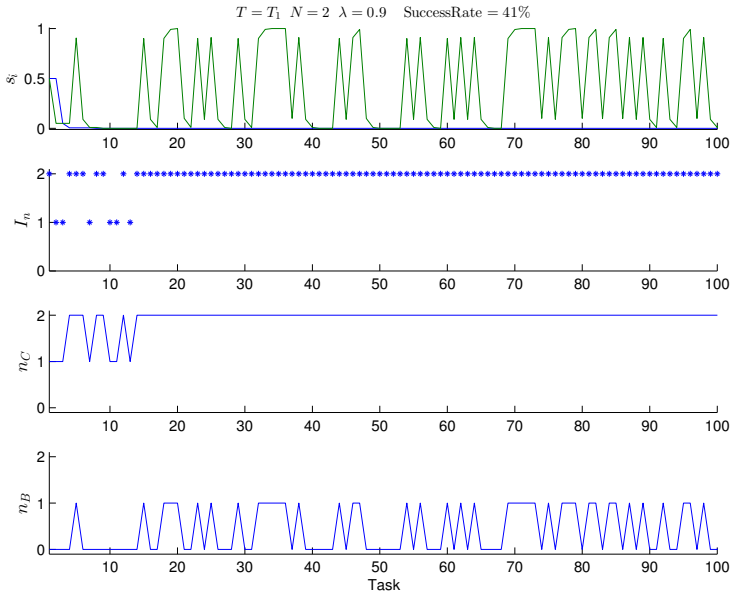

(a)

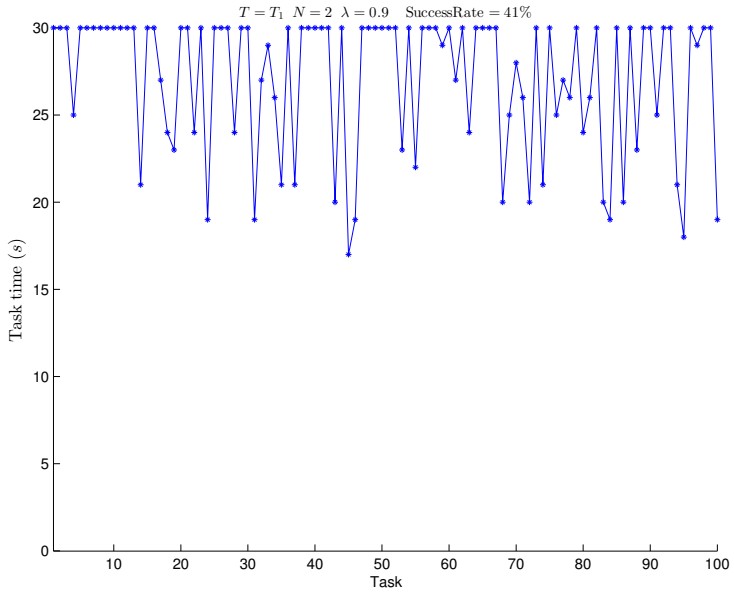

(b)

Figure 6.5: A group of $N = 2$ robotic fish deals with Task 1.

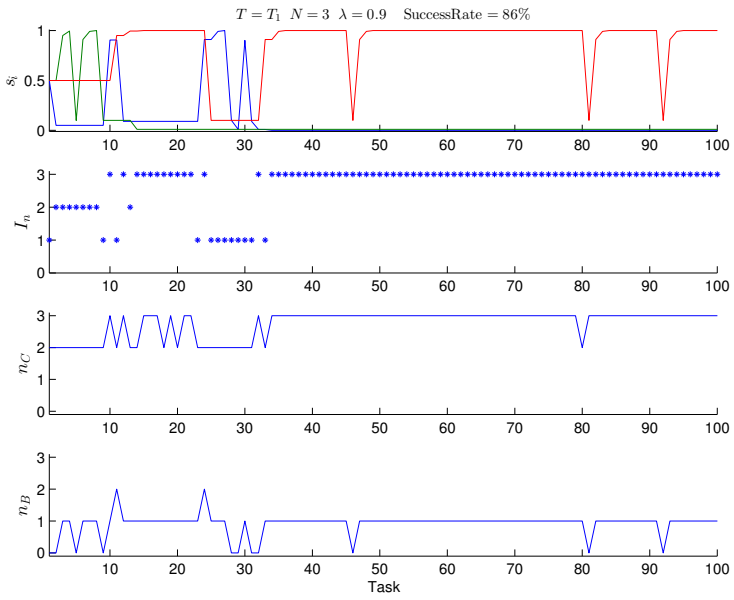

(a)

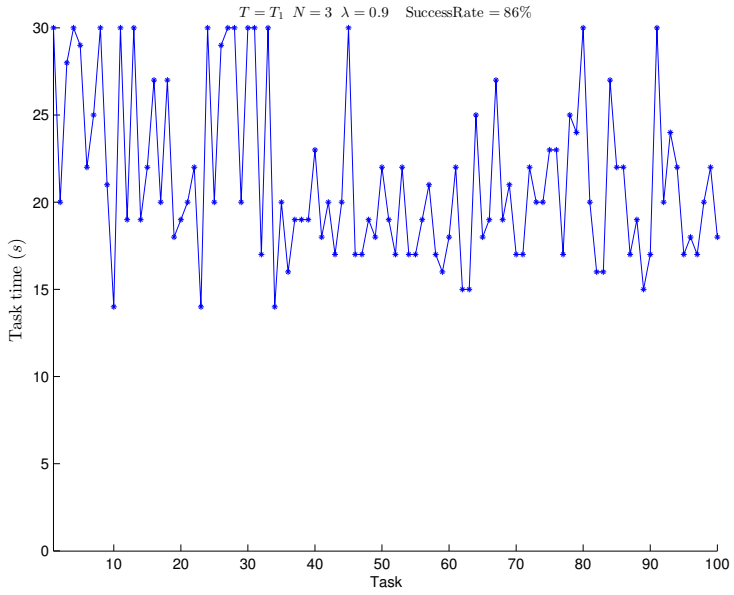

(b)

Figure 6.6: A group of $N = 3$ robotic fish deals with Task 1.

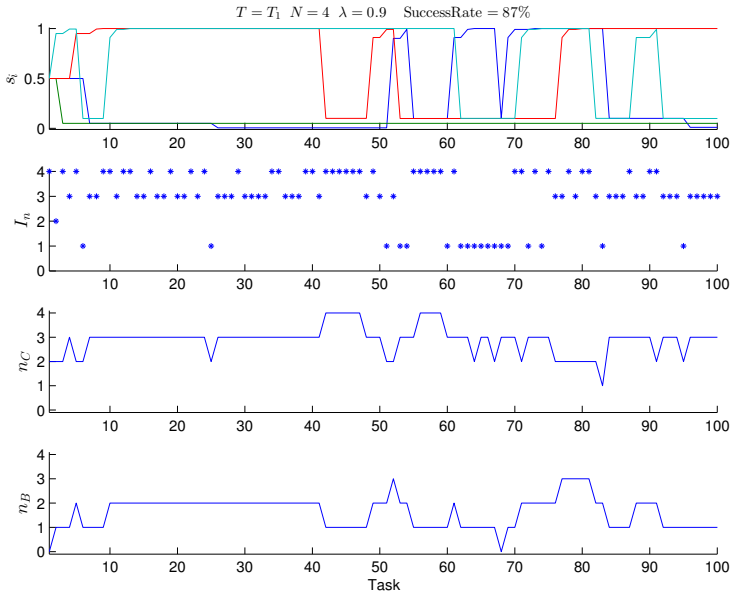

(a)

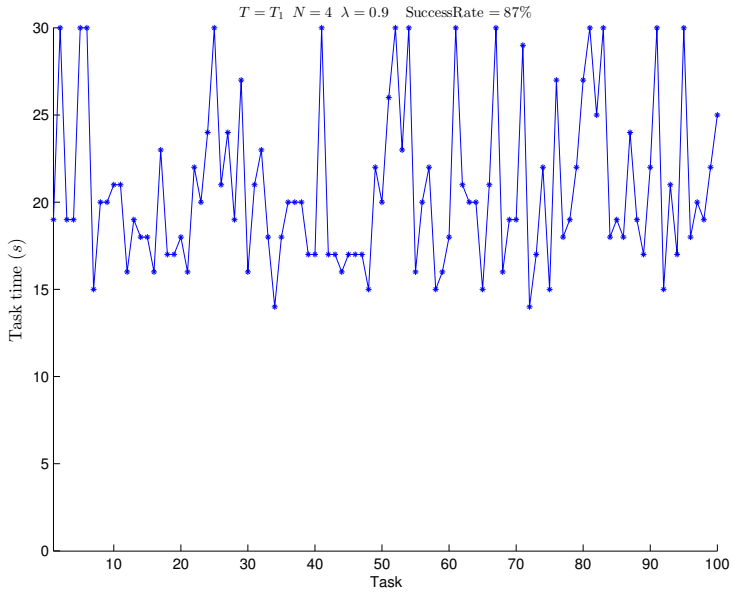

(b)

Figure 6.7: A group of $N = 4$ robotic fish deals with Task 1.

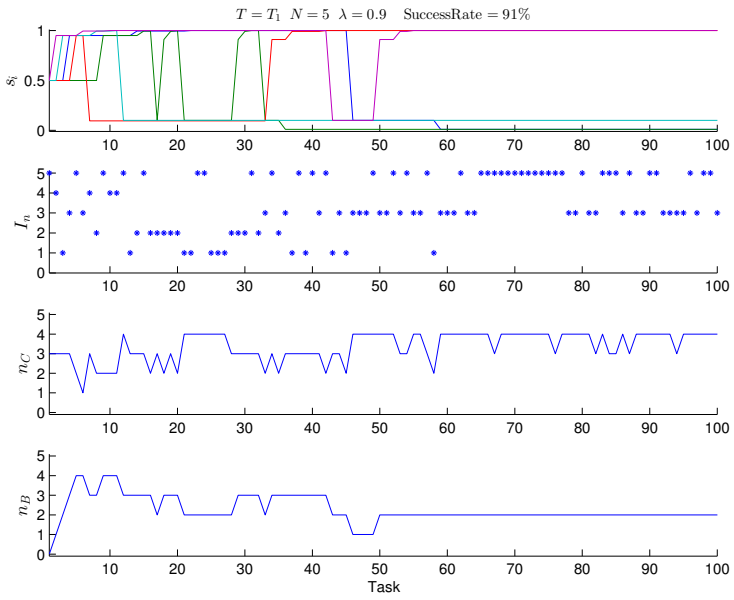

(a)

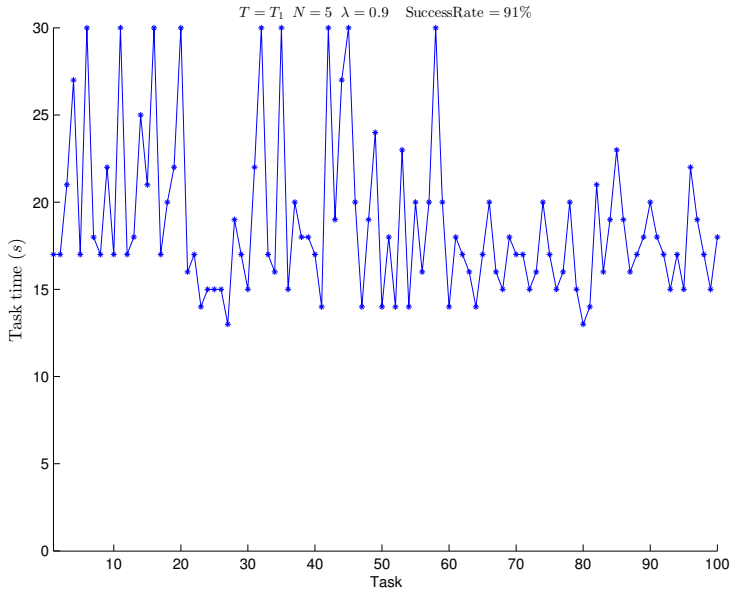

(b)

Figure 6.8: A group of $N = 5$ robotic fish deals with Task 1.

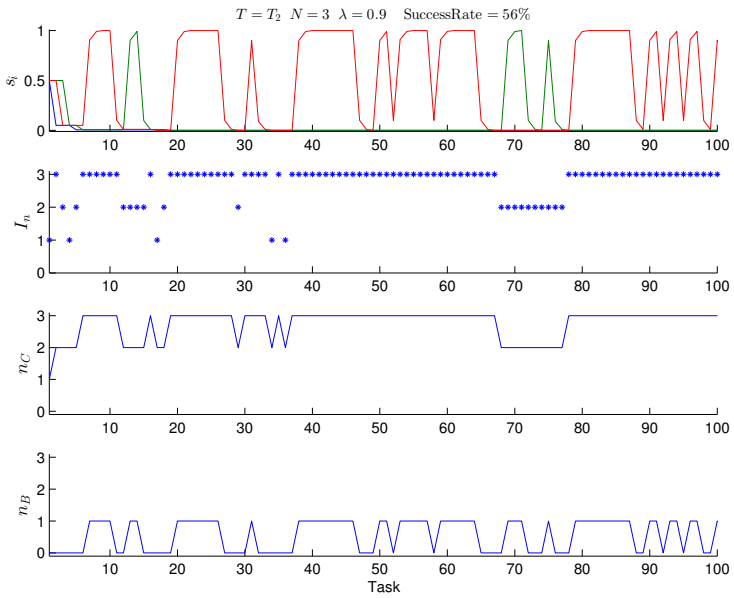

(a)

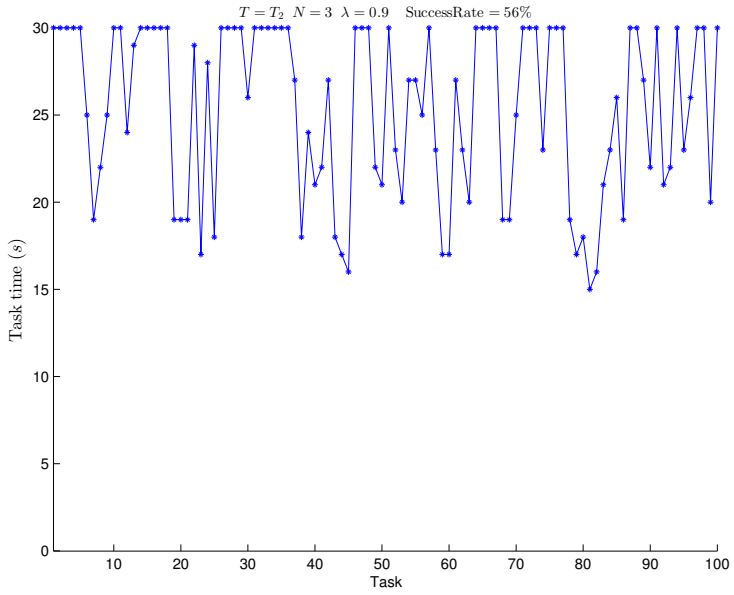

(b)

Figure 6.9: A group of $N = 3$ robotic fish deals with Task 2.

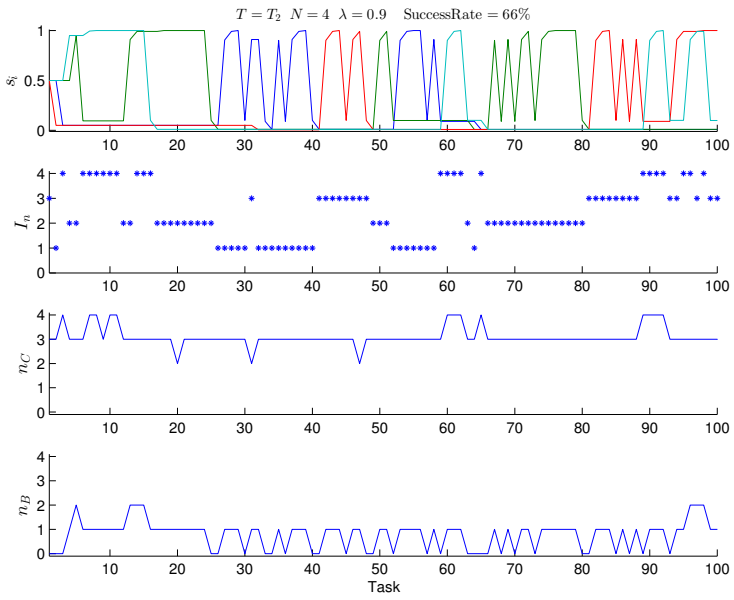

(a)

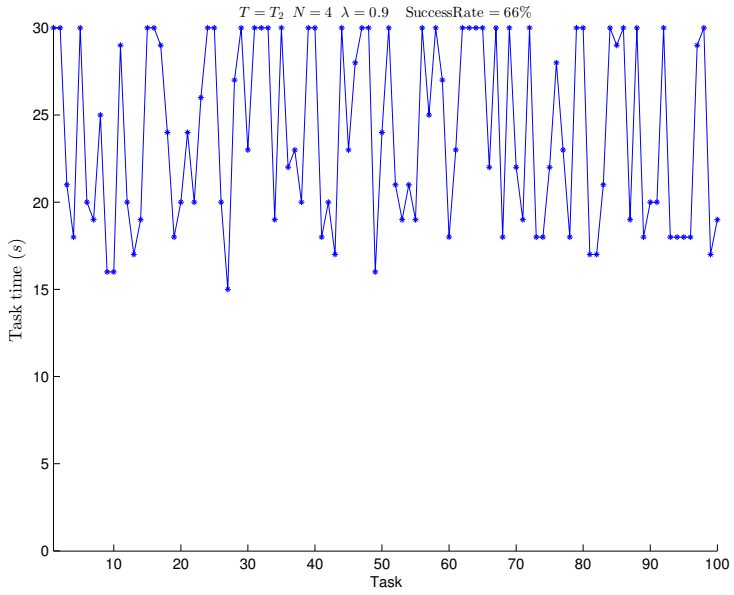

(b)

Figure 6.10: A group of $N = 4$ robotic fish deals with Task 2.

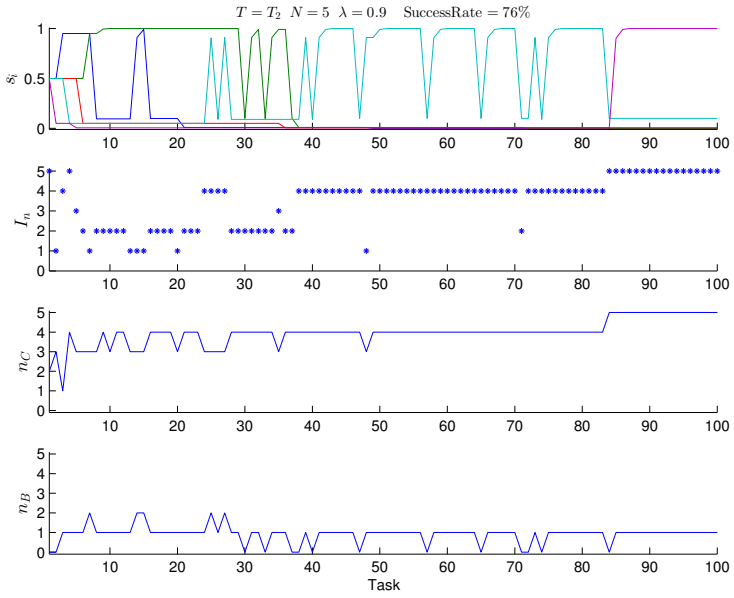

(a)

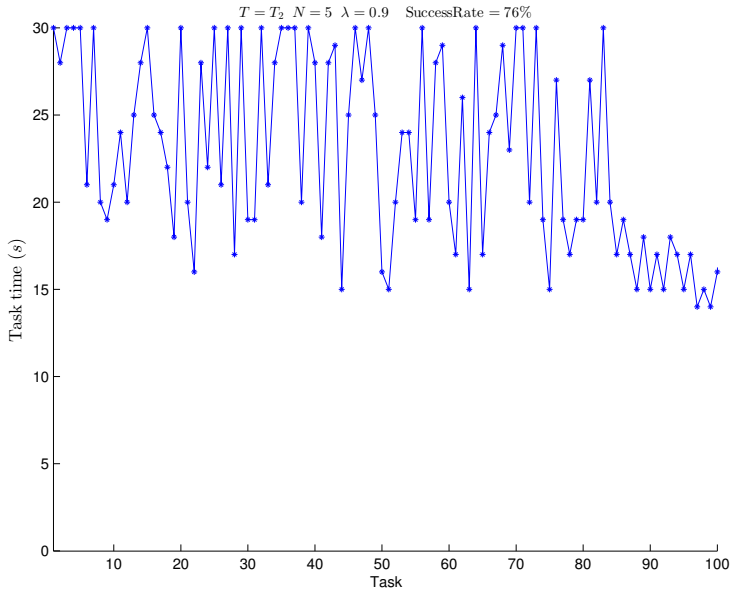

(b)

Figure 6.11: A group of $N = 5$ robotic fish deals with Task 2.

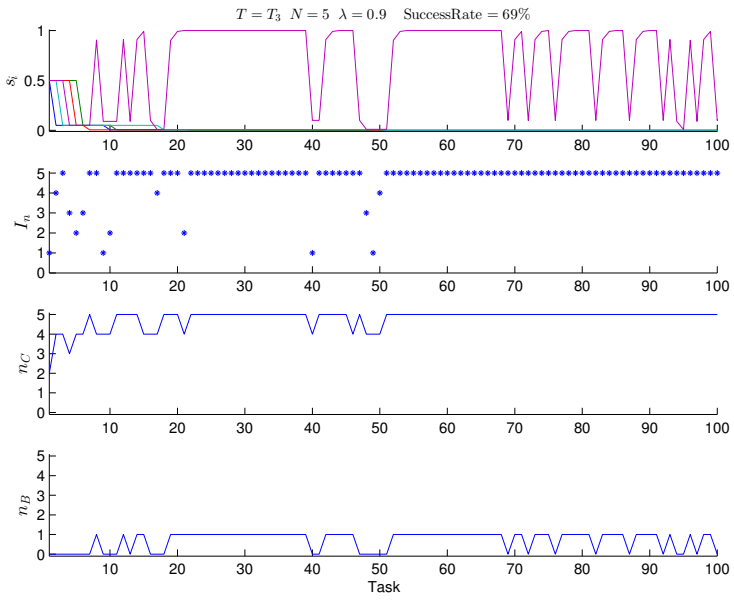

(a)

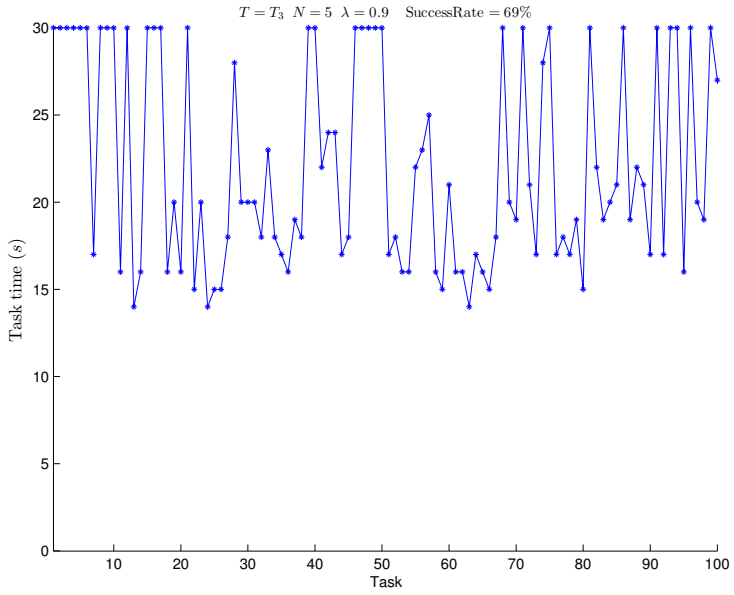

(b)

Figure 6.12: A group of $N = 5$ robotic fish deals with Task 3.

6.4 Simulation results

In this section, we first repeat the evolution with fixed tasks by simulations similar to what has been done in experiments in the previous section, but within a much larger region in the parameter space. Then we investigate the situation when the difficulty of the tasks can change during a single evolution process.

6.4.1 Evolution with fixed tasks

We choose several typical situations to show the evolutionary process with fixed tasks. We choose group size $N = 10$ and $T = 0.1N, 0.4N, 0.9N$ to represent the easy task, moderate one, and difficult one, respectively. The strategy update rate λ is set to 0.4 as a long-term evolution and 0.9 as a short-term one. Then 10000 tasks are performed in a single evolution.

The simulation results are shown in Fig. 6.13 $-$ 6.18. Similar to what has been shown in the experiments, the strategies s_i of the N fish, the label of the initiator I_n, the number of C-players n_C, the number of bold fish n_B, and the success rate are shown in each figure. In addition, a histogram is used to show the percentage of the roles for each fish during a single evolution.

From the figures, one can check that the number of C-players n_C is around a lower level when the task is easier, while n_C is in a higher level when the task is more difficult. This result is consistent with what we have indicated by experiments. In addition, a more interesting phenomenon is shown by the simulation results that *the number of C-players is always around T*. To show this clearly, we have drawn the value of T in red in the subplot n_C in each figure. On the other hand, *the number of bold fish n_B is always around $N - T$*, which is also consistent with what we have indicated by experiments. Similarly, the value of $N - T$ has been drawn in red in the subplot n_B in each figure.

Then we focus on the dynamics of strategies s_i and the label of the initiator I_n together with the percentage of the roles for each fish during a single evolution. One can find that when the update rate $\lambda = 0.9$, the strategies of the individuals in the group show a strong tendency for diversity and the process of role differentiation has occurred. This phenomenon is identical with what has been shown in the experiments. However, when the update rate $\lambda = 0.4$, which has not been adopted in experiments, the percentage of the roles for each fish looks similar with each other's. It implies that *the diversity of personalities and the process of role differentiation emerge in a short-term evolution*.

Finally, the simulations also show that the success rate increases as the update rate λ increases when T is fixed, while the success rate decreases as T increases when

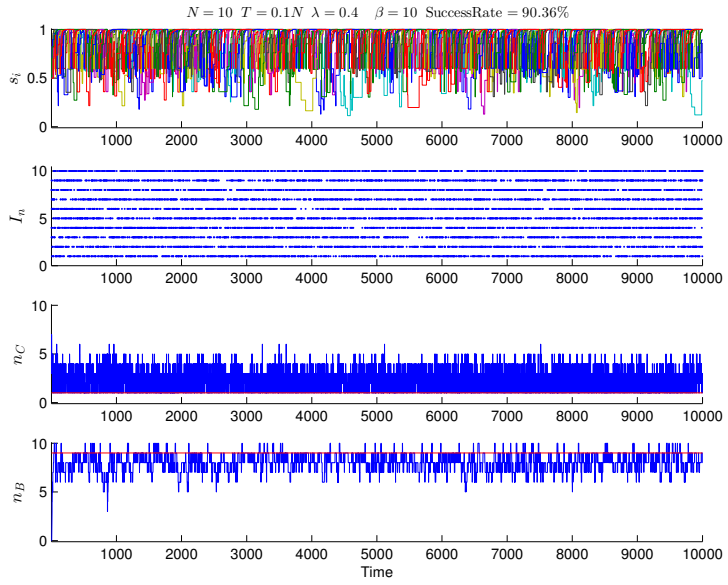

(a)

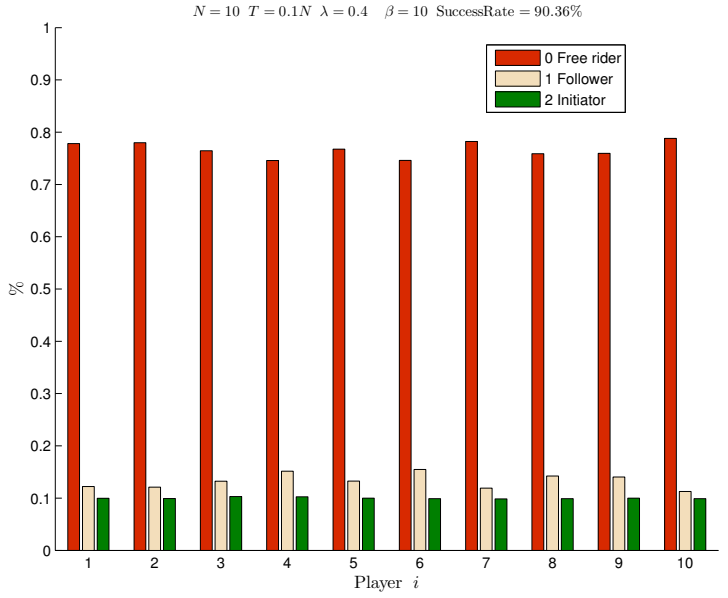

(b)

Figure 6.13: A group of $N = 10$ robotic fish deals with fixed tasks, where $T = 0.1N$ and strategy update rate $\lambda = 0.4$.

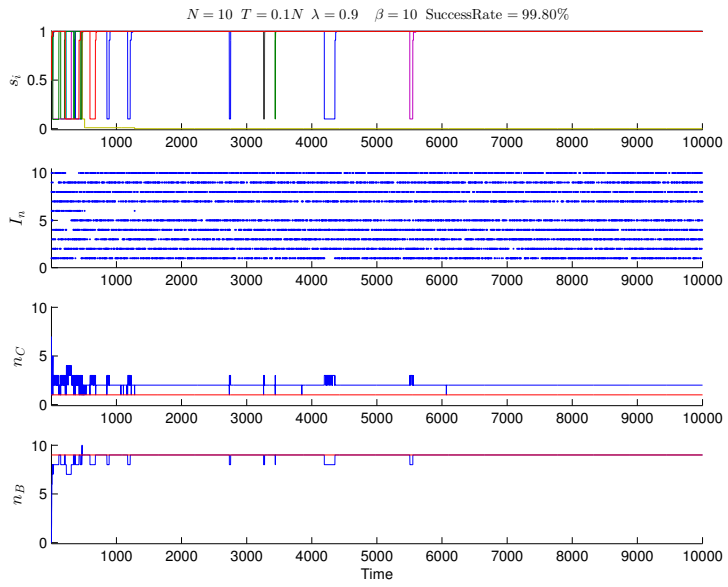

(a)

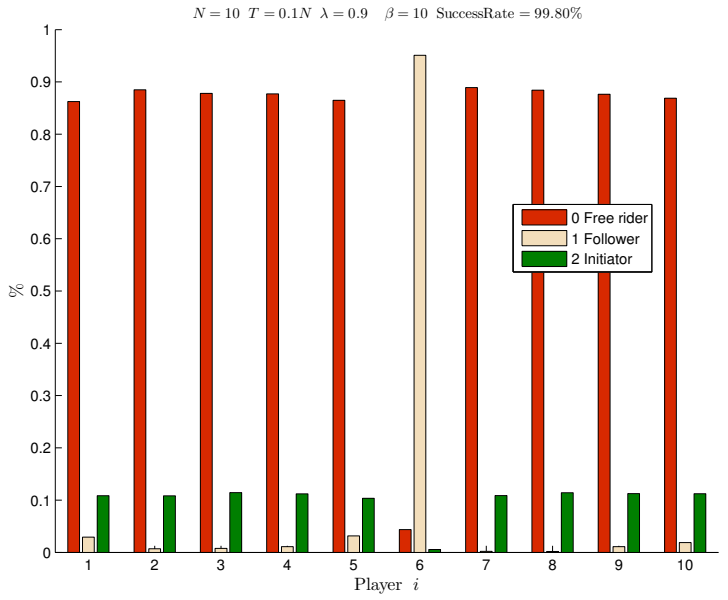

(b)

Figure 6.14: A group of $N = 10$ robotic fish deals with fixed tasks, where $T = 0.1N$ and strategy update rate $\lambda = 0.9$.

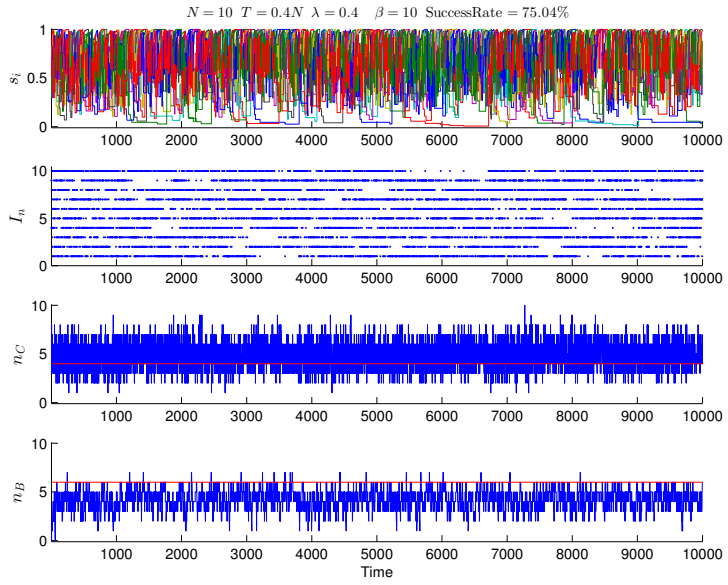

(a)

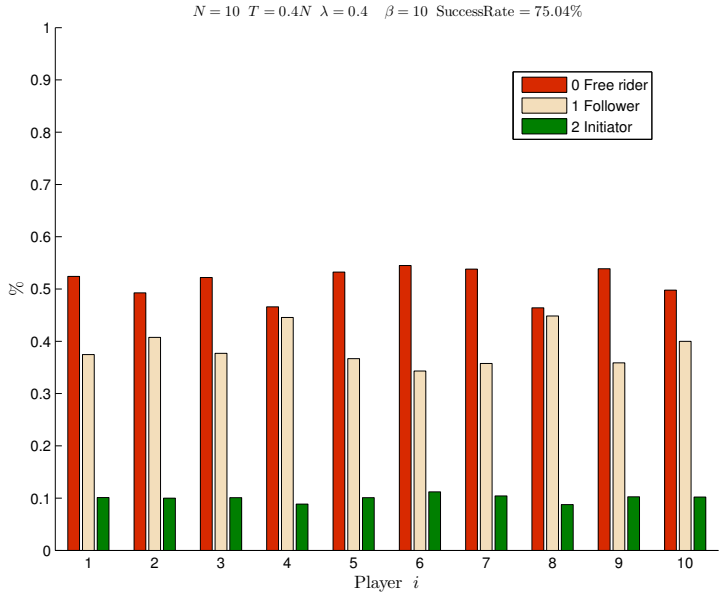

(b)

Figure 6.15: A group of $N = 10$ robotic fish deals with fixed tasks, where $T = 0.4N$ and strategy update rate $\lambda = 0.4$.

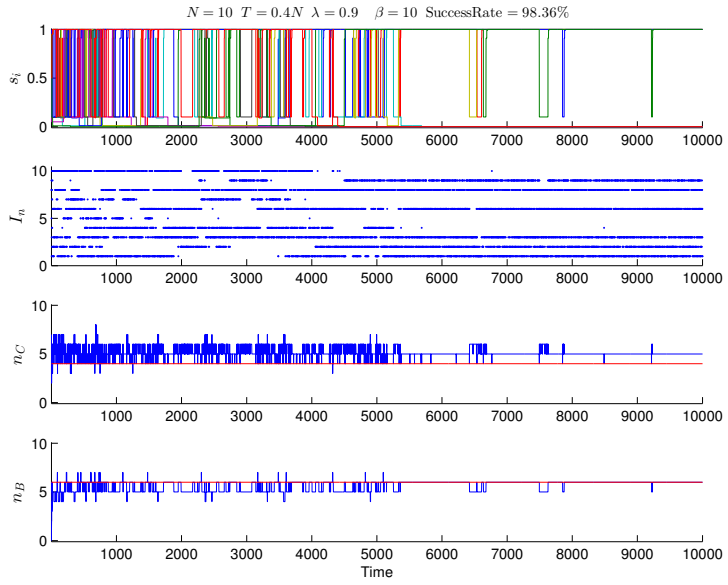

(a)

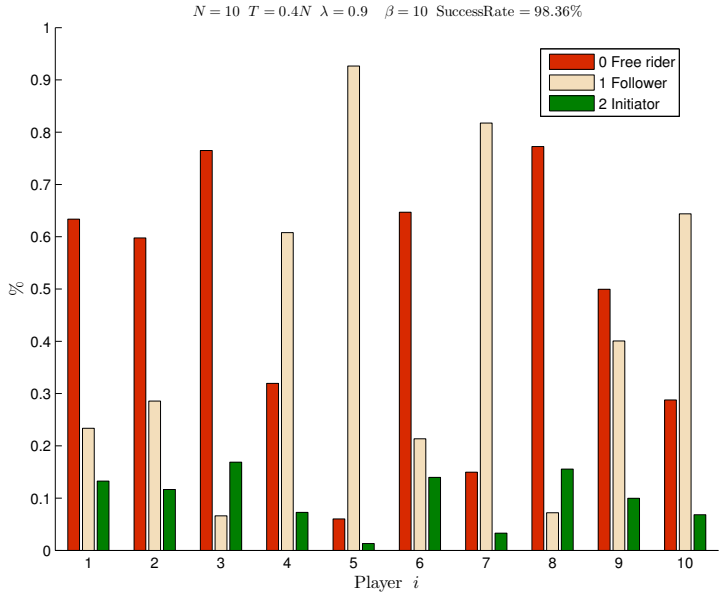

(b)

Figure 6.16: A group of $N = 10$ robotic fish deals with fixed tasks, where $T = 0.4N$ and strategy update rate $\lambda = 0.9$.

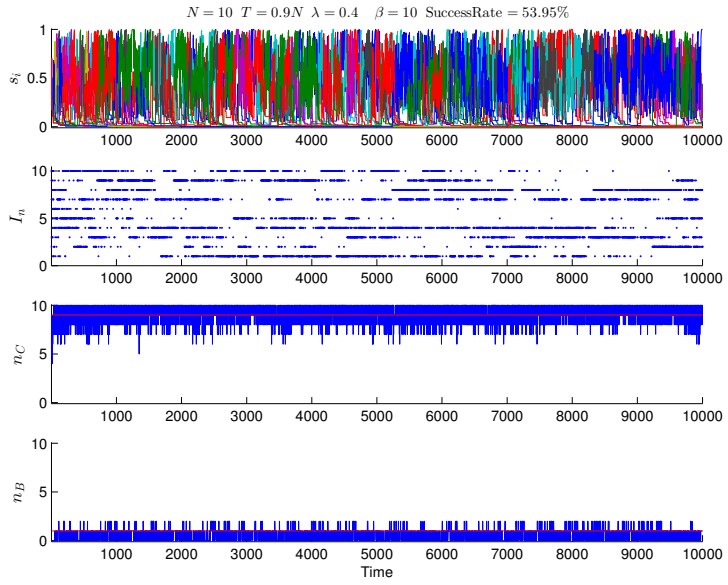

(a)

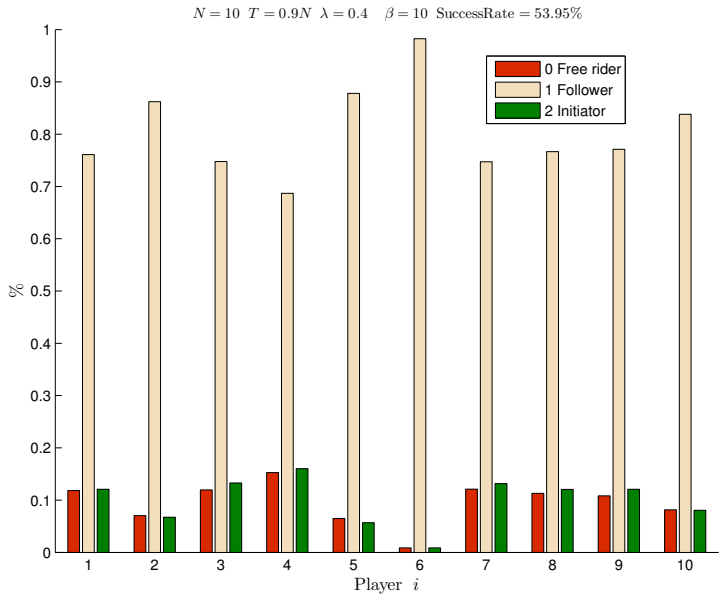

(b)

Figure 6.17: A group of $N = 10$ robotic fish deals with fixed tasks, where $T = 0.9N$ and strategy update rate $\lambda = 0.4$.

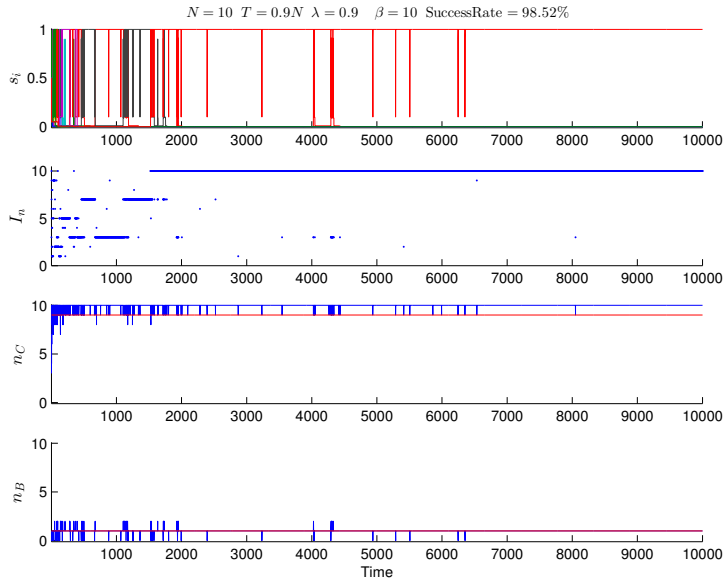

(a)

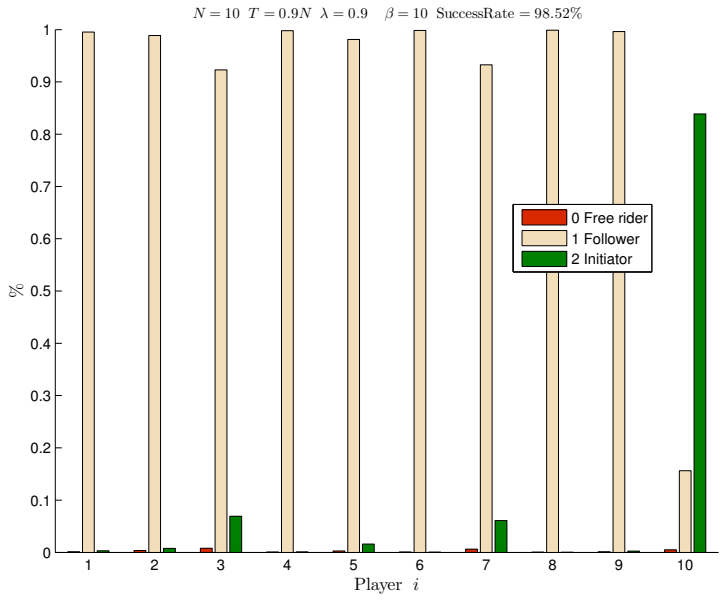

(b)

Figure 6.18: A group of $N = 10$ robotic fish deals with fixed tasks, where $T = 0.9N$ and strategy update rate $\lambda = 0.9$.

the update rate λ is fixed. Note that the large update rate implies the emergence of the diversity of personalities in the group as we have mentioned. Thus it can be seen as an evidence of the conclusion from the experiments that the diversity of the personalities in the group results in a good performance of doing a certain obstacle removing task.

6.4.2 Further statistical analysis

In order to show more situations viewed from more general angles, we present statistical results for the evolution with fixed tasks. We choose the group size $N = 2, 3, ..., 11, 20, 30$, the strategy update rate $\lambda = 0.1, 0.2, ..., 0.9$, and threshold $T = 0.1N, 0.2N, ..., N$. Each evolution consists of 10000 tasks as well. In order to get the statistical results, each data point is the average of 100 runs.

The simulation results are shown in Fig. 6.19 − 6.34. Here we focus on four quantities: (a) $\frac{n_C}{N}$, the proportion of C-players in the group; (b) $\bar{s}_i$, the average strategies of the group; (c) $\frac{n_B}{N}$, the proportion of bold fish in the group; and (d) the success rate.

For each fixed group size N, we investigate the dynamics of the four quantities under different update rate λ and different T. We select the cases of $N = 2, 6, 30$ as typical situations and show the corresponding simulation results in Fig. 6.19 − 6.30. One can check that the dynamics of these four focused quantities are in accordance with the above conclusions. We want to clarify here why some differences in details exist among the three typical cases $N = 2, 6, 30$. We can see from Fig. 6.27 − Fig. 6.30 that the curves separate with each other and show a quite clear tendency when $N = 30$. Although the curves when $N = 2, 6$ show similar tendencies, some cross and overlap exist, especially when $N = 2$. The reason is that the sampling step of T, $0.1N$, is not large enough to distinguish the impact of two neighboring sampling points of T on the group, when the group size N is too small. As N increases, this situation gets better and then completely disappears when N exceeds 6. That is why we choose $N = 2, 6, 30$ as typical cases to show the results.

We further compare the dynamics of these quantities under the same task difficulty level relative to the group size N, $\frac{T}{N}$. Two typical cases of $T = 0.1N$ and $T = N$ are shown in Fig. 6.31 − 6.34. Combining with the results when $N = 2, 6, 30$, we find that the group size N hardly affects the tendency of the focused quantities.

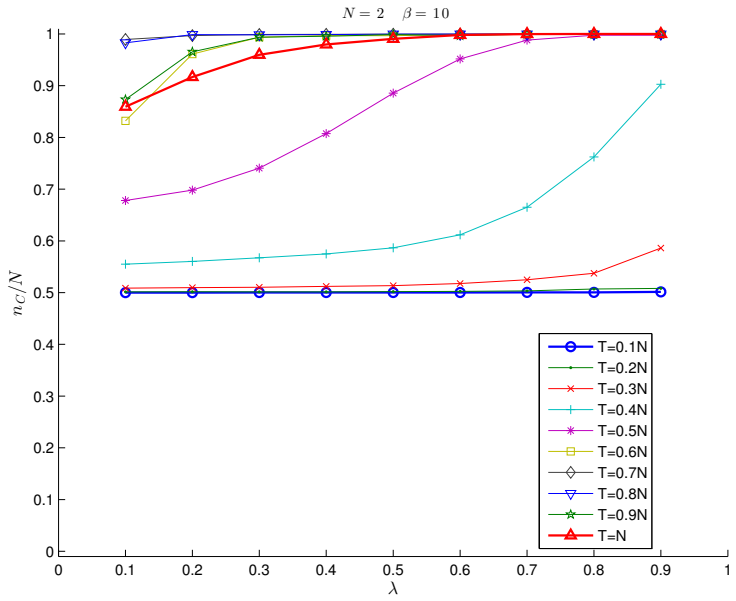

Figure 6.19: The proportion of C-players in the group for different T when $N = 2$.

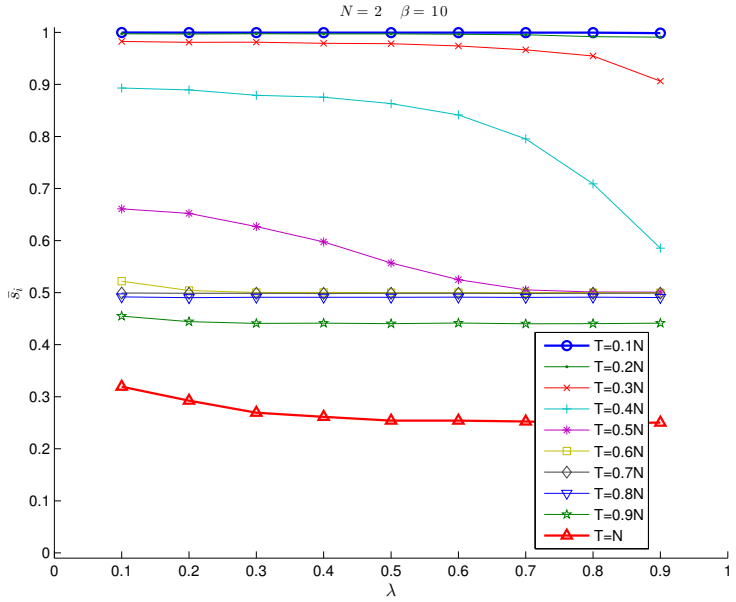

Figure 6.20: The average strategy of the group for different T when $N = 2$.

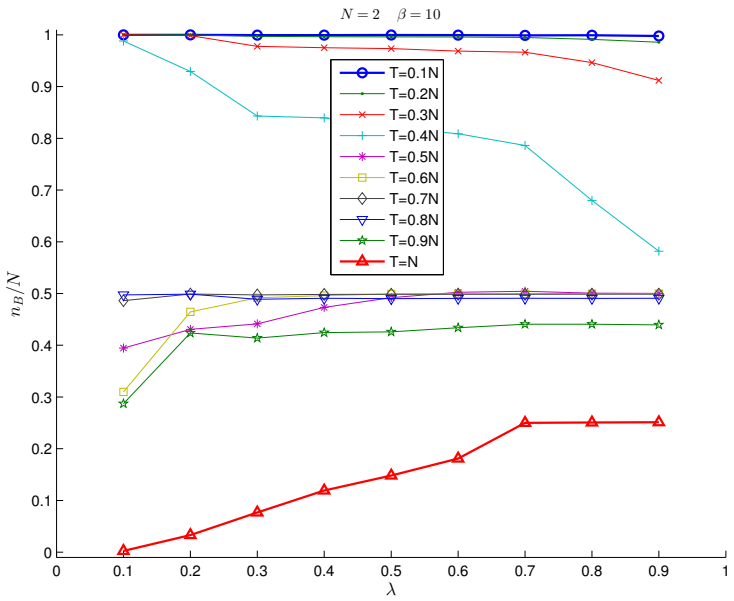

Figure 6.21: The proportion of bold fish in the group for different T when $N = 2$.

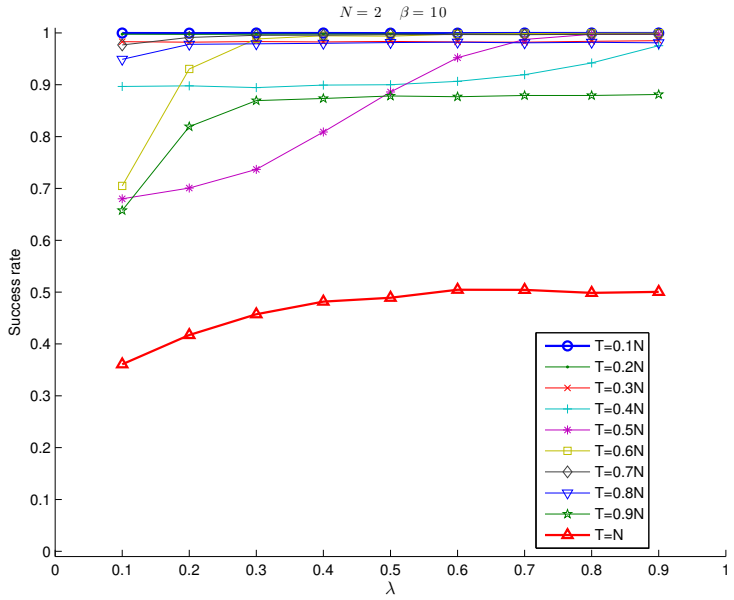

Figure 6.22: The success rate for different T when $N = 2$.

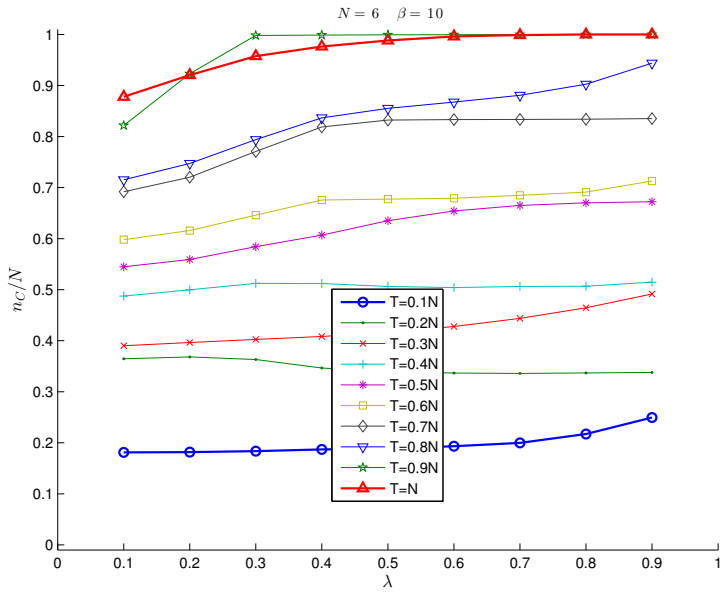

Figure 6.23: The proportion of C-players in the group for different T when $N = 6$.

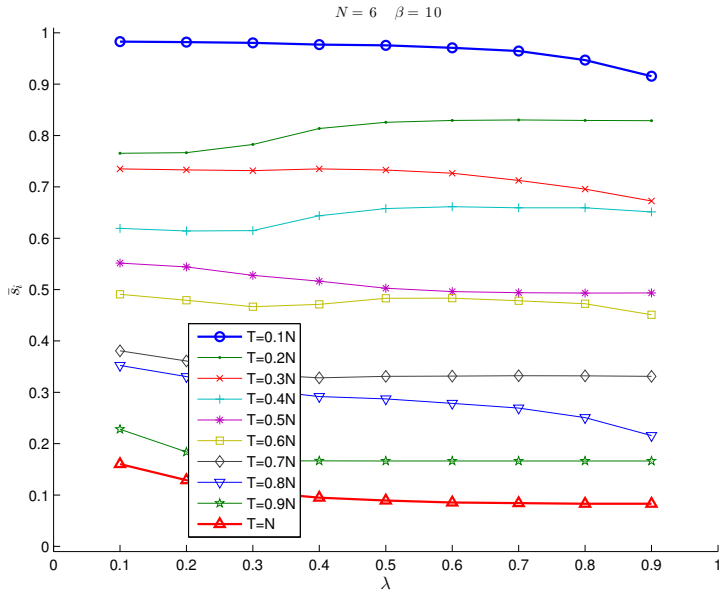

Figure 6.24: The average strategy in the group for different T when $N = 6$.

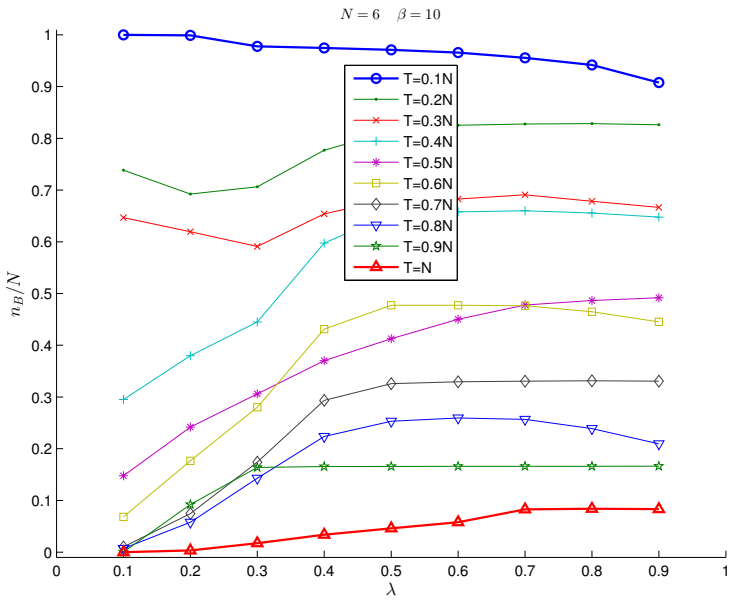

Figure 6.25: The proportion of bold fish in the group for different T when $N = 6$.

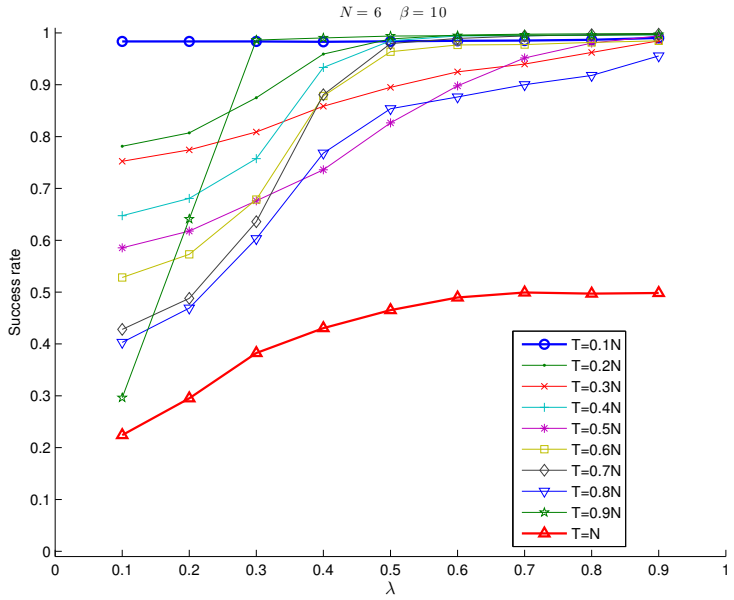

Figure 6.26: The success rate for different T when $N = 6$.

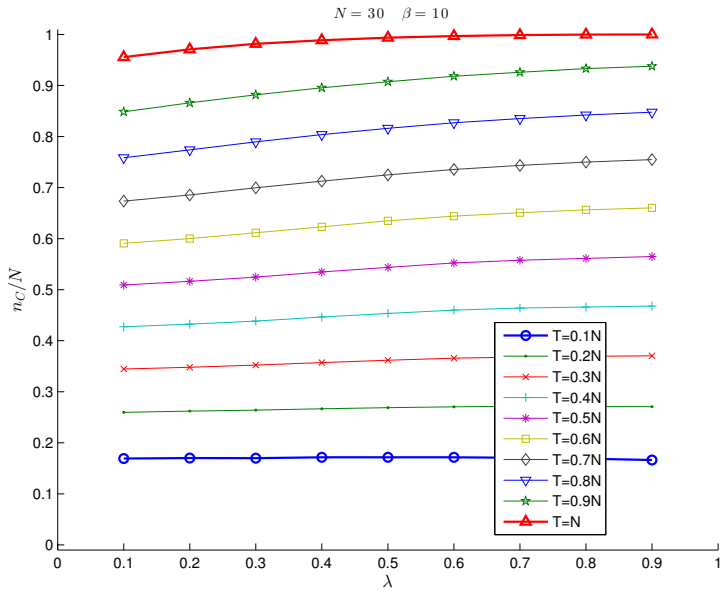

Figure 6.27: The proportion of C-players in the group for different T when $N = 30$.

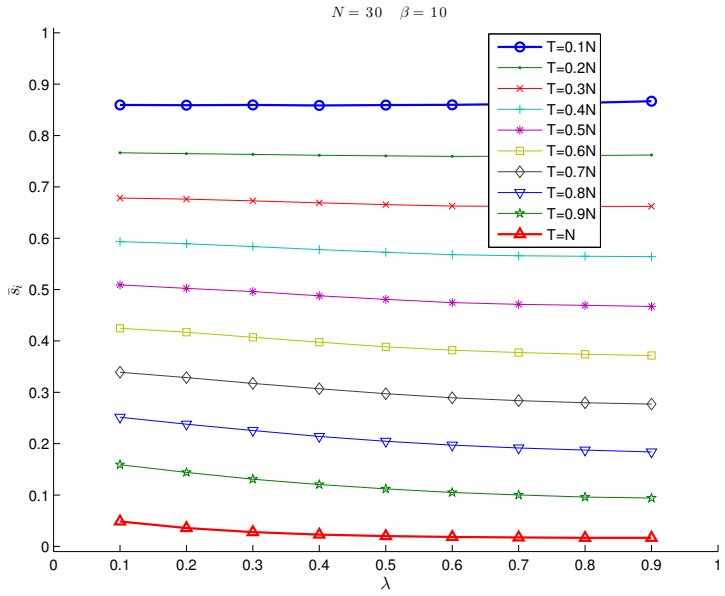

Figure 6.28: The average strategy in the group for different T when $N = 30$.

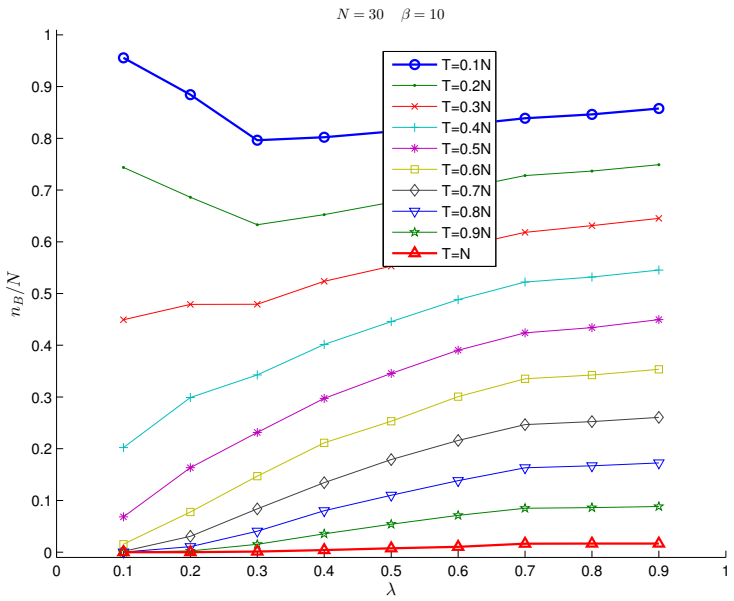

Figure 6.29: The proportion of bold fish in the group for different T when $N = 30$.

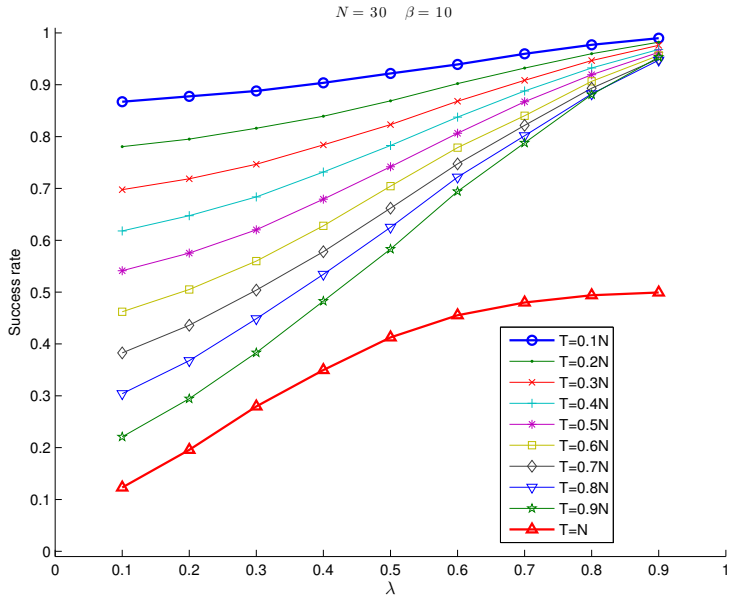

Figure 6.30: The success rate for different T when $N = 30$.

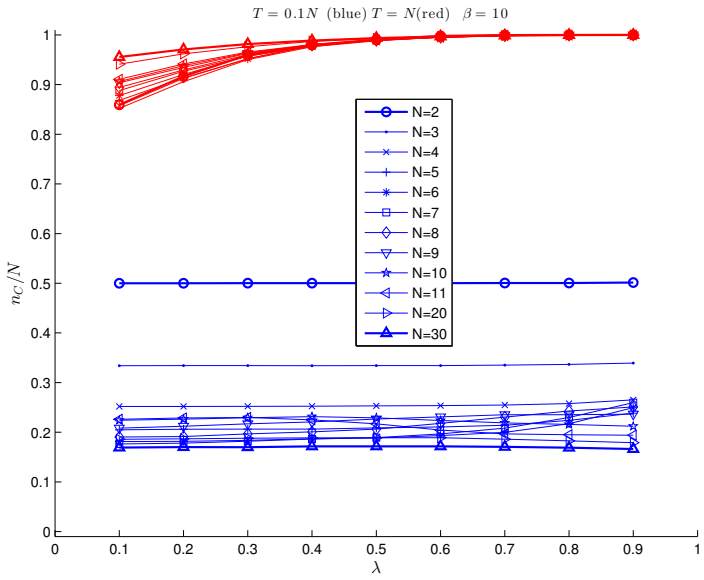

Figure 6.31: The proportion of C-players in the group for different N when $T = 0.1N$ and $T = N$.

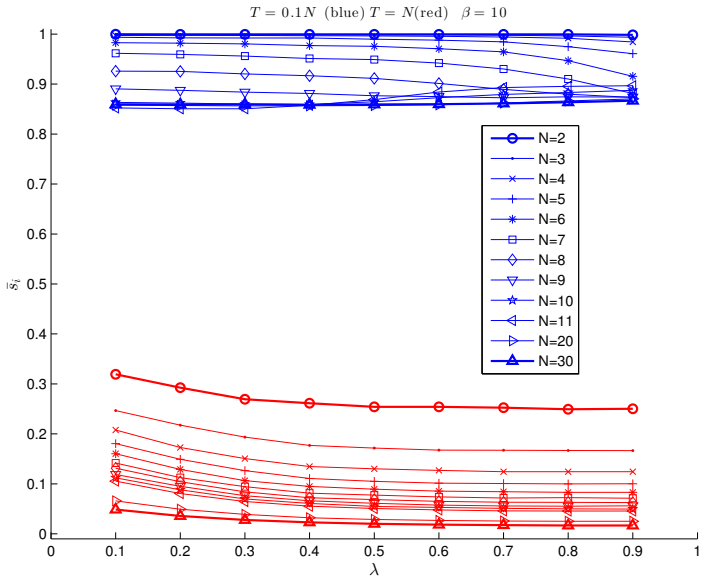

Figure 6.32: The average strategy of the group for different N when $T = 0.1N$ and $T = N$.

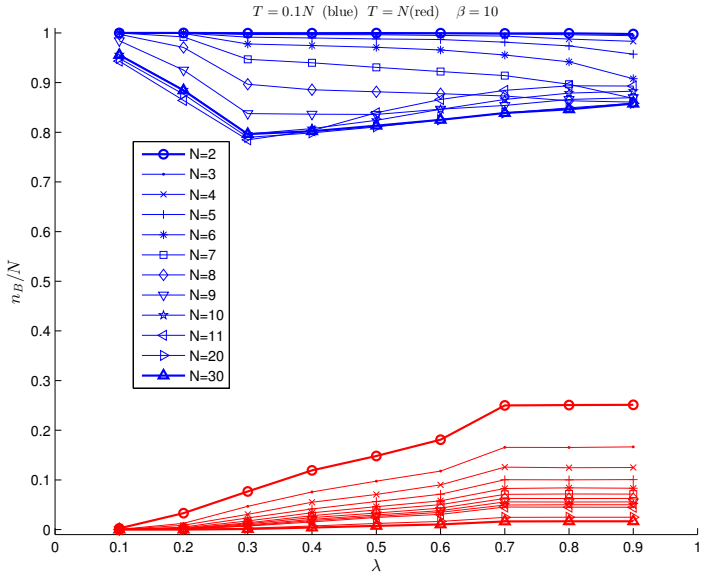

Figure 6.33: The proportion of bold fish in the group for different N when $T = 0.1N$ and $T = N$.

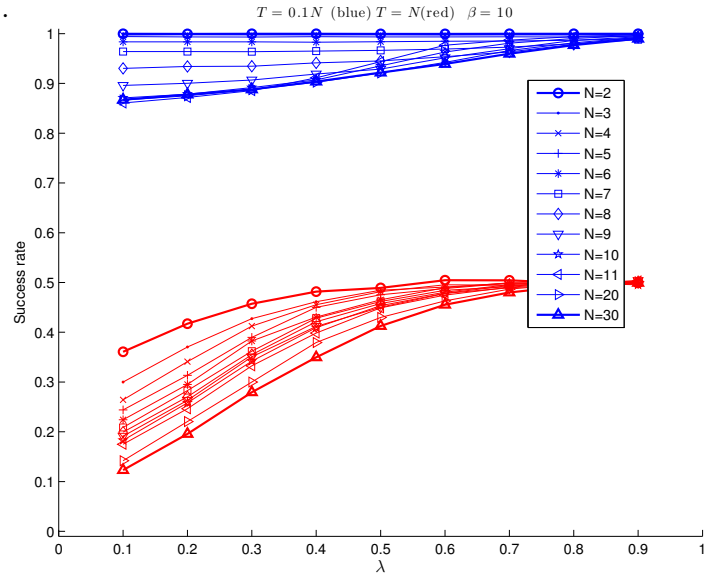

Figure 6.34: The success rate for different N when $T = 0.1N$ and $T = N$.

6.4.3 Evolution with changed tasks

All the results above focus on the evolution during which the difficulty of obstacle removing task is fixed. Now we are interested in the situation when the difficulty of tasks can change during a single evolution process.

We still choose $N = 10$ and $\lambda = 0.1, 0.4, 0.9$. Each evolution consists of 10000 tasks as well. T is set to $0.1N$ for the first 2000 tasks, then increases to $0.9N$ from task 2001 to 4000, and decreases back to $0.1N$ from task 40001 to the end of the evolution.

The simulation results are shown in Fig. 6.35 − 6.37. The strategies s_i of the N fish, the label of the initiator I_n, the number of C-players n_C, the number of bold fish n_B, and the success rate are shown in each figure. Moreover, the curves of T and $N - T$ are drawn in red in the subplots n_C and n_B, respectively.

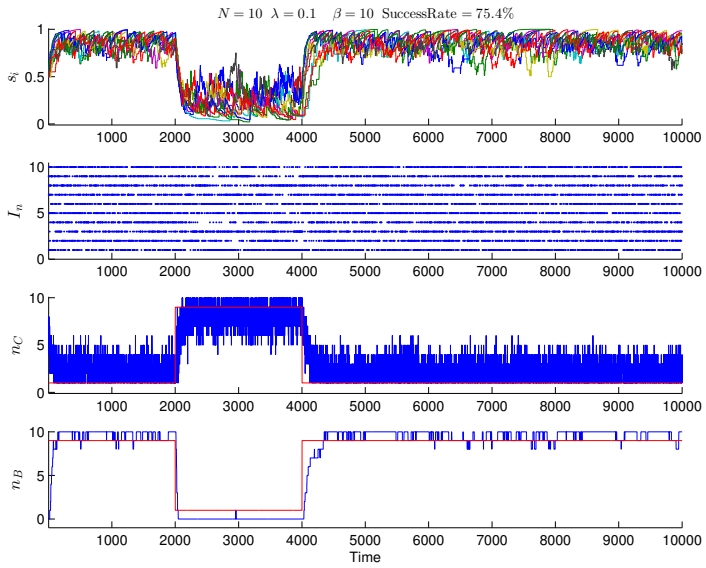

Figure 6.35: A group of $N = 10$ robotic fish deals with changed tasks, where strategy update rate $\lambda = 0.1$.

When T changes from $0.1N$ to $0.9N$, n_C and n_B can quickly converge to the new T and $N - T$, respectively. It means that when the difficulty of task changes from easy to hard, the group can quickly adapt itself to the new situation by self-adaptation during the evolution. On the other hand, when T decreases from $0.9N$ to $0.1N$, the group can still quickly adapt itself to the new situation when the strategy update rate λ is low, but costs much time for higher update rate λ. As we mentioned,

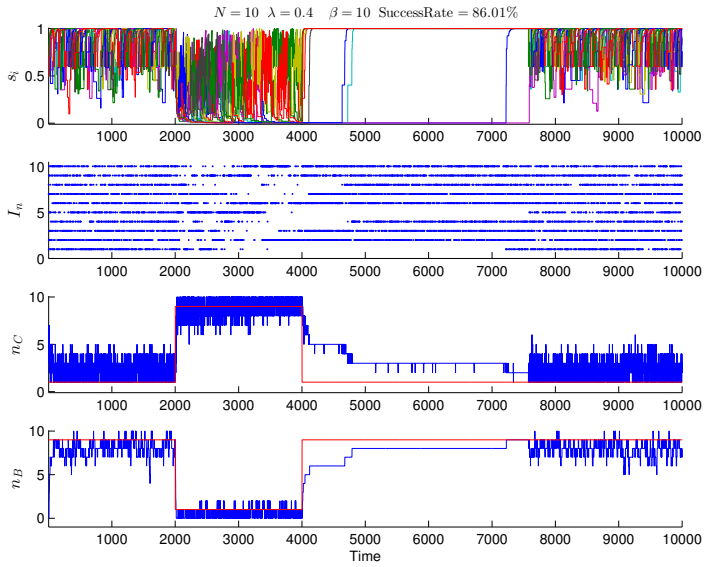

Figure 6.36: A group of $N = 10$ robotic fish deals with changed tasks, where strategy update rate

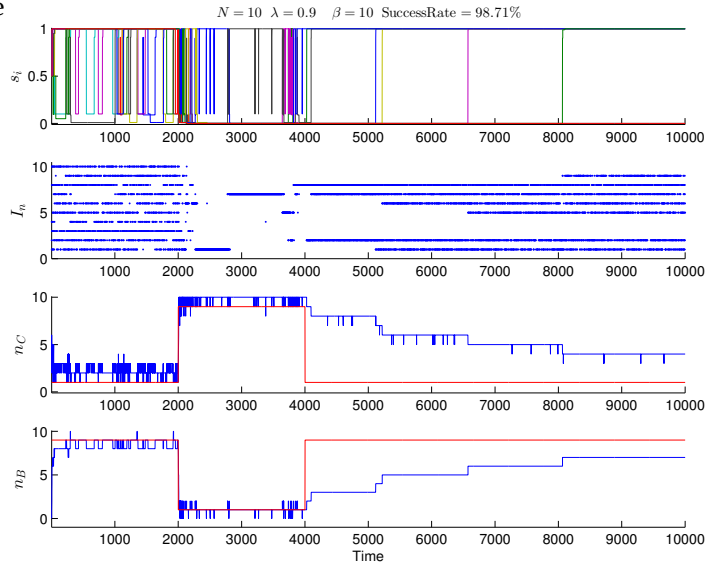

Figure 6.37: A group of $N = 10$ robotic fish deals with changed tasks, where strategy update rate $\lambda = 0.9$.

the short-term evolution results in the diversity of personalities and the process of role differentiation in the group. Thus we can conclude that the group spends much time to adapt itself to an easier task due to the diversity of personalities and the process of role differentiation emerge in the group. In conclusion, *the fish group has the ability of self-adaptation to fit with the difficulties of the obstacle removing tasks, even though the difficulty may change and is unknown to the fish group and the fish do not communicate with each other; moreover, large diversity of personalities may slow down the regulation process when the task difficulty decreases*.

6.5 Discussion and conclusion

In this section, we first summarize the results from both experiments and simulations, and show further analysis. Then we give the conclusion and future work.

6.5.1 Discussion

We summarize the results according to the two aspects we focus on: how personality evolves, and how effective leadership emerges in the fish group. Based on these, we further analyze how groups of robotic fish solve the obstacle removing tasks.

Evolution of personalities of individuals

In view of the evolution of personalities of individuals in the group, we identify that more bold fish emerge in the group when the obstacle removing tasks are easier. Moreover, a more interesting phenomenon is shown that the number of bold fish n_B is always around the difference between group size N and the threshold T which presents the difficulty of the tasks. If we think a little further, the personality which shows the fish's willingness of being an initiator can be seen as the confidence of the fish in success causing an effective leadership. Then the above conclusion can be understood as follows: when the task is more difficult, fewer fish have enough confidence to be an initiator; however, more fish have such kind of confidence when the task is easier.

After gaining insight into more details, we further find that the diversity of the personalities and the process of role differentiation emerge in a short-term evolution run.

Emergence of effective leadership in the group

Note that the emergence of effective leadership in the group is implied by the success of the task. Then we consider the group's performance, which can be quantified by achieving success or not when doing the task. For a given obstacle removing task, more diversity of personalities in the group results in a better performance for achieving success faster.

On the other hand, the fish group has the ability of self-adaptation to fit with the difficulties of obstacle removing tasks, although the difficulty may change and is unknown to the fish group and the fish do not communicate with each other; moreover, the diversity of personalities may slow down the regulation process when the task difficulty decreases. We also find the number of C-players is always around the threshold T which presents the difficulty of the tasks. Due to the ability of self-adaptation, the fish group can solve the obstacle removing tasks with appropriate number of C-players, as shown in the following part.

In addition, we verify that our conclusions above are applicable for all group size N we tested, and we conjecture that it holds for all group sizes.

How the groups solve the obstacle removing tasks

From the results above, we arrive at an important fact that the diversity of personalities is a crucial factor in determining the group's performance in doing the obstacle removing tasks in our setting. This inspires us to analyze how the groups solve the obstacle removing tasks with and without diversity of personalities, respectively.

Case (I): Without diversity of personalities. All fish in the group almost have the same level of willingness to be an initiator from a statistical perspective. Then the fish will initiate a collective movement in turns during the evolution process, and the frequency of each fish to be a C-player is similar to each other's. As is shown before, a reasonable number of C-players, which corresponds with the group's estimation of the difficulty of the task, participate in pushing the obstacle for each task. Obviously, the energy consumption of each fish is almost balanced in this case.

Case (II): With diversity of personalities. The process of role differentiation has occurred after a few steps of the evolution. Some of the fish have high level of willingness to be an initiator while others rarely want to initiate a collective movement in doing the obstacle removing tasks. Thus the frequency of fish with high level of willingness to be an initiator is obvious larger than that of the others. Moreover, the number of such fish is smaller when the task is more difficult. Then, for a difficult task, once an initiator occurs, lots of others will follow, since the one who rarely wants to be an initiator always has great willingness to follow others. Thus the number of cooperators will keep a high level and then the group still can achieve

success with high probability.

Considering the situations in experiments or even in real biological system, the model confirms the intuitive interpretation that the level of willingness to be an initiator also affects how quickly the initiator emerges. For example, if all members of the group have the same level of willingness to be an initiator, then the higher this level is, the faster the initiator emerges. In other words, the bolder individual would like to be an initiator itself, but the shyer one prefers to wait for others' decision. From this perspective, the time cost of the group to do the obstacle removing task is short in this case. This characteristic is important if there exists any requirement of the time used to complete the forging task.

6.5.2 Conclusion

In this chapter, a new framework, using multi-robotic fish system as an experimental tool and evolutionary game theory as the theoretical tool, has been proposed to investigate the evolution of personalities and the emergence of effective leadership in bio-inspired robotic fish groups. The proposed framework takes advantages of its two components. On the one hand, the design of the robotic fish and its locomotion control, which imitate the physical structures and locomotion properties of real fish, allow us to get much closer to the situations of fish groups in nature. On the other hand, evolutionary game theory is powerful in understanding interactive behavior in animal groups. To verify the usefulness of our proposed framework in investigating the behaviors of robotic fish groups, leadership in an obstacle removing scenario has been chosen as a case study. An N-player snowdrift game has been proposed and used to model the obstacle removing scenario with N robotic fish. Personality has been introduced as the player's strategy to present the robotic fish's willingness to initiate a collective movement in an obstacle removing task. The experiments by groups of robotic fish have been carried out to study the evolution of personalities and the emergence of effective leadership in the fish groups. In addition, the effectiveness of our game model has been verified by fitting with the experimental data. Thus simulations have also been carried out as effective complements of the experimental results.

Currently, we are exploring the application of the proposed framework to investigate more behaviors of robotic fish groups. We are also extending the robotic fish system in the framework to a heterogeneous system consisting of both robotic fish and real fish. Such a heterogeneous system may help biologists to understand better the interactive behaviors in real fish schools.

Chapter 7

Conclusions and Future Research

In this chapter, we summarize our work in this thesis and give recommendations for future research.

7.1 Concluding remarks

This thesis has investigated control and coordination issues for robotic multi-agent systems using biomimetic robotic fish teams. The robotic fish and the experimental platform have been studied. To replicate the outstanding performance of real fish in nature, we have studied three control issues of robotic fish, from individual to group, in Chapter 3, 4, and 5, respectively. Based on these biomimetically inspired control tools, in Chapter 6, we have developed a multi-robotic fish setup using evolutionary game theoretic ideas to construct a new framework to study the diversification of personalities and emergence of leadership that are critical for the completion of group tasks.

In Chapter 3, we have investigated the locomotion control of an individual robotic fish. A simple but effective CPG model has been proposed. The key point in our proposed CPG model is to use partially linearized oscillators instead of nonlinear ones. This design differs significantly from the standard CPG models. While our CPG contains the basic features of its biological counterparts and is capable of producing coordinated patterns of rhythmic activity, due to the partially linearized structures of the oscillators, the computational costs of our CPG model is greatly reduced and all the structural parameters can be selected more intuitively and easily according to the request of the dynamic performance of the CPG model. In addition, the complete control architecture, mainly composed of the proposed CPG model and a transition layer, has been built up. The transition layer is used to transform higher level control commands into accessible inputs to the CPG for producing suitable coordinated patterns of rhythmic activity. In order to reduce the number of the control parameters, a PSO based method has been used to find an optimal point in the parameter space, where a maximum speed can be achieved. As a result, only

two control parameters, which are the frequency for speed control and the offset of the motors for direction control, are sufficient for the whole locomotion control implementation. Furthermore, a large number of numerical simulations and physical experiments have been performed to show that the performance of our CPG-based method is reliable and its application is easy and simple.

Chapter 4 has investigated another control issue of robotic fish inspired by the observation that formations of synchronized fish may swim with less energy consumption. We have designed distributed control laws for groups of robotic fish to lock the phases of their sinusoidal body waves in an antiphase fashion. The phase dynamics of the body waves of the robotic fish have been modeled by coupled Kuramoto oscillators. We have proven that when such phase dynamics are coupled through real-time communications with a diamond-shape topology, they can be synchronized with the desirable relative phase differences of zero or π to mimic the fish swimming patterns predicted in the corresponding biological studies. Both computer simulations and physical experiments have been performed to show the effectiveness and robustness of the proposed control strategies.

In Chapter 5, we have proposed an evolutionary game model to control groups of robotic fish and have further studied the emergence and evolution of cooperation among them in multi-robot water polo matches. This control issue is based on inspiration from the coordination behaviors of fish schooling and other collective motions for social animals. A novel modified snowdrift game has been proposed to model simplified multi-robot water polo matches. The cooperation coefficient has been introduced to quantify the well-known synergy effect and the learning coefficient has been defined to describe the robots' learning capability. We have studied the evolutionary stability of reactive strategies in infinite populations when the cooperation coefficient takes different values. Furthermore,we have analyzed robotic fish's tendencies to collaborate and have found that robots prefer to cooperate with teammates when cooperation is efficient and play alone otherwise. In addition, an update rule for the cooperation coefficient has been designed and we have shown that the cooperation efficiency can be improved when robots cooperate more. Moreover, we have found through simulations that when the cooperation coefficient coevolves with the population dynamics, cooperation efficiency gets improved under better learning capabilities.

Chapter 6 has developed a new framework, using multi-robotic fish system as the experimental tool and evolutionary game theory as the theoretical tool, to investigate the evolution of personalities and the emergence of effective leadership in bio-inspired robotic fish groups. To verify the usefulness of our proposed framework in investigating the phenomenon in coordinated multi-agent systems, leadership in an obstacle removing scenario has been chosen as a case study. An N-player

evolutionary game has been proposed to model the obstacle removing scenario with N robotic fish. Then the personality, which is considered in this research to be each fish's willingness to initiate a collective movement in an obstacle removing task, has been introduced to the game model as the player's strategy. The experiments by groups of robotic fish have been carried out to study the evolution of personalities and the emergence of effective leadership in the robotic fish groups. We have identified by experiments that the diversity of personalities in a group, which emerges in the short-term evolution, is a crucial factor in determining the group's performance in the obstacle removing tasks. We have further analyzed how the groups solve the tasks with and without diversity of personalities, respectively. Moreover, we have found that the robotic fish group has the ability of self-adaptation to cope with the level of difficulties of obstacle removing tasks. In addition, the effectiveness of our game model has been verified by perfect fitting the experimental data. Then simulations have also been carried out as effective complements to the experimental results.

7.2 Recommendations for future research

We identify three directions for future research.

• CPG with sensory feedback for locomotion control

Chapter 3 has studied a CPG-based method for locomotion control of an individual robotic fish. However, the proposed CPG model is open-loop since the robotic fish has no sensor. Currently, we are exploring to integrate several sensors, such as pose sensors and pressure sensors, into the body of the robotic fish. Then it is of interest to add some sensory information as coupling terms to obtain a CPG with sensory feedback. This design will allow the robotic fish to adjust its locomotion pattern by self-regulation to fit complex environment and better interact with its neighbors when swimming in schools.

• Coordination strategy with more motion dynamics for formation control

Chapter 4 has shown an antiphase synchronization strategy that can coordinate the body waves of a formation of swimming robotic fish. However, the proposed strategy has only considered the phase dynamics of the robotic fish. Currently, we are exploring to study a more comprehensive coordination control strategy that considers more motion dynamics of the robotic fish, such as the amplitudes and frequencies of the oscillator model. This design, which considering all aspects of the

robotic fish motion dynamics that may affect their interactions in water, is of clear advantage that better performance of robotic fish may be achieved when swimming together. Moreover, this design of coordination strategy together with the sensor feedback added to CPG model will offer an opportunity to investigate what kind of formation of robotic fish may swim with less energy consumption.

• **Evolving heterogeneous system consisting of both robotic fish and real fish**

Based on the idea shown in Chapter 5, Chapter 6 has proposed a new framework, combining multi-robotic fish systems and evolutionary game theory, to investigate phenomena in coordinated multi-robotic fish systems. Leadership in an obstacle removing scenario has been chosen as a case study to show the power of the proposed evolving multi-robotic fish system when investigating the phenomenon in robotic fish groups. It is of great interest to extend the multi-robotic fish system in the framework to a heterogeneous system consisting of both robotic fish and real fish. In other words, we are exploring to add one or more robotic fish to a group of real fish. Then we can control the behavior of robotic fish and investigate how the fish group will evolve when some of the members (i.e., the robotic fish) change their behavior. This design, the evolving heterogeneous system consisting of both robotic fish and real fish, may provide us a novel and better way of understanding the fish behaviors in nature.

Bibliography

[1] J. A. Acebron, L. L. Bonilla, C. J. P. Vicente, F. Ritort, and R. Spigler. The kuramoto model: A simple paradigm for synchronization phenomena. *Reviews of Modern Physics*, 77:137–185, 2005.

[2] T. Balch and R. C. Arkin. Behavior-based formation control for multirobot teams. *IEEE Transactions on Robotics and Automation*, 14:926–939, 1998.

[3] J. L. Baxter, E. K. Burke, J. M. Garibaldi, and M. Norman. Multi-robot search and rescue: A potential field based approach. In *Autonomous Robots and Agents*, volume 76, chapter 2, pages 9–16. Springer Berlin Heidelberg, 2007.

[4] C. Bernstein, A. Kacelnik, and J. R. Krebs. Individual decisions and the distribution of predators in a patchy environment. *Journal of Animal Ecology*, 57(3):1007–1026, 1988.

[5] L. E. Blume. The statistical mechanics of strategic interaction. *Games and Economic Behavior*, 5:387–424, 1993.

[6] Y. Bourquin. *Self-organization of locomotion in modular robots*. Master's Thesis, Department of Informatics, University of Sussex, 2005.

[7] F. Bullo, J. Cortes, and S. Martinez. *Distributed Control of Robotic Networks*. Princeton University Press, Princeton, 2009.

[8] L. Busoniu, R. Babuska, and B. D. Schutter. A comprehensive survey of multiagent reinforcement learning. *IEEE Transactions on Systems, Man, and Cybernetics, Part C: Applications and Reviews*, 38:156–172, 2008.

[9] D. W. Casbeer, D. B. Kingston, R. W. Beard, and T. W. McLain. Cooperative forest fire surveillance using a team of small unmanned air vehicles. *International Journal of Systems Science*, 37(6):351–360, 2006.

[10] J. F. Chang. A performance comparison between genetic algorithms and particle swarm optimization applied in constructing equity portfolios. *International Journal of Innovative Computing, Information and Control*, 5(12(B)):5069–5079, 2009.

[11] T. H. Chung, G. A. Hollinger, and V. Isler. Search and pursuit-evasion in mobile robotics: A survey. *Autonomous Robots*, 31(4):299–316, 2011.

[12] N. Correll and A. Martinoli. Multirobot inspection of industrial machinery. *IEEE Robotics and Automation Magazine*, 16:103–112, 2009.

[13] I. D. Couzin, J. Krause, N. R. Franks, and S. A. Levin. Effective leadership and decision-making in animal groups on the move. *Nature*, 434(7025):513–516, 2005.

[14] A. Crespi and A. J. Ijspeert. Online optimization of swimming and crawling in an amphibious snake robot. *IEEE Transactions on Robotics*, 24(1):75–87, 2008.

[15] A. Crespi, D. Lachat, A. Pasquier, and A. J. Ijspeert. Controlling swimming and crawling in a fish robot using a central pattern generator. *Autonomous Robots*, 25:3–13, 2008.

[16] F. Delcomyn. Neural basis for rhythmic behaviour in animals. *Science*, 210(4469):492–498, 1980.

[17] J. Deng and X. Shao. Hydrodynamics in a diamond-shaped fish school. *Journal of Hydrodynamics, Ser. B*, 18:438–442, 2006.

[18] A. Dhariwal, G. S. Sukhatme, and A. A. G. Requicha. Bacterium-inspired robots for environmental monitoring. In *Proc. of the IEEE International Conference on Robotics and Automation (ICRA '04)*, pages 1436–1443, 2004.

[19] M. Doebeli and C. Hauert. Models of cooperation based on the prisoner's dilemma and the snowdrift game. *Ecology Letters*, 8:748–766, 2005.

[20] J. R. Dyer, A. Johansson, D. Helbing, I. D. Couzin, and J. Krause. Leadership, consensus decision making and collective behaviour in humans. *Philosophical Transactions of the Royal Society B: Biological Sciences*, 364(1518):781–789, 2009.

[21] B. E. Eskridge, E. Valle, and I. Schlupp. Using experience to promote the emergence of leaders and followers. In *Proc. of the 2013 European Conference on Complex Systems*, 2013.

[22] D. F. Feng, G. Cho, and R. F. Doolittle. Determining divergence times with a protein clock: update and reevaluation. *Proceedings of the National Academy of Sciences*, 94(24):13028–13033, 1997.

[23] J. Gore, H. Youk, and A. van Oudenaarden. Snowdrift game dynamics and facultative cheating in yeast. *Nature*, 459:253–256, 2009.

[24] S. Grillner. Neural control of vertebrate locomotion - central mechanisms and reflex interaction with special reference to the cat. *Feedback and motor control in invertebrates and vertebrates*, pages 35–56, 1985.

[25] J. L. Harcourt, T. Z. Ang, G. Sweetman, R. A. Johnstone, and A. Manica. Social feedback and the emergence of leaders and followers. *Current Biology*, 19(3):248–252, 2009.

[26] J. L. Harcourt, G. Sweetman, A. Manica, and R. A. Johnstone. Pairs of fish resolve conflicts over coordinated movement by taking turns. *Current Biology*, 20(2):156–160, 2010.

[27] D. He, Q. Wang, C. Rong, and G. Xie. Generating high-speed three-dimensional dynamic quadruped walking using an evolutionary search. In *Proc. of the International Conference on Informatics in Control, Automation and Robotics*, pages 167–172, 2009.

[28] M. Hebbel, R. Kosse, and W. Nistico. Modeling and learning walking gaits of biped robots. In *Proc. of the Workshop on Humanoid Soccer Robots of the 2006 IEEE-RAS International Conference on Humanoid Robots*, pages 40–48, 2006.

[29] J. Hofbauer and K. Sigmund. *Evolutionary games and population dynamics*. Cambridge University Press, 1998.

[30] Y. Hu, W. Zhao, and L. Wang. Vision-based target tracking and collision avoidance for two autonomous robotic fish. *IEEE Transactions on Industrial Electronics*, 56:1401–1410, 2009.

[31] A. J. Ijspeert. Central pattern generators for locomotion control in animals and robots: A review. *Neural Networks*, 21(4):642–653, 2008.

[32] A. J. Ijspeert, A. Crespi, D. Ryczko, and JM. Cabelguen. From swimming to walking with a salamander robot driven by a spinal cord model. *Science*, 315:1416–1420, 2007.

[33] A. J. Ijspeert, J. Hallam, and D. Willshaw. Evolving swimming controllers for a simulated lamprey with inspiration from neurobiology. *Adaptive Behavior*, 7(2):151–172, 1999.

[34] R. A. Johnstone and A. Manica. Evolution of personality differences in leadership. *Proceedings of the National Academy of Sciences*, 108(20):8373–8378, 2011.

[35] C. Karakuzu. Parameter tuning of fuzzy sliding mode controller using particle swarm optimization. *International Journal of Innovative Computing, Information and Control*, 6(10):4755–4770, 2010.

[36] E. Katsnelson, U. Motro, M. W. Feldman, and A. Lotem. Evolution of learned strategy choice in a frequency-dependent game. *Proceedings of the Royal Society B: Biological Sciences*, 279(1731):1176–1184, 2012.

[37] J. Kennedy and R. C. Eberhart. Particle swarm optimization. In *Proc. of the IEEE International Conference on Neural Networks*, pages 1942–1948, 1995.

[38] H. Kimura, Y. Fukuoka, and A. H. Cohen. Adaptive dynamic walking of a quadruped robot on natural ground based on biological concepts. *The international Journal of Robotics Research*, 26(5):475–490, 2007.

[39] A. J. King. Follow me! I 'm a leader if you do; I 'm a failed initiator if you don 't? *Behavioural Processes*, 84(3):671–674, 2010.

[40] J. Krause, D. Hoare, S. Krause, C. K. Hemelrijk, and D. I. Rubenstein. Leadership in fish shoals. *Fish and Fisheries*, 1(1):82–89, 2000.

[41] J. Krause and G. D. Ruxton. *Living in groups*. Oxford University Press, 2002.

[42] R. J. Kuo, C. C. Huang, and T. L. Hu. Normal vector-controlled particle swarm optimization algorithm for solving bi-level linear programming problem. *ICIC Express Letters*, 4(5(A)):1417–1424, 2010.

[43] Intelligent Control Laboratory. Control and optimization of robotic fish. Technical report, Peking university, 2010.

[44] J. C. Liao, D. N. Beal, G. V. Lauder, and M. S. Triantafyllou. Fish exploiting vortices decrease muscle activity. *Science*, 302:1566–1569, 2003.

[45] M. J. Lighthill. Note on the swimming of slender fish. *Journal of Fluid Mechanics*, 9:305–317, 1960.

[46] W. F. Loomis. *Four billion years: an essay on the evolution of genes and organisms*. Sinauer Associates, Incorporated, 1988.

[47] K. H. Low. Mechatronics and buoyancy implementation of robotic fish swimming with modular fin mechanisms. *Proceedings of the Institution of Mechanical Engineers, Part I: Journal of Systems and Control Engineering*, 221(3):295–309, 2007.

[48] K. McIsaac and J. Ostrowski. Motion planning for anguilliform locomotion. *IEEE Transactions on Robotics and Automation*, 19(4):637–625, 2003.

[49] M. Milinski, R. D. Sommerfeld, H. J. Krambeck, F. A. Reed, and J. Marotzke. The collective-risk social dilemma and the prevention of simulated dangerous climate change. *Proceedings of the National Academy of Sciences of the United States of America*, 105:2291–2294, 2008.

[50] S. Nakayama, M. C. Stumpe, A. Manica, and R. A. Johnstone. Experience overrides personality differences in the tendency to follow but not in the tendency to lead. *Proceedings of the Royal Society B: Biological Sciences*, 280(1769):20131724, 2013.

[51] C. Niehaus, T. Röfer, and T. Laue. Gait optimization on a humanoid robot using particle swarm optimization. In *Proc. of the Second Workshop on Humanoid Soccer Robots in conjunction with the 2007 IEEE-RAS International Conference on Humanoid Robots*, 2007.

[52] M. A. Nowak and K. Sigmund. Tit for tat in heterogeneous populations. *Nature*, 355:250–253, 1992.

[53] J. Ostrowski and J. Burdick. Gait kinematics for a serpentine robot. In *Proc. of the IEEE International Conference on Robotics and Automation (ICRA '96)*, pages 1294–1299, 1996.

[54] D. Pais and N. E. Leonard. Adaptive network dynamics and evolution of leadership in collective migration. *Physica D: Nonlinear Phenomena*, 267:81–93, 2014.

[55] D. A. Paley, N. E. Leonard, R. Sepulchre, D. Grunbaum, and J. K. Parrish. Oscillator models and collective motion. *IEEE Control Systems Magazine*, 27:89–105, 2007.

[56] E. Pennisi. How did cooperative behavior evolve? *Science*, 309:93, 2005.

[57] O. Petit and R. Bon. Decision-making processes: the case of collective movements. *Behavioural Processes*, 84(3):635–647, 2010.

[58] S. A. Rands, G. Cowlishaw, R. A. Pettifor, J. M. Rowcliffe, and R. A. Johnstone. Spontaneous emergence of leaders and followers in foraging pairs. *Nature*, 423(6938):432–434, 2003.

[59] W. Ren and R. W. Beard. Consensus seeking in multiagent systems under dynamically changing interaction topologies. *IEEE Transactions on Automatic Control*, 50:655–661, 2005.

[60] C. Reynolds. Flocks, herds and schools: A distributed behavioral model. In *ACM SIGGRAPH Computer Graphics*, volume 21, pages 25–34, 1987.

[61] C. Rong, Q. Wang, Y. Huang, G. Xie, and L. Wang. Autonomous evolution of high speed quadruped gaits using particle swarm optimization. In *RoboCup 2008: Robot Soccer World Cup XII*, pages 259–270. Springer, 2009.

[62] N. Roy and G. Dudek. Collaborative robot exploration and rendezvous: Algorithms, performance bounds and observations. *Autonomous Robots*, 11(2):117–136, 2001.

[63] W. H. Sandholm, E. Dokumaci, and F. Franchetti. Dynamo: Diagrams for evolutionary game dynamics, version 1.1. 2011. http://www.ssc.wisc.edu/∼whs/dynamo.

[64] M. Sfakiotakis, D. M. Lane, and B. C. Davies. An experimental undulating-fin device using the parallel bellows actuator. In *Robotics and Automation, 2001. Proceedings 2001 ICRA. IEEE International Conference on*, volume 3, pages 2356–2362, 2001.

[65] M. Sfakiotakis, D. M. Lane, and J. B. C. Davies. Review of fish swimming modes for aquatic locomotion. *IEEE Journal of Oceanic Engineering*, 24:237–252, 1999.

[66] J. Shao, L. Wang, and J. Yu. Development of multiple robotic fish cooperation platform. *International Journal of Systems Science*, 38(3):257–268, 2007.

[67] J. Shao, L. Wang, and J. Yu. Development of an artificial fish-like robot and its application in cooperative transportation. *Control Engineering Practice*, 16(5):569–584, 2008.

[68] Y. Shi and R. C. Eberhart. A modified particle swarm optimizer. In *Proc. of the IEEE International Conference on Evolutionary Computation*, pages 69–73, 1998.

[69] S. Stocker. Models for tuna school formation. *Mathematical Biosciences*, 156:167–190, 1999.

[70] P. Stone. *Layered learning in multiagent systems: A winning approach to robotic soccer*. Ph.D. Thesis, School of Computer Science, Carnegie Mellon University, 1998.

[71] R. S. Sutton and A. G. Andrew. *Reinforcement learning: An introduction*. Cambridge Univ Press, 1998.

[72] G. Szabó and G. Fáth. Evolutionary games on graphs. *Physics Reports*, 446:97–216, 2007.

[73] G. Szabó and C. Tőke. Evolutionary prisoner's dilemma game on a square lattice. *Physical Review E*, 58:69–73, 1998.

[74] Y. Taguchi, H. Nakano, A. Utani, A. Miyauchi, and H. Yamamoto. A competitive particle swarm optimization for finding plural acceptable solutions. *ICIC Express Letters*, 4(5(B)):1899–1904, 2010.

[75] M. S. Triantafyllou and G. S. Triantafyllou. An efficient swimming machine. *Scientific American*, 272:64–70, 1995.

[76] D. P. Tsakiris, M. Sfakiotakis, A. Menciassi, G. La Spina, and P. Dario. Polychaete-like undulatory robotic locomotion. In *Proc. of the IEEE International Conference on Robotics and Automation (ICRA '05)*, pages 3018–3023, 2005.

[77] P. E. Turner and L. Chao. Prisoner's dilemma in an RNA virus. *Nature*, 398:441–443, 1999.

[78] C. Wang, B. Wu, M. Cao, and G. Xie. Modified snowdrift games for multi-robot water polo matches. In *Proc. of the 24th Chinese Control and Decision Conference*, pages 164–169, 2012.

[79] C. Wang, G. Xie, L. Wang, and M. Cao. CPG-based locomotion control of a robotic fish: Using linear oscillators and reducing control parameters via PSO. *International Journal of Innovative Computing, Information and Control*, 7:4237–4249, 2011.

[80] D. Weihs. Hydromechanics of fish schooling. *Nature*, 241:290–291, 1973.

[81] D. Weihs. Some hydrodynamical aspects of fish schooling. In *Swimming and Flying in Nature*, pages 703–718. Plenum Publishing Corporation, 1975.

[82] F. J. Weissing. Animal behaviour: Born leaders. *Nature*, 474(7351):288–289, 2011.

[83] M. Wolf, G. S. Van Doorn, and F. J. Weissing. On the coevolution of social responsiveness and behavioural consistency. *Proceedings of the Royal Society B: Biological Sciences*, 278(1704):440–448, 2011.

[84] B. Wu, P. M. Altrock, L. Wang, and A. Traulsen. Universality of weak selection. *Physical Review E*, 82:046106, 2010.

[85] C. Wu and L. Wang. Where is the rudder of a fish: The mechanism of swimming and control of self-propelled fish school. *Acta Mechanica Sinica*, 26:45–65, 2010.

[86] W. Zhao, Y. Hu, G. Xie, L. Wang, and Y. Jia. Development of vision-based autonomous robotic fish and its application in water-polo-attacking task. In *Proc. of the 2008 American Control Conference (ACC)*, pages 568–573, 2008.

[87] W. Zhao, J. Yu, Y. Fang, and L. Wang. Development of multi-mode biomimetic robotic fish based on central pattern generator. In *Proc. of the IEEE/RSJ International Conference on Intelligent Robots and Systems*, pages 3891–3896, 2006.

Summary

In the past years, astonishing dynamical behaviors in fish schools and other social animal groups in nature have become the focus of multi-disciplinary studies. Rooted in control engineering and reaching out to biology, this thesis uses biomimetic robotic fish teams as a powerful means to investigate the control and coordination issues for robotic multi-agent systems. We first study three control issues of robotic fish, from individual to group, to replicate the outstanding performance of real fish in nature. Based on these biomimetically inspired control tools, we develop a multi-robotic fish setup using evolutionary game theoretic ideas to construct a new framework to investigate phenomena in coordinating multi-agent systems. New theoretical results developed in this thesis are useful for control engineers and provide insight for biologists, while the improved experimental techniques pave ways for further robotic study.

To learn from the outstanding locomotion skills of real fish in nature, we first investigate the locomotion control of an individual robotic fish. A complete control architecture, mainly composed of a simple but effective CPG model and a transition layer, is built up. Our proposed CPG model has a key feature of using partially linearized oscillators. This design differs significantly from the standard CPG models. While our CPG contains the basic features of its biological counterparts and is capable of producing coordinated patterns of rhythmic activity, due to the partially linearized structures of the oscillators, the computational costs of our CPG model is greatly reduced and all the structural parameters can be selected more intuitively and easily according to the request of the dynamic performance of the CPG model. The designed transition layer is used to transform higher level control commands into accessible inputs to the CPG for producing suitable coordinated patterns of rhythmic activity. Furthermore, aiming to reduce the number of the control param-

eters, a PSO based method is used to find an optimal point in the parameter space, where a maximum speed can be achieved. As a result, only two control parameters, which are the frequency for speed control and the offset of the motors for direction control, are sufficient for the whole locomotion control implementation.

Inspired by the observation that formations of synchronized fish may swim with higher energy efficiency, we then design distributed control laws for formations of swimming robotic fish generating antiphase sinusoidal body waves. The phase dynamics of the body waves of the biomimetic robotic fish is modeled by coupled Kuramoto oscillators. It is proven that when such phase dynamics are coupled through real-time communications with a diamond-shape topology, they can be synchronized with the desirable relative phase differences of zero or π to mimic the fish swimming patterns predicted in the corresponding biological studies.

Based on inspiration from the coordination behaviors of fish schooling and other collective motions for social animals, we further propose an evolutionary game model to control groups of robotic fish and study the emergence and evolution of cooperation among them in multi-robot water polo matches. A novel modified snowdrift game is proposed to model the simplified multi-robot water polo matches. A cooperation coefficient is introduced to quantify the well-known synergy effect and a learning coefficient is defined to describe the robots' learning capability. Then we study the evolutionary stability of reactive strategies in infinite populations when the cooperation coefficient takes different values. We further analyze robotic fish's tendencies to collaborate. It is found that robots prefer to cooperate with teammates when cooperation is efficient and play alone otherwise. To gain insight into how the cooperation coefficient affects the cooperation tendencies, we design an update rule to allow the cooperation coefficient to evolve when robots learn to improve their performances. It is found that when the cooperation coefficient co-evolves with the population dynamics, cooperation efficiency gets improved under better learning capabilities.

Finally, we develop a new framework, using multi-robotic fish system as the experimental tool and evolutionary game theory as the theoretical tool, to investigate phenomena in coordinated bio-inspired robotic fish groups. Leadership in an obstacle removing task is chosen as a case study to verify the usefulness of our proposed framework. An N-player evolutionary game is proposed to model the obstacle removing task with N robotic fish. Then the personality, which is considered in this research to be each fish's willingness to initiate a collective movement in a group task, is introduced to the game model as the player's strategy. We carry out experiments by groups of robotic fish to study the evolution of personalities and the emergence of effective leadership in the robotic fish team. It is identified by experiments that the divergence of personalities in a group, which emerges in the short-term

evolution, is a crucial factor in determining the group's performance in the obstacle removing tasks. We further analyze how the groups solve the tasks with and without diversity of personalities, respectively. Moreover, it is found that the robotic fish group has the ability of self-adaptation to cope with the level of difficulties of group tasks.

Samenvatting

In de afgelopen jaren is het verbazingwekkende dynamische gedrag van scholen vissen en andere groepen sociale dieren in de natuur in de belangstelling komen te staan van multidisciplinair onderzoek. In dit proefschrift passen we fundamentele gereedschappen uit de regeltechniek toe op biologische systemen om de regeling en coördinatie van robot multi-agent systemen te bestuderen. We bestuderen daarvoor drie regeltechnische kwesties voor zowel een individuele robotvis, als een groep robotvissen. Daarbij bootsen we de buitengewone prestaties van echte vissen in de natuur na. Gebruikmakend van deze natuur nabootsende regel gereedschappen in combinatie met speltheorie, ontwikkelen we een multi-robotvis setup om een nieuw kader op te stellen om bepaalde fenomenen in het coördineren van multi-agent systemen te onderzoeken. De nieuwe theorie in dit proefschrift is nuttig voor regeltechnici en geeft inzicht aan biologen, terwijl de verbeterde experimentele technieken de weg vrijmaken voor verregaand robot onderzoek.

We beginnen met het onderzoeken van de motoriekregeling van een individuele robotvis om te leren van de buitengewone motorische vaardigheden van echte vissen in de natuur. Een volledige regelingsarchitectuur is opgebouwd, hoofdzakelijk samengesteld uit een simpel maar effectief CPG model en een transitie laag. De spil van het door ons voorgestelde CPG model maakt gebruik van gedeeltelijk gelineariseerde oscillators. Dit ontwerp verschilt significant van de standaard CPG modellen. Ons CPG model bevat de basis functies van zijn biologische tegenhangers en kan gecoördineerde patronen van ritmische activiteit produceren. Door de gedeeltelijk gelineariseerde structuur van de oscillators is de rekentijd van ons CPG model sterk gereduceerd en kunnen we alle structurele parameters meer intuïtief selecteren. Deze selectie is afhankelijk van de dynamische prestaties van het CPG model. De ontworpen transitie laag wordt gebruikt om hogere regelingscomman-

dos te vertalen in voor de CPG toegankelijk ingangssignalen, die daarmee een gecoördineerd patroon van ritmische activiteit kan produceren. Bovendien is een op PSO gebaseerde methode gebruikt om een optimum in de parameterruimte te vinden voor een maximale snelheid, met als doel het aantal regel parameters te reduceren. Als gevolg daarvan zijn slecht twee parameters, zijnde de snelheidsfrequentie en de offset van de richtingsregelaar van de motors, voldoende om de gehele motoriek regeling te implementeren.

Vervolgens ontwerpen we gedistribueerde regelingen voor formaties van zwemmende robotvissen, die sinusoïde lichaamsgolven genereren in antifase. Deze regeling is geïnspireerd door de observatie dat formaties van gesynchroniseerde vissen mogelijkerwijs met een hogere energie efficiëntie zwemmen. De fase dynamica van de lichaamsgolven van de natuurgetrouwe robotvis is gemodelleerd door een gekoppelde Kuramoto oscillator. Wanneer de fase dynamica gekoppeld zijn door real-time communicatie met een diamant-vormige topologie is bewezen dat de vissen kunnen synchroniseren met een gewenst relatief fase verschil van nul of π radialen. Daarmee bootsen we zwempatronen na die voorspeld zijn in overeenkomstige biologische studies.

Ten derde presenteren we een evolutionair spel model om groepen robotvissen te regelen. Dit model is gebaseerd op het gecoördineerde gedrag van vissen in scholen en andere collectieve bewegingen van sociale dieren. We richten ons daarbij op de opkomst en evolutie van samenwerking tussen de vissen in een multi-robotvis water polo wedstrijd. Een nieuw aangepast sneeuwdrift spel is opgesteld om vereenvoudigde multi-robotvis water polo wedstrijden te modelleren. Een samenwerkingcoëfficiënt is geïntroduceerd om het bekende synergie effect te kwantificeren. Daarnaast definiëren we een leercoëfficiënt ten aanzien van de leercapaciteiten van de vissen. Vervolgens bestuderen we de evolutionaire stabiliteit van de reactieve strategieën in oneindige populaties voor verschillende waarden van de samenwerkingcoëfficiënt. Verder blijkt dat robots een voorkeur voor samenwerking hebben wanneer samenwerking efficiënt is, wanneer dit niet het geval is spelen ze alleen. We ontwerpen een verversingsregel om de samenwerkingcoëfficiënt te laten evolueren wanneer de robots leren hun prestaties te verbeteren. Daarmee verwerven we inzicht hoe het samenwerkingcoëfficiënt de neiging tot samenwerking beïnvloedt. Het blijkt dat wanneer de samenwerkingcoëfficiënt zich tegelijk met de populatie dynamica ontwikkelt, de efficiëntie van de samenwerking verbeterd door betere leer bekwaamheden van de robots.

Tot slot ontwikkelen we een nieuw kader om fenomenen binnen groepen van gecoördineerde biologisch geïnspireerde robotvissen te onderzoeken. Daarbij gebruiken we een multi-robotvis systeem als experimenteel gereedschap en evolutionaire speltheorie als theoretisch gereedschap. Het fenomeen van leiderschap bij een

obstakel verwijdering taak is gekozen als een casestudy om het nut van het door ons voorgestelde kader aan te tonen. We stellen een evolutionair spel met N spelers voor om de obstakel verwijder taak te modelleren voor een groep met N robotvissen. Daarna introduceren we persoonlijkheid in het spel als de spelers strategie. Persoonlijkheid in dit onderzoek is de bereidheid van elke vis om een collectieve beweging in een groep te initiëren. Met behulp van experimenten met groepen robotvissen bestuderen we de evolutie van persoonlijkheden en de opkomst van effectief leiderschap binnen een robotvis team. De experimenten tonen aan dat de divergentie van persoonlijkheden in een groep op de korte termijn, een cruciale factor is in het bepalen van groepsprestaties in obstakel verwijdering taken. Verder analyseren we hoe groepen de taken oplossen met en zonder diversiteit van persoonlijkheden. Bovendien blijkt dat een groep robotvissen een vermogen tot zelfaanpassing heeft om de moeilijkheidsgraad van de groepstaak het hoofd te bieden.

ISBN: 978-90-367-7371-3